

Chemical Organization Theory for Reaction-Diffusion Systems and its Application to Virus Infection Models

A thesis submitted in fulfillment of the requirements
for the degree of Doctor rerum naturalis (Dr. rer. nat.)

brought before the Rat der Fakultät für Mathematik und Informatik
of the Friedrich Schiller University of Jena

by Mathematician (Diploma) Stephan Peter
born 8th April 1982 in Nordhausen

Supervisor & Examiner: Prof. Dr. Bashar Ibrahim, Gulf University for Science and Technology, Kuwait

Examiner: Prof. Dr. Peter Dittrich, University of Jena

Date of defense: 31th March 2022

Zusammenfassung

Die Ergebnisse dieser Arbeit sind in vier Kapitel unterteilt. Im ersten Kapitel wird die Chemische Organisationstheorie (COT) erweitert auf Reaktionsdiffusionssysteme (RDS). Das heißt, die Menge der persistenten Spezies eines RDS wird beschrieben auf der Ebene des zugrundeliegenden Reaktionsnetzwerks. Es wird bewiesen, dass die Menge der persistenten Spezies einer jeden beschränkten Lösung eines RDS eine Verteilte Organisation (englisch: distributed organization (DO)) ist. Dabei wird auch die innere Struktur solcher DOs offengelegt und bewiesen, dass die Menge aller DOs eines gegebenen RDS immer einen Verband bildet. Es wird gezeigt, dass die genannten Resultate verschiedene Informationen zur Beschreibung des gesamten potenziellen Langzeitverhaltens aller beschränkten Lösungen des RDS liefern. Im zweiten Ergebniskapitel wird beispielhaft skizziert, wie Informationen über Diffusion und verschiedene Randbedingungen für die Spezies als zusätzliche Reaktionen in das Reaktionsnetzwerk integriert werden können, um aus diesem alle DOs zu bestimmen, die als Mengen persistenter Spezies in Frage kommen. Im dritten Kapitel werden verschiedene In-Host-Influenza A Virusinfektionsmodelle gewöhnlicher Differenzialgleichungen analysiert, indem jeweils all ihre Organisationen bzw. DOs bestimmt werden. Im letzten Kapitel wird diese Technik bei der Anwendung auf SARS-Cov-19 Virusinfektionsmodelle dahingehend erweitert, dass auch Modelle partieller Differenzialgleichungen einschließlich Host-to-host-Modellen analysiert werden. Schließlich werden alle Modelle beider Viren in eine Hierarchie integriert. Die Informationen, die dadurch generiert werden, werden bezüglich der theoretischen Resultate über Persistenz aus dem ersten Kapitel analysiert und diskutiert.

Abstract

The results of this work comprise four sections. In the first section, Chemical Organization Theory (COT) is extended toward reaction-diffusion systems (RDS). That is, the set of persistent species in RDS is described by linking their dynamics with the underlying network structure using an extension of COT. More precisely, it is proven that for every bounded solution of an RDS the set of persistent species is a distributed organization (DO). Also, the inner structure of such DOs is revealed as well as the fact that the set of DOs always forms a lattice. It is shown that these results provide various information about the potential dynamical behavior of the RDS. In the second section of the Results it is exemplified how knowledge about diffusion and different boundary conditions can be integrated as further reactions into the reaction network to compute all DOs from it, which are possibly persistent. In the third section, several in-host Influenza A virus infection dynamics ODE models are analyzed by computing the set of their organizations resp. DOs. In the last section, this technique is extended by analyzing ODE and PDE models of Cov-SARS-19 virus infection dynamics within and between hosts. Finally, all models of both viruses are put together into one hierarchy. The information gained from the structures and the hierarchy of the models is discussed with regard to the results about persistence from the first section.

List of publications

This work is based on the first four of the following list of publications:

1. Stephan Peter, Bashar Ibrahim and Peter Dittrich. "Linking network structure and dynamics to describe the set of persistent species in reaction diffusion systems", *SIAM J. Applied Dynamical Systems* (2021), Vol. 20, No. 4, pp. 2037 – 2076.
 2. Stephan Peter, Peter Dittrich and Bashar Ibrahim. "Structure and Hierarchy of SARS-CoV-2 Infection Dynamics Models Revealed by Reaction Network Analysis". *Viruses* 13.1 (2021), page 14.
 3. Stephan Peter, Martin Hölzer, Kevin Lamkiewicz, Pietro Speroni di Fenizio, Hassan Al Hwaer, Manja Marz, Stefan Schuster, Peter Dittrich and Bashar Ibrahim. "Structure and Hierarchy of Influenza Virus Models Revealed by Reaction Network Analysis". *Viruses* 11.5 (2019), page 449.
 4. Stephan Peter, Fanar Ghanim, Peter Dittrich and Bashar Ibrahim, "Organizations in reaction-diffusion systems: Effects of diffusion and Boundary conditions", *Ecological Complexity* 43 (2020), page 100855.
-
5. Stephan Peter, Matthias Schirmer, Philippe Lathan, Georg Stimpfl, Bashar Ibrahim. "Performance analysis of a solar-powered multi-purpose supply container", *MDPI Sustainability*, 2022 (submitted).
 6. Peter Kreyssig, Christian Wozar, Stephan Peter, Tomas Veloz, Bashar Ibrahim, Peter Dittrich. "Effects of small particle numbers on long-term behaviour in discrete biochemical systems", *Bioinformatics*, Volume 30, Issue 17, Pages i475–i481, 2014.
 7. Stephan Peter, Tomas Veloz, Peter Dittrich. "Feasibility of Organizations - A Refinement of Chemical Organization Theory with Application to P Systems", *Eleventh International Conference on Membrane Computing*, Springer, 2010.
 8. Stephan Peter, Sten Grimmer, Susanne Lipfert, Andre Seyfarth. "Variable Joint Elasticities in Running", *Informatik aktuell - Autonome Mobile Systeme 2009*, 129–136, Springer Berlin Heidelberg.

Acknowledgements

I thank my supervisors Prof. Dr. Dittrich and Prof. Dr. Bashar Ibrahim for their great support and advice. I thank the co-authors Prof. Dr. Manja Marz, Prof. Dr. Stefan Schuster, Dr. Peter Kreyssig, Christian Wozar, Dr. Tomas Veloz, Dr. Sten Grimmer, Susanne Lipfert, Prof. Dr. Andre Seyfarth, Fanar Ghanim, Martin Hölzer, Kevin Lamkiewicz, Prof. Dr. Pietro Speroni di Fenizio and Hassan Al Hwaeer for their contributions. Also I thank Dr. Hendrik Huthoff as well as Dr. Frank Wessely for carefully reading the manuscripts and Prof. Dr. Tobias Oertel-Jäger for discussing distributed organizations.

Contents

Zusammenfassung	iii
Abstract	v
List of publications	vii
Acknowledgements	ix
1 Introduction	1
2 Methods	5
2.1 Reaction Networks and Dynamical Systems	5
2.2 Coloring scheme for species involved in virus infection dynamics	8
2.3 Deriving the underlying reaction network from a dynamical system	8
2.4 Computing the organizations of a reaction network	9
2.5 The signature of a reaction network	11
2.6 Persistence	12
3 Results	13
3.1 Linking network structure and dynamics to describe the set of persistent species in reaction diffusion systems	13
3.1.1 Persistence	13
3.1.2 Comparison of different concepts of persistence	17
3.1.3 Distributed Organizations	20
3.1.4 The role closedness plays in the dynamics	24
3.1.5 DOs and persistence	28
3.1.6 Analysis of a DO lattices	34
3.1.7 Comparisons and hierarchies of several models using their signature	35
3.1.8 Example I	36
3.1.9 Example II	38
3.1.10 Example III	39
3.2 Organizations in Reaction-Diffusion Systems: Effects of Diffusion and Boundary Conditions	43
3.2.1 Example Ia	43
3.2.2 Example Ib	44
3.2.3 Example Ic	44
3.2.4 Summary	44
3.3 Structure and Hierarchy of Influenza A Virus Infection Models	49
Models	49
Hierarchy of influenza A virus models	61
3.4 Structure and Hierarchy of SARS-Cov-2 Virus Infection Models	65
In-Host Models	65

Host-To-Host Models	68
A Linked In-Host/Host-To-Host Model	71
Hierarchy of Models	72
4 Conclusions	75
4.1 Future work	76
Bibliography	79
A Reactions of Influenza-A virus infection dynamics models	87
B Reactions of SARS-Cov-2 virus infection dynamics models	91

List of Abbreviations

ODE	Ordinary Differential Equation
PDE	Partial Differential Equation
COT	Chemical Organization Theory
RDS	Reaction Diffusion System
DO	Distributed Organization
BC	Boundary Condition
IAV	Influenza A Virus
RNA	Ribonucleic Acid
SARS-CoV-2	Severe acute respiratory syndrome coronavirus type 2
CoV	SARS-CoV-2

List of Symbols

\mathcal{S}	finite set of species	section 2.1
$s_i \in \mathcal{S}$	Species	section 2.1
$n = \mathcal{S} $	Number of species	section 2.1
\mathcal{R}	finite set of reactions	section 2.1
$r_j \in \mathcal{R}$	Reaction	section 2.1
$m = \mathcal{R} $	Number of reactions	section 2.1
$(\mathcal{S}, \mathcal{R})$	Reaction network	section 2.1
$\phi(c)$	Abstraction of c = species of c with non-zero concentration	section 2.1
\mathbb{N}_0	Set of natural numbers including 0	section 2.1
$a_{ij} \in \mathbb{N}_0$	Number of s_i in the LHS of the reaction r_j	section 2.1
$b_{ij} \in \mathbb{N}_0$	Number of s_i in the RHS of the reaction r_j	section 2.1
$n_{ij} = b_{ij} - a_{ij} \in \mathbb{Z}$	Element of the stoichiometric matrix	section 2.1
$\text{supp}(r_j)$	Support of reaction r_j	section 2.1
$N \in \mathbb{Z}^{n \times m}$	Stoichiometric matrix	section 2.1
v	Feasible flux	section 2.1
$v()$	Flux vector function	section 2.1
$k_j > 0$	Reaction constants of r_j	section 2.1
$t \geq 0$	Time variable	section 2.1
$\Omega \subseteq \mathbb{R}^p, p \in \mathbb{N}$	Domain with $0 < \int_{\Omega} dx < \infty$	section 2.1
$x \in \Omega$	Space variable	section 2.1
\mathbb{R}_+^n	Set of vectors of non-negative reals, i.e., $\mathbb{R}_+^n \equiv \{(c_1, \dots, c_n)^T \in \mathbb{R}^n : c_1, \dots, c_n \geq 0\}$	section 2.1
$d_i \geq 0$	Diffusion rate of the species s_i	section 2.1
ν	External normal vector to the boundary $\delta\Omega$	section 2.1
$c()$	Solution of a RDS	section 2.1
$(t_l)_{l=1}^{\infty}$	Sequence of points in time	section 2.1
$\hat{v} = \hat{v}(c, (t_l)_{l=1}^{\infty})$	Total flux (with respect to c and $(t_l)_{l=1}^{\infty}$)	section 2.1
$\text{clos}_1(S) = \text{clos}_1^1(S)$	Union of S and the set of all species produced reactions $r_j \in \mathcal{R}$ with $\text{supp}(r_j) \subseteq S$	definition 2.4.1
$\text{clos}_1^k(S)$	$= \text{clos}_1(\text{clos}_1^{k-1}(S)), k \geq 1, \text{clos}_1^0(S) \equiv S$	definition 2.4.1
$\text{clos}(S)$	Closure of a subset $S \subseteq \mathcal{S}$ of species $= \cup_{k \in \mathbb{N}} \text{clos}_1^k(S)$	definition 2.4.1
$S^\epsilon \subseteq \mathbb{R}_+^n$	ϵ -neighborhood of S = concentration vectors with $c_i > \epsilon \forall s_i \in S$	definition 3.1.1
$S^{\epsilon, \delta} \subseteq \mathbb{R}_+^n$	(ϵ, δ) -neighborhood of S = concentration vectors with $c_i > \epsilon \forall s_i \in S$ and $c_i \leq \delta \forall s_i \notin S$	definition 3.1.1
$F(C) = F(C; c, (t_l)_{l=1}^{\infty})$	Frequency of occurrence of the set $C \subseteq \mathbb{R}_+^n$ of concentration vectors w.r.t. a solution c and $(t_l)_{l=1}^{\infty}$	definition 3.1.2
$P(c)$	Set of persistent subsets of species with respect to solution c of a RDS	definition 3.1.3

$$\Phi(c) = \cup_{S \in P(c)} S$$
$$D \in \mathbb{R}^{n \times n}$$

Set of persistent species w.r.t. c
Fickian diffusivity (diagonal) matrix

definition 3.1.3
section 3.1.5

Chapter 1

Introduction

Reaction systems are widely used to describe and to study phenomena in various areas such as biochemistry [88] and evolutionary biology [46, 93]. Those systems often base on ODEs or PDEs and are usually very complex. To understand them it is a common approach to analyze the reaction networks they rely on. Reaction network theory provides various approaches to deal with such complexity, for example, deficiency [27, 47], RAF theory (Reflexively Autocatalytic and Food-generated) [88], hemical organization theory (COT) [19], subnetwork analysis [17], elementary modes [81], graph theory [33, 82], and Lyapunov functions [63]. Among others, these approaches allow for analyzing the behavior of dynamical reaction systems basing on ODEs or PDEs like for example reaction-diffusion systems (RDS). Such analyses include the question of which species can persist in the long-run [78, 72].

Persistence is the main topic of the first section of the results chapter in which COT is applied to RDS. Therefore, COT is extended appropriately by generalizing organizations towards distributed organizations (DOs). Then two main results are obtained:

1. The set of persistent species of a bounded solution of a reaction-diffusion system is always a DO.
2. The set of DOs of a reaction network is always a lattice.

This means, that for a given RDS we know all the possibly persistent subsets of species by computing the DOs of the underlying reaction network. Which of these DOs is approached in a concrete simulation depends on the initial conditions and the reaction constants which were chosen. Finally we provide simulation examples. The relation between the RDS, their underlying reaction networks, simulations and COT is depicted in Figure 1.1.

In the second section of the results chapter the effects of diffusion and different boundary conditions on the DOs are discussed by providing three examples. The main idea is to modify the reaction network appropriately to incorporate boundary conditions.

In the third section of the results chapter COT is applied to the analysis of virus infection dynamics models of Influenza A, that is, in-host ODE models. Influenza is an infectious respiratory disease, annually infecting 5 – 15 % of the human population and causing epidemics that result in 3 – 5 million severe cases with 300,000 – 500,000 deaths each year [89]. The annual recurrence of epidemics is caused by the continuous alteration of seasonal influenza viruses, which enables them to efficiently escape the immune system even due to previous infections or vaccinations [77]. The major burden of disease in humans is caused by seasonal influenza A (IAV) and influenza B viruses, causing symptoms varying from mild respiratory disease characterized by fever, sore throat, headache and muscle pain to severe and in some cases lethal pneumonia and secondary bacterial infections [54].

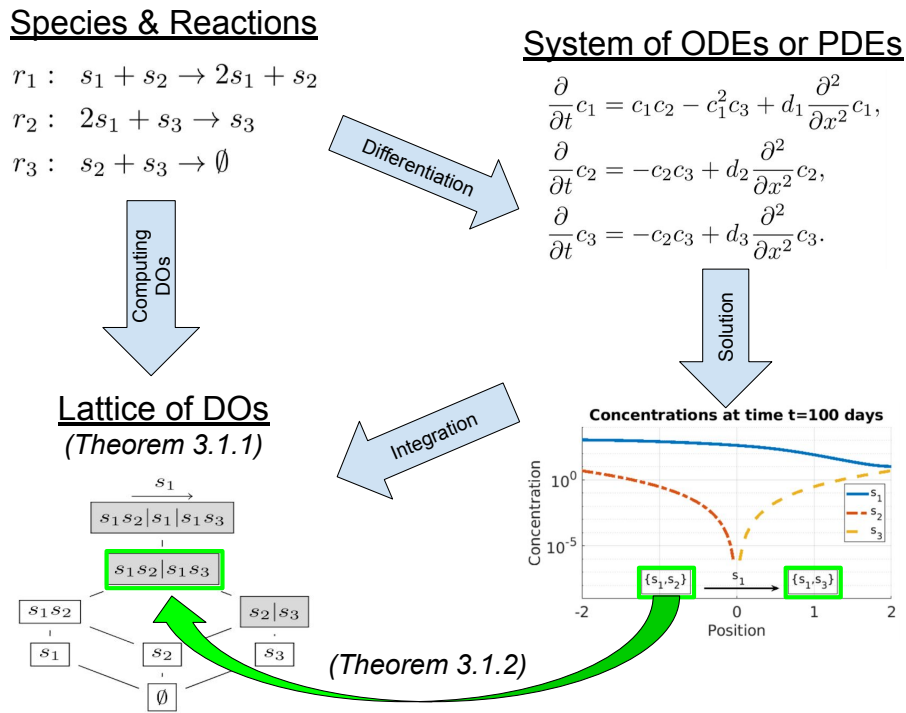


FIGURE 1.1: [76] Illustration of the relation between a dynamical system (upper right), its solutions (lower right), its underlying reaction network (upper left), and the lattice of DOs (lower left) of the reaction network for Example 1 presented in Section 3.1.8. Systems of ODEs or PDEs are built from reaction networks by fixing the derivatives of the species concentrations according to the reaction rules. Integrating all the solutions of a dynamical system leads back to the reaction network and reveals the lattice of DOs. Also notated in the figure, the main results of this paper: The set of persistent species of every bounded solution of a RDS is a DO (theorem 3.1.2) and the set of DOs of every reaction network forms a lattice (theorem 3.1.1). It is shown how the fact that every potentially persistent set of species is part of the lattice of DOs allows for studying the interplay of different subsets of species with regard to their persistence.

The long-term spread of influenza viruses in the human population and the acute nature of influenza virus epidemics is driven by the global movement of these viruses. Differences in seasonal epidemics caused by influenza viruses are mainly driven by differences in the rates of virus evolution. The single-stranded RNA segments of influenza viruses, which are located inside the virus particle (or virion), evolve rapidly and thus can escape the host's immune response very efficiently.

Several ordinary differential equations (ODEs) models have been developed to provide insight into within-host dynamics of influenza A virus infections (for reviews see [84, 9, 21, 11, 35]). These models work in a time scale of days and describe the concentration dynamics of target cells, immune system components, viral load, and sometimes co-infecting pathogens. The models differ in terms of complexity and state space dimensions, which are between 3 and 15 for the models examined here. While the low-dimensional models can be analyzed completely and in a straightforward way (e.g. by calculating their fixed points and stability analysis), the characterization of the entire behavioral spectrum of complex models is more difficult (see for example

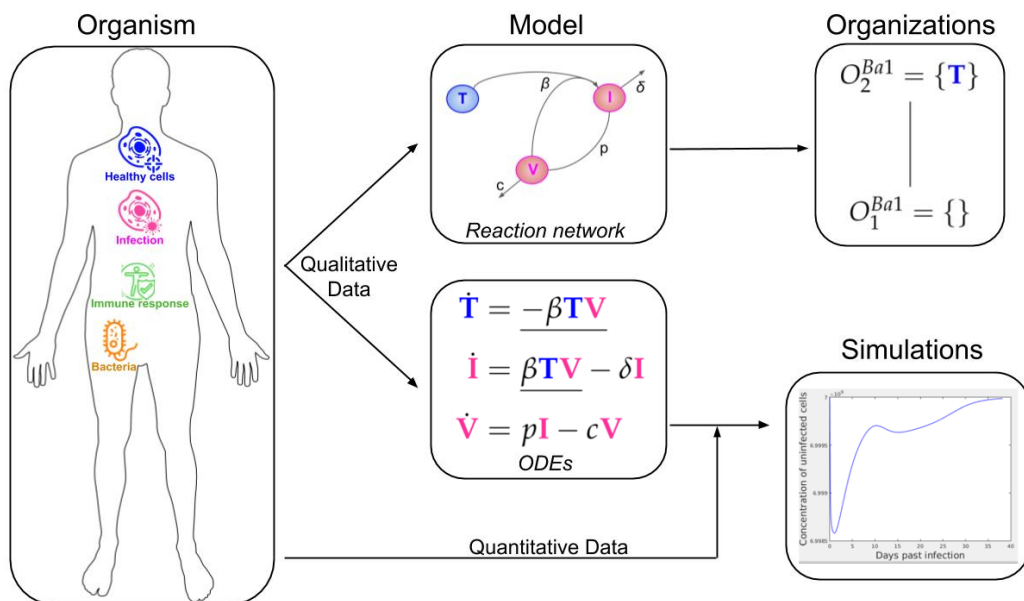


FIGURE 1.2: [75] Relation between measured data, ordinary differential equations (ODE) model, and hierarchy of organizations.

[58]).

We present an approach to understand the overall structure of these models that allows them to be related to each other in a simple way. To this end, we apply chemical organization theory [19, 59] to obtain a hierarchical decomposition of each model into chemical organizations. A chemical organization is a sub-set of species (i.e. dimensions or model components, like for example uninfected cells or viruses) that cannot generate any other species (property of closure) and that can self-maintain its own species, i.e., any species consumed by a process within the organization can be regenerated by a process within the organization. The organizations of an ODE model are rigorously related to its long-term dynamics in the following way: Given a stationary state of the ODE model, the set of species with strictly positive concentrations must be an organization [19]. The same is true for all practically relevant periodic and chaotic attractors [72]. Note that the advantage of this approach is that decomposition into organizations is based solely on the model structure (i.e., reaction rules) and thus is independent of kinetic details, like rate constants. The relation between measured data, ODE model, and organizations is depicted in Figure 1.2.

By applying the method to twelve models of influenza A virus infection we found different types of model structures ranging from two to eight organizations. Furthermore the models' organizations imply a partial order among models. The resulting hierarchy of models can help to select a suitable model for certain data or serve as a framework for further model development.

We provide reaction network files for all models and a software tool for computing their organizations (<https://github.com/stephanpeter/orgsflu>).

In the fourth section of the results chapter the analysis of infection dynamics models is extended to models of SARS-CoV-2 infection dynamics. The current SARS-CoV-2 pandemic has required huge efforts from global society and the scientific community to track, understand, and combat its proliferation. Models of the infection dynamics can help understanding SARS-CoV-2 pathogenesis, develop

optimal treatments, and introduce appropriate measures to prevent the spread of the virus. There are a multitude of modeling approaches with different properties, applications and aims that can be classed into categories of in-host models (e.g., [3, 11, 42, 22, 94, 91, 1, 90]) versus host-to-host models (such as [68, 100, 30, 57]), discrete versus continuous models and ODE versus PDE models (for an overview we refer to [25, 24, 49, 96]). There is an accumulating body of literature on SARS-CoV-2 infection dynamics that make use of these various tools and provide datasets that can be analyzed retrospectively once consensus modeling strategies have been derived [48, 50]. The aforementioned models have in common that they rely on an identifiable reaction network, for instance, a set of species and a set of reactions that describe the possible interactions of these species. In Section 3.3, we have shown that for Influenza A virus infection dynamics, reaction network analysis (especially COT [28]) provides metrics to understand, analyze, and categorize different in-host ODE models. In this section, we apply reaction network analysis, especially COT, to SARS-CoV-2 infection dynamics. Thereby we extend our previous approach presented in Section 3.3 into several directions: We incorporate in-host, host-to-host, and linked models consisting either of ODEs or PDEs. Finally, we combine the models of SARS-CoV-2 with Influenza A in order to compare the dynamics for both viruses. Therefore we describe the structure of a set of representative models of SARS-Cov-2 infection dynamics. For each of these models, we then derive the signature. The signature of a model gives a brief overview of its potential dynamical behavior, which allows for relating several models to each other and combining them in a hierarchy. We link the respective hierarchy of SARS-CoV-2 with that of Influenza A virus from Section 3.3. This novel method can be used as an instrument for a deeper understanding of infection dynamics models and further for an appropriate construction of future virus infection models.

All models, as well as the software tools used to do the analysis, can be found on Github (<https://github.com/stephanpeter/orgs-covid>).

In the Conclusions, the results of this work are discussed and summarized. Also, open questions remaining for future studies are listed.

Chapter 2

Methods

2.1 Reaction Networks and Dynamical Systems

Given a finite set $\mathcal{S} = \{s_1, \dots, s_n\}$ of n species (or molecules), together with a finite set $\mathcal{R} = \{r_1, \dots, r_m\}$ of m reactions, we call $(\mathcal{S}, \mathcal{R})$ a (chemical) reaction network. Each reaction $r_j \in \mathcal{R}$, $j = 1, \dots, m$, can be depicted by a so-called reaction equation using a right arrow,

$$\sum_{i=1}^n a_{ij} s_i \rightarrow \sum_{i=1}^n b_{ij} s_i \quad (2.1)$$

where $a_{ij}, b_{ij} \in \mathbb{N}_0 \equiv \mathbb{N} \cup \{0\}$, $i = 1, \dots, n$, $j = 1, \dots, m$. The difference between the matrices $A = (a_{ij}) \in \mathbb{N}^{n \times m}$ and $B = (b_{ij}) \in \mathbb{N}^{n \times m}$ is called the *stoichiometric matrix* $N = B - A \in \mathbb{Z}^{n \times m}$. For a reaction $r_j \in \mathcal{R}$, $j \in \{1, \dots, m\}$, the set of species s_i (reactants) with $a_{ij} > 0$ is called *support* of r_j and denote it by $\text{support}(r_j)$ or $\text{supp}(r_j)$. Note that if a species $s_i \in \mathcal{S}$ is reduced by a reaction $r_j \in \mathcal{R}$, that is $n_{ij} < 0$, then $s_i \in \text{supp}(r_j)$, that is, $a_{ij} > 0$. For a reaction $r_j \in \mathcal{R}$, $j \in \{1, \dots, m\}$, the species s_i with $b_{ij} > 0$ are called *products* of r_j .

A dynamical system can be derived from a reaction network by assigning to each species $s_i \in \mathcal{S}$, $i = 1, \dots, n$ and every time $t \in \mathbb{R}_+ \equiv \{u \in \mathbb{R} : u \geq 0\}$, a nonnegative concentration value $c_i(t)$. A map ϕ mapping a concentration vector back to a subset of species from the power set $\mathcal{P}(\mathcal{S})$ of the set of species, that is,

$$\phi : \mathbb{R}_{\geq 0}^n \rightarrow \mathcal{P}(\mathcal{S}), c \mapsto \phi(c), \quad (2.2)$$

is called *abstraction*, if

$$\phi(c) \equiv \{s_i \in \mathcal{S} : c_i > 0 \text{ for any } i \in \{1, \dots, n\}\}. \quad (2.3)$$

Thus, $\phi(c)$ is the subset of species that contains exactly those species that have a strictly positive concentration value. Species with concentration equal zero do not belong to $\phi(c)$. The abstraction ϕ plays an important role in this work, since it allows for linking the concentration vectors of a solution of a dynamical system with its underlying reaction network.

Now the question is considered of how the reactions rule the concentration values of the species in a dynamical system. For a given subset $S \subseteq \mathcal{S}$ of species, a vector $v \in \mathbb{R}_+^n$ is called a *feasible flux* with respect to S if for all $r_j \in \mathcal{R}$, $j = 1, \dots, m$, it holds that

$$v_j \begin{cases} > 0, & \text{iff } \text{support}(r_j) \subseteq S, \\ = 0, & \text{otherwise.} \end{cases} \quad (2.4)$$

A function

$$v : \mathbb{R}_+^n \rightarrow \mathbb{R}_+^m, c \mapsto v(c), \quad (2.5)$$

that is Lipschitz continuous on every bounded subset of \mathbb{R}_+^n , is called *flux vector function*, if for every $c \in \mathbb{R}_+^n$ the vector $v(c)$ is a feasible flux with respect to $\phi(c)$. Thus the flux vector function maps any vector of concentrations to a vector of reaction rates. If, for example, mass-action kinetics is applied ($v_j(c) = k_j \cdot c_1^{a_{1j}} \cdot \dots \cdot c_n^{a_{nj}}$ with real *reaction constants* $k_j > 0$, $j = 1, \dots, m$) to constructing v , then v is a flux vector function, because then it holds true that $v_j(c)$ is strictly positive if and only if the concentrations of all the species from the support of $r_j \in \mathcal{R}$ are strictly positive. This represents the common assumption that a reaction is active if and only if all of its reactants are present at the same time and place [27].

By defining the derivatives of the concentrations with respect to time we obtain a dynamical system as a system of ordinary differential equations (ODEs),

$$\frac{d}{dt}c(t) = \dot{c}(t) = N \cdot v(c(t)), \quad (2.6)$$

which describes how the change of the concentrations of the species from \mathcal{S} results from the concentrations via the set of reactions \mathcal{R} . In this case, the reaction network *underlies* the dynamical system. By adding initial conditions $c(0) = c^0 \in \mathbb{R}_+^n$, an *initial value problem* is obtained.

If, besides the time variable t , we add a space variable $x \in \Omega$ from a connected domain $\Omega \subset \mathbb{R}^p$, $p \in \mathbb{N}$, with $0 < \int_{\Omega} dx < \infty$ and a C^2 smooth boundary $\partial\Omega$, we can model effects like diffusion by differentiating twice with respect to x . Thus we arrive at describing the dynamics of the concentrations $c_i(x, t)$, $i = 1, \dots, n$, of the species for each location $x \in \Omega$ by a system of partial differential equations (PDEs),

$$\frac{\partial}{\partial t}c_i(x, t) = \underbrace{N \cdot v(c(x, t))}_{\text{reactions}} + \underbrace{d_i \frac{\partial^2}{\partial x^2}c_i(x, t)}_{\text{diffusion}}, \quad i = 1, \dots, n, \quad (2.7)$$

where $d_i \geq 0$, $i = 1, \dots, n$, are the *diffusion coefficients* of the species. By adding twice-continuously differentiable nonnegative *initial conditions*

$$c_i(x, 0) = c_i^0(x) \geq 0, \quad x \in \Omega, \quad i = 1, \dots, n, \quad (2.8)$$

and *homogeneous Neumann boundary conditions* (BCs),

$$\frac{\partial}{\partial \nu}c_i(x, t) = 0, \quad x \in \partial\Omega, \quad i = 1, \dots, n, \quad (2.9)$$

where $\nu \in \mathbb{R}^n$ is the external normal vector to the boundary $\delta\Omega$, we get a boundary value problem (BVP), a so-called reaction-diffusion system (RDS) with a solution

$$c : \Omega \times \mathbb{R}_+ \rightarrow \mathbb{R}^n, (x, t) \mapsto c(x, t). \quad (2.10)$$

We assume that each its derivatives $\frac{\partial c}{\partial t}$ and $\frac{\partial^2 c}{\partial x^2}$ is continuous with respect to x and t (for $t = 0$, continuity with respect to t holds from above only). Thus the solution c itself is continuous with respect to x and t too. We furthermore assume that it is bounded, that is, there exists a real $K \in \mathbb{R}$ such that $|c(x, t)| < K$ for all $x \in \Omega$, $t \geq 0$. Under certain conditions the existence and uniqueness of a solution to an RDS as

defined above results from standard theorems [32].

We call a monotonously increasing sequence $(t_j)_{j=1}^{\infty}$ of nonnegative real numbers tending towards infinity with

$$1 \leq t_{j+1} - t_j \leq Z, j \in \mathbb{N},$$

for some $Z \in \mathbb{R}_+$ a *sequence of points in time*. We call a vector

$$\hat{v} = \hat{v}(c, (t_l)_{l=1}^{\infty}) \equiv \lim_{j \rightarrow \infty} \frac{1}{t_{j+1} - t_j} \int_{t_j}^{t_{j+1}} \int_{x \in \Omega} v(c(x, t)) dx dt \in \mathbb{R}_+^m \quad (2.11)$$

constructed from a single solution c of an RDS by using the sequence $(t_j)_{j=1}^{\infty}$ of points in time a *total flux* with respect to c and $(t_j)_{j=1}^{\infty}$ if

$$N\hat{v} = 0. \quad (2.12)$$

Thus double-integration of a solution of an RDS connects the dynamics to a property of the underlying reaction network, namely the stoichiometric matrix. Note that the total flux is not necessarily a feasible flux for any subset of species. In the first part of this work we focus on the question of which of the components \hat{v}_j , $j = 1, \dots, m$, of the vector \hat{v} are strictly positive and which are equal to zero. Each of the components that is strictly positive represents a reaction that is active in the long-run of the solution c of the RDS. Thus, the components of \hat{v} with $\hat{v}_j > 0$ determine, which species must persist in the long-run to support the respective reactions r_j .

In [19] it was shown that if an ODE system approaches a fixed point, then the set of persistent species is an organization in the sense of COT. An organization is a subset $S \subseteq \mathcal{S}$ of species that is

1. closed, that is, none of the reactions supported by this subset of species produces a species that is not contained in this subset
2. and self-maintaining, that is, there is a feasible flux $\hat{v} \in \mathbb{R}_+^m$ such that $N \cdot \hat{v} \geq 0$.

We will introduce COT in more detail in the preliminaries section. Since we regard bounded solutions only, all the results of this work concerning the dynamics of RDSs hold for $N\hat{v} = 0$. Only in Section 2.5 and in Section 3.1.3 the inequality $N\hat{v} \geq 0$ is used.

In [72] we have generalized the fixed points result from [19] mentioned above. We have shown that whenever the solution of an ODE system approaches an arbitrary attractor that exhibits only one single subset of persistent species, this subset is an organization [72]. Such attractors might include periodic or even chaotic behavior. But we have also cited solutions of RDSs with other types of attractors, for example, heteroclinic orbits, that exhibit more than one subset of persistent species, which are distributed with respect to time [69]. We had proven that for such solutions the minimal subsets of persistent species are organizations, but we could not prove that statement for all subsets of persistent species or for their union [72].

In the first part of this work we generalize the techniques developed for ODE systems in [72] to RDSs with solutions exhibiting more than one subset of persistent species, especially systems with spatial extension and diffusion effects, that is, involving PDEs. We provide simulation results of RDSs exhibiting solutions c with total fluxes \hat{v} that are not feasible fluxes. Instead, reactions that would be active for a feasible flux are inactive. This is due to a temporal or spatial separation of the

persistent species among several subsets. We show that neither these subsets nor their union is necessarily an organization in the sense of classical COT. We therefore generalize the definition of organization towards distributed organizations (DOs) to capture the newly identified phenomenon of the persistent species being distributed. Note that, like organizations, DOs solely depend on the reaction network underlying the dynamical system. We finally arrive at two main results. First, given a reaction network, the set of DOs forms a lattice which hierarchically relates the DOs to one another. Second, for every solution of an RDS the set of persistent species is always a DO of the underlying reaction network. Whereas the first result provides information about the overall structure of a reaction network the second one characterizes the inner structure of the set of persistent species with regard to a single solution of an RDS. We show how connecting these two perspectives supports reaction network analysis. The overall situation is illustrated in Figure 1.1.

2.2 Coloring scheme for species involved in virus infection dynamics

The following coloring scheme for particular classes of species is introduced. It is used for the analysis of the virus infection dynamics models in the second part of the results.

- Uninfected (target) cells or those resistant/refractory to infection are marked in blue, e.g., T .
- Infected cells, partially or latently infected cells, and viruses are marked in magenta, e.g., I and V .
- Species belonging to the active immune response are marked in green. It is worth noting that the first two models analyzed in this paper [61, 5] do not explicitly have immune system components.
- Bacterial co-infection species are marked in orange. These species are only occurring in Smith's model [85].
- Text referring to any other species is marked in black, for example, transient target cell states, passive immune system, or dead cells.

2.3 Deriving the underlying reaction network from a dynamical system

The method presented here is in accordance with literature dealing with the relationship between reaction systems and differential equations [87, 26]. The in-host ODE model from Almcera [3] (see Figure 2.1) is used as a showcase to describe how from the ODEs or PDEs of a dynamical system the underlying reaction network is derived:

Each summand of each ODE (or PDE) is translated into a reaction as illustrated by the transition from Subfigures (a) to (b) in Figure 2.1. On the left-hand side of each reaction formula, there is a set of species, the so-called support of a reaction. The support of a reaction is the unique set of species that are needed to run the reaction. If only one of the species of the support of the reaction is missing then that reaction is not active. The term (of the ODE (or PDE)) that belongs to that reaction

must be zero if and only if the concentration of at least one of the species in the support of that reaction is zero. The number of the appearance of each species of a reaction on the right-hand side of a reaction is bigger or less than the number on the left-hand side depending on whether the regarding term has a positive or negative sign in the ODE (or PDE) of the regarding species.

As an example we consider the reaction R_3 . The corresponding summand is $c_V \mathbf{E} \mathbf{V}$. It is zero if and only if the concentration of at least one of \mathbf{E} or \mathbf{V} is zero. Thus the support of R_3 contains exactly the species \mathbf{E} and \mathbf{V} . On the left-hand side of the reaction equation of R_3 the species \mathbf{E} resp. \mathbf{V} appear only to the power of one because of the power of \mathbf{E} resp. \mathbf{V} is one in $c_V \mathbf{E} \mathbf{V}$. Since the summand $c_V \mathbf{E} \mathbf{V}$ appears only in the ODE of \mathbf{V} , namely with a negative sign, the right-hand side of the reaction equation of R_3 contains one less of \mathbf{V} than the left-hand side. The number of \mathbf{E} is equal on both sides of the reaction equation since the amount of \mathbf{E} is not affected by the reaction R_3 .

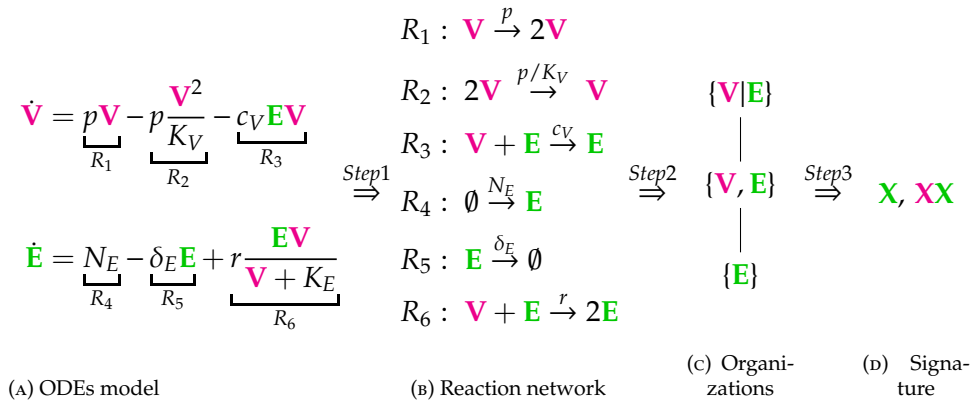


FIGURE 2.1: [73] The in-host part of the Almcocera Model

[3, 11] has two variables resp. ODEs (see Subfigure (A)): viruses (\mathbf{V}) and T-cells (\mathbf{E}).

This is the starting point of our method consisting of three steps briefly described below. Step 1: We derive from the ODE system a set of six reactions (see Subfigure (B)): R_1, \dots, R_6 . Step 2: We compute from the set of reactions the set of organizations (an organization is a subset of species with specific properties as described below in this Chapter): $\{\mathbf{V}, \mathbf{E}\}$ and $\{\mathbf{E}\}$. We arrange the organizations in a Hasse diagram (see Subfigure (C)), where organizations get bigger from bottom to top and are linked by a line, if the lower organization is a subset of the upper one. Step 3: We derive from the set of organizations the signature of the model (see Subfigure (D)). For our example, the signature is \mathbf{X}, \mathbf{XX} , where \mathbf{X} represents the organization $\{\mathbf{E}\}$ and \mathbf{XX} represents $\{\mathbf{V}, \mathbf{E}\}$.

2.4 Computing the organizations of a reaction network

COT is a branch of reaction network theory which deals with analyzing reaction networks to understand the behavior of dynamical systems. In recent decades many properties of reaction networks were proven to be useful for this purpose. The first steps in that direction were taken by Feinberg, Horn, and Jackson [27, 47]. They defined the terms *deficiency*, *balance*, and *reversibility* to draw conclusions about the steady states, their stability, and the persistence of species in dynamical systems.

Inspired by Fontana and Buss [31], abstract models of autopoiesis [93], autocatalytic set evolution [23, 53, 79], and artificial chemistries [8, 51], Dittrich and Speroni

di Fenizio [19] introduced COT in order to describe the time evolution of complex chemical systems undergoing qualitative transitions in their species compositions. Given a reaction network as a set of species and a set of reaction rules, COT identifies a hierarchy of closed and self-maintaining subsets of species, which are called organizations [19]. A chemical organization is derived from the rules of the reaction network [19] and thus is independent of kinetic details, such as rate constants. The COT approach allows for analyzing, understanding, and engineering complex, high-dimensional systems by decomposing them into a Hasse diagrams of interrelated organizations. This allows for tracking qualitative transitions as movements in the hierarchy of organizations [60, 65, 75]. Furthermore, there is a proven link to the long-term behavior, that is, all trajectories of a dynamical system converge to organizations [72, 56]. The approach can be applied in various domains where models can be formulated as reaction networks, such as atmospheric and combustion chemistry [15], evolutionary biology [46], systems biology [52], ecology [95], complex systems [44], computer science [67], and social sciences [20].

Now we state the basics of COT [29] by first introducing the closure of a subset of species and then defining organizations.

Definition 2.4.1 (Closure of a subset of species). *Given a reaction network $(\mathcal{S}, \mathcal{R})$ and a subset $S \subseteq \mathcal{S}$ of species, we define the set operation*

$$\text{clos}_1(S) \equiv S \cup \{s_i \in \mathcal{S} : \exists r_j \in \mathcal{R} : \text{supp}(r_j) \subseteq S, b_{ij} > 0\}, \quad (2.13)$$

that is, the set of species from S , together with all species, that are produced by the reactions, which are active on S . From this we define a monotonously increasing sequence of sets

$$\begin{aligned} \text{clos}_1^0(S) &= S, \\ \text{clos}_1^1(S) &= \text{clos}_1(S), \\ \text{clos}_1^2(S) &= \text{clos}_1(\text{clos}_1(S)), \\ \text{clos}_1^3(S) &= \text{clos}_1(\text{clos}_1(\text{clos}_1(S))), \\ &\dots \\ \text{clos}_1^{k_{\min}+1}(S) &= \text{clos}_1(\text{clos}_1^{k_{\min}}(S)), \end{aligned}$$

where $k_{\min} = \min\{k \in \mathbb{N}_0 : \text{clos}_1^{k+1}(S) = \text{clos}_1^k(S)\}$. Since the set of species and the set of reactions are finite, k_{\min} is finite and thus the closure of S is unique and finite. We call the set

$$\text{clos}(S) \equiv \text{clos}_1^{k_{\min}}(S) \quad (2.14)$$

the closure of S .

For every subset S of species, the closure $\text{clos}(S)$ of S does not contain the support of any reaction that produces a species which is not already contained in S . We call this property, to which the closure of any subset of species pertains, the *closedness property*. This and self-maintenance are the properties of an organization. We assume that the set \mathcal{S} of all species of a reaction network $(\mathcal{S}, \mathcal{R})$ is closed.

Definition 2.4.2 (Closedness, self-maintenance and organizations). *Given a reaction network $(\mathcal{S}, \mathcal{R})$ and a subset $S \subseteq \mathcal{S}$ of species we then call S*

1. *self-maintaining if there is a feasible flux v with respect to S such that*

$$Nv \geq 0, \quad (2.15)$$

that is, all elements of $N \cdot v$ are zero;

2. closed if

$$\text{clos}(S) = S; \quad (2.16)$$

3. an organization if it is self-maintaining and closed.

2.5 The signature of a reaction network

All organizations of a given reaction network can be arranged in a so-called Hasse diagram. For the In-host Almcocera example model the Hasse diagram is shown in Figure 2.1 (C). From the bottom to the top the organizations have increasing size, indicating an increasing number of species. A line is drawn between two organizations if and only if one is a subset of the other and there is no organization between them. Thus, there is a line between the organizations $\{\mathbf{E}\}$ and $\{\mathbf{V}, \mathbf{E}\}$.

We derive from the set of organizations the **signature** of the model (see Figure 2.1 (D)). For our example, the signature is \mathbf{X}, \mathbf{XX} , where \mathbf{X} represents the organization $\{\mathbf{E}\}$ and \mathbf{XX} represents $\{\mathbf{V}, \mathbf{E}\}$.

The signature tells us via colored Xs (see Section 2.2), which of the types of species are contained in the organizations of the model. We maintain this coloring throughout this work. Note that we use underlining $\underline{\mathbf{X}}$ to tag host-to-host species in contrast to in-host species.

One should understand the following aspects concerning the method presented above:

The long-term behavior of simulations of the dynamics of the model can be easily estimated from the signature: We know from [72] that there is always an organization representing the species persisting in the long-run. Thus species that are not contained in any organization will go extinct for sure after a sufficiently long time period. On the other hand, species that are contained in all organizations of a model, will persist in the long-run for sure. If a species is contained in some organizations of a model but not in all, it has the potential to persist but also to go extinct. It depends on the applied kinetic laws, the initial conditions, and the reaction constants, which case occurs.

A hierarchy of a set of models can be constructed relying on their signatures. Like the set of organizations of one model, it can again be visualized as a Hasse diagram. The more combinations of colors a signature contains, the higher is its position in the Hasse diagram and the bigger is the variety of its potential dynamical behavior. If all combinations of colors of one signature are present in a second signature, then the models can be linked by a line. Kinetic laws: Note that except for reaction R_6 , where Michaelis–Menten kinetics are applied, all the other reactions of this example follow mass-action kinetics. The technique of computing and analyzing chemical organizations used in this work applies to both these kinetic laws.

Distributed organizations: When the species \mathbf{V} and \mathbf{E} are separated (we say “distributed”), the reaction R_3 is inactive. Then, due to the remaining for reactions, the set $\{\mathbf{V}, \mathbf{E}\}$ is still self-maintaining and closed and thus some kind of an organization. We write $\{\mathbf{V}|\mathbf{E}\}$ (instead of $\{\mathbf{V}, \mathbf{E}\}$) to denote this and call $\{\mathbf{V}|\mathbf{E}\}$ a “distributed organization.”

2.6 Persistence

Persistence comprises various ideas from different fields, for example ecology, chemistry, and biology. It is applied to a huge multitude of different model types like for example, discrete and continuous models, ODE and PDE models, deterministic or stochastic models, models with and without a spatial dimension, and so on. As for all these types of models, for the RDSs discussed in this work there are a number of different terms related to persistence, such as permanence [45, 69, 18, 12], coexistence [43, 69], extinction [2, 43], strong persistence [2], uniform persistence [43], etc. For an overview of these concepts we refer the reader to [45, 2]. There are many aspects of persistence regarding dynamical systems. For example, persistence can be analyzed with regard to a single species or a whole system of species. Also, persistence concerning a single solution and all possible solutions of an RDS arising from different initial conditions or reaction constants can be distinguished. Furthermore, there are different grades of persistence, e.g., weak or strong persistence. In this work we are concerned with subsets of persistent species in regard to a single solution of an RDS and link it with the persistence of all solutions of any RDS that has the same underlying reaction network.

Chapter 3

Results

3.1 Linking network structure and dynamics to describe the set of persistent species in reaction diffusion systems

This section is organized as follows. We first state the concept of persistence this work relies on. Then we compare this concept to two other concepts of persistence, one stronger and one weaker than ours. Then we define distributed organizations (DOs) and prove that they always form a lattice as one of the two main results of this work. We discuss the role of closed subsets of species in the dynamics. Subsequently, as the second main result, we prove that the set of persistent species with respect to a solution of a RDS is always a DO of the underlying reaction network. Then we show how to apply the fore-mentioned results to analyze DO lattices and to draw conclusions about the long-term behavior of RDS. Then we state some remarks on how to compare several DO lattices and how to put them into hierarchies. Finally, we present three example simulation results and discuss them with respect to our theoretical results.

3.1.1 Persistence

In this subsection we present the concept of persistence on which this study relies. For this purpose we first define two kinds of neighborhoods, which are special subsets of the state space of concentration vectors. We also define a frequency of occurrence for any subset of the state space and, based on that, we introduce persistent subsets of species. From the persistence of a subset of species we derive the persistence of a species, which we analyze further and compare to other grades of persistence based on the limits superior and the limits inferior of the concentration values of that species. In this subsection, we assume that the solution $c_i(x, t)$ of an RDS introduced in Section 2.1 is nonnegative for all $t > 0$, $x \in \Omega$, $s_i \in \mathcal{S}$. We will prove this in Section 3.1.4.

Definition 3.1.1 (Neighborhood of a subset of species in the space of concentrations). *Given a subset $S \subseteq \mathcal{S}$ of species and real numbers $\varepsilon, \delta > 0$, we call the set*

$$S^{\varepsilon, \delta} \equiv \{c \in \mathbb{R}_+^n : c_s \begin{cases} > \varepsilon & \text{iff } s \in S \\ \leq \delta & \text{iff } s \notin S \end{cases}\} \subseteq \mathbb{R}_{\geq 0}^n \quad (3.1)$$

of concentration vectors the (ε, δ) -neighborhood of S , and for $\delta = \infty$ we call the set

$$S^\varepsilon \equiv S^{\varepsilon, \infty} \equiv \{c \in \mathbb{R}_+^n : c_s > \varepsilon \text{ iff } s \in S\} \subseteq \mathbb{R}_{\geq 0}^n \quad (3.2)$$

of concentration vectors the ε -neighborhood of S .

There are lower and upper boundaries for the flux vector function values $v(c)$ depending on whether or not c is in some special ε -neighborhoods. The following remark provides these boundaries, which we need to prove the results of this work.

Remark 3.1.1 (Boundaries of the fluxes). *Given an RDS with underlying reaction network $(\mathcal{S}, \mathcal{R})$, a reaction $r_j \in \mathcal{R}$ for a $j \in \{1, \dots, m\}$, and a subset $S \subseteq \mathcal{S}$ of species, the following hold:*

- *If $\text{supp}(r_j) \subseteq S$ then for all $\varepsilon > 0$ there is a lower boundary $L(\varepsilon) > 0$ for the flux vectors $v_j(c)$ such that*

$$0 < L(\varepsilon) < v_j(c) \quad (3.3)$$

for all $c \in S^\varepsilon$.

- *If $\text{supp}(r_j) \not\subseteq S$ then for all $\varepsilon > 0$ there is an upper boundary $U(\varepsilon) > 0$ for the flux vectors $v_j(c)$ such that*

$$0 \leq v_j(c) \leq U(\varepsilon) \Leftrightarrow c \notin \text{support}(r_j)^\varepsilon \quad (3.4)$$

and $\lim_{\varepsilon \rightarrow 0} U(\varepsilon) = 0$.

Proof. The proof follows from the definition of the flux vector function $v()$ in the introduction, that is, its continuity and feasibility property, and from the definitions of neighborhoods in Definition 3.1.1. \square

Remark 3.1.2 (Disjoint decomposition of ε -neighborhoods). *Given a reaction network $(\mathcal{S}, \mathcal{R})$, a subset $\tilde{S} \subseteq \mathcal{S}$ of species, and real numbers $\varepsilon, \delta > 0$. Then the ε -environment \tilde{S}^ε of \tilde{S} is a disjoint union of (ε, δ) -environments $S^{\varepsilon, \delta}$ of all subsets $S \subseteq \mathcal{S}$ of species with $\tilde{S} \subseteq S$. That is,*

$$\tilde{S}^\varepsilon = \bigsqcup_{\tilde{S} \subseteq S} S^{\varepsilon, \delta}. \quad (3.5)$$

This holds true especially for $\varepsilon = \delta$.

This is illustrated in Figure 3.1. Definition 3.1.2 is a pre-stage to persistence and shows the strong relation to the construction of the vector \hat{v} sketched in Equation 2.11.

Definition 3.1.2 (Frequency of occurrence of concentration vectors). *Given a solution c of an RDS, a subset $C \subseteq \mathbb{R}_+^n$ of the set of concentration vectors, and a sequence $(t_j)_{j=1}^\infty$ of points in time, we call the nonnegative number*

$$F(C; c, (t_j)_{j=1}^\infty) \equiv \limsup_{l \rightarrow \infty} \frac{1}{t_{j+1} - t_j} \int_{t_j}^{t_{j+1}} \int_{\{x \in \Omega: c(x, t) \in C\}} dx dt \quad (3.6)$$

the frequency of occurrence of C (with respect to c and $(t_j)_{j=1}^\infty$) and write for short $F(C)$ if it is clear to which solution c and which sequence $(t_j)_{j=1}^\infty$ it relates.

Now we state the main definition of persistence regarding a single solution c of an RDS.

Definition 3.1.3 (Persistent subsets of species and persistent species). *Given a solution c of an RDS with an underlying reaction network $(\mathcal{S}, \mathcal{R})$, we call a subset $S \subseteq \mathcal{S}$ of species persistent (with respect to c) if for all sequences $(t_j)_{j=1}^\infty$ of points in time there is an $\varepsilon > 0$*

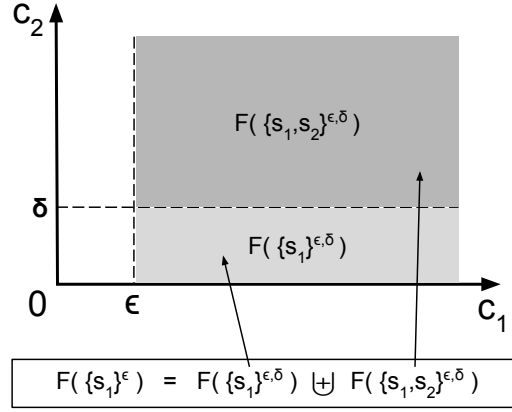


FIGURE 3.1: [76] Illustration of Remark 3.1.2 for an example with two species s_1 and s_2 . The ϵ -environment of $\{s_1\}$ is a disjoint union of the (ϵ, δ) -environments of $\{s_1\}$ and $\{s_1, s_2\}$.

such that for all $\delta > 0$ the frequency of occurrence $F(S^{\epsilon, \delta})$ of $S^{\epsilon, \delta}$ with respect to c and $(t_j)_{j=1}^\infty$ is strictly positive, that is,

$$F(S^{\epsilon, \delta}) = \limsup_{j \rightarrow \infty} \frac{1}{t_{j+1} - t_j} \int_{t_j}^{t_{j+1}} \int_{\{x \in \Omega: c(x, t) \in S^{\epsilon, \delta}\}} dx dt > 0. \quad (3.7)$$

We denote the set of persistent subsets of species $P(c)$, i.e.,

$$P(c) \equiv \{S \subseteq \mathcal{S} : S \text{ is persistent with respect to } c\}. \quad (3.8)$$

We call a single species $s \in \mathcal{S}$ persistent (with respect to c) if s is contained in at least one of the persistent subsets of species, i.e.,

$$s \in \cup \{S \subseteq \mathcal{S} : S \in P(c)\}. \quad (3.9)$$

We say that a species $s \in \mathcal{S}$ goes extinct (with respect to c) if it is not persistent with respect to c . We denote the set of persistent species $\Phi(c)$, i.e.,

$$\Phi(c) \equiv \{s \in \mathcal{S} : s \text{ is persistent with respect to } c\} = \cup \{S \subseteq \mathcal{S} : S \in P(c)\}. \quad (3.10)$$

See Figure 3.2 for an illustration of the concept of persistence introduced above. It is important to note that Definition 3.1.3 draws a clear distinction between the species within a persistent set S and those outside of S . More precisely, a strictly positive frequency of occurrence of S not only demands the co-occurrence of the species from S but also the simultaneous disappearance of the species that are not elements of S . Our second simulation example in Section 3.1.9 illustrates this clearly, since there we have an RDS with solution c with a set $P(c) = \{\{s_1\}, \{s_2\}, \{s_3\}, \{s_1, s_2\}, \{s_1, s_3\}, \{s_2, s_3\}\}$ of persistent subsets of species. But the set $\mathcal{S} = \{s_1, s_2, s_3\}$ of all species is not persistent even though it contains persistent species.

Whereas in Definition 3.1.3 we derived the persistence of a single species from the persistence of subsets of species, in Lemma 3.1.1 we provide an immediate criterion for the persistence of a single species.

Lemma 3.1.1 (ϵ -neighborhood criterion for persistent species). *Given a solution c of a RDS with an underlying reaction network $(\mathcal{S}, \mathcal{R})$, a species $s_i \in \mathcal{S}$ is persistent with respect*

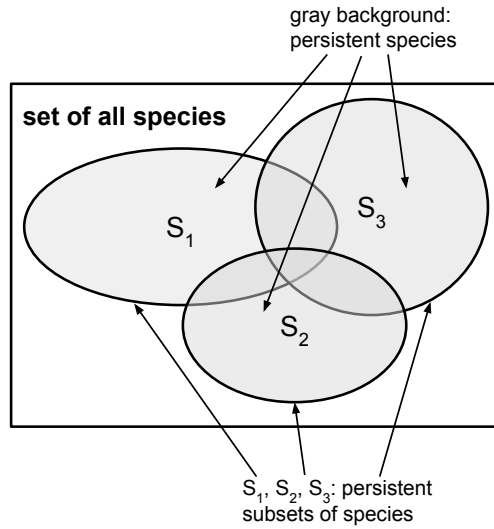


FIGURE 3.2: [76] Overview of the terms regarding persistence as defined and used in this work.

to c , that is,

$$s_i \in \Phi(c) = \cup_{S \in P(c)} S \quad (3.11)$$

if and only if for all sufficiently small $\varepsilon > 0$ and every sequence $(t_j)_{j=1}^{\infty}$ of points in time the frequency $F(\{s_i\}^{\varepsilon})$ of occurrence of $\{s_i\}^{\varepsilon}$ is strictly positive, that is,

$$F(\{s_i\}^{\varepsilon}) \equiv \limsup_{l \rightarrow \infty} \frac{1}{t_{l+1} - t_l} \int_{t_l}^{t_{l+1}} \int_{\{x \in \Omega: c_i(x,t) > \varepsilon\}} dx dt > 0. \quad (3.12)$$

Proof. 1. First we prove that Equation 3.12 follows from $s_i \in \Phi(c)$. Thus, we assume, that s_i is persistent, that is, there is a persistent subset $S \in P(c)$ with $s_i \in S$. Then for all sequences $(t_j)_{j=1}^{\infty}$ of points in time there is an $\varepsilon > 0$ such that for all $\delta > 0$,

$$F(S^{\varepsilon, \delta}) = \limsup_{j \rightarrow \infty} \frac{1}{t_{j+1} - t_j} \int_{t_j}^{t_{j+1}} \int_{\{x \in \Omega: c(x,t) \in S^{\varepsilon, \delta}\}} dx dt > 0, \quad (3.13)$$

and so

$$\begin{aligned} 0 &< F(S^{\varepsilon, \delta}) \\ &= \limsup_{j \rightarrow \infty} \frac{1}{t_{j+1} - t_j} \int_{t_j}^{t_{j+1}} \int_{\{x \in \Omega: c(x,t) \in S^{\varepsilon, \delta}\}} dx dt \\ &\leq \limsup_{j \rightarrow \infty} \frac{1}{t_{j+1} - t_j} \int_{t_j}^{t_{j+1}} \int_{\{x \in \Omega: c(x,t) \in S^{\varepsilon}\}} dx dt \\ &\leq \limsup_{j \rightarrow \infty} \frac{1}{t_{j+1} - t_j} \int_{t_j}^{t_{j+1}} \int_{\{x \in \Omega: c(x,t) \in \{s_i\}^{\varepsilon}\}} dx dt \\ &= \limsup_{j \rightarrow \infty} \frac{1}{t_{j+1} - t_j} \int_{t_j}^{t_{j+1}} \int_{\{x \in \Omega: c(x,t) > \varepsilon\}} dx dt. \end{aligned} \quad (3.14)$$

From Definition 3.1.2 it follows that $F(\{s_i\}^\varepsilon) > 0$ for all sufficiently small $\varepsilon > 0$.

2. Now we prove the other direction, that is, we assume that there is an $\varepsilon > 0$ such that for every sequence $(t_j)_{j=1}^\infty$ of points in time, Equation 3.12 holds true. So for all $\delta > 0$,

$$\begin{aligned} 0 &< F(\{s_i\}^\varepsilon) \\ &\stackrel{\text{Remark 3.1.2}}{=} F\left(\bigcup_{s_i \in \mathcal{S}} S^{\varepsilon, \delta}\right) \\ &= \sum_{s_i \in \mathcal{S}} F(S^{\varepsilon, \delta}). \end{aligned} \quad (3.15)$$

Since the sum is finite, there is a subset $S \subseteq \mathcal{S}$ of species with $F(S^{\varepsilon, \delta}) > 0$ and $s_i \in S$. Thus S is persistent, and the proof is completed. \square

In the supplementary material we provide Lemma 3.1.3 and Lemma 3.1.2. The latter is necessary to prove the former, and Lemma 3.1.1 is needed for the proofs of both. Both Lemma 3.1.3 and Lemma 3.1.2 are not necessary to prove the main results of this work. But Lemma 3.1.3 helps in assessing our concept of persistence of a species as defined in Definition 3.1.3 by comparing it to two other types of persistence which can be derived from the concentration values of a species as well. Briefly, Lemma 3.1.3 states that for a given solution c of an RDS with an underlying reaction network $(\mathcal{S}, \mathcal{R})$ and an arbitrary species $s_i \in \mathcal{S}$, the following two conclusions hold:

$$\liminf_{t \rightarrow \infty} \int_{x \in \Omega} c_i(x, t) dx > 0 \Rightarrow s_i \text{ is persistent w.r.t. } c \Rightarrow \limsup_{t \rightarrow \infty} \int_{x \in \Omega} c_i(x, t) dx > 0. \quad (3.16)$$

This shows that our concept of persistence can be regarded as a refinement of other definitions of persistence. Mincheva and Siegel [62], by using so-called Volpert indices, proved for an RDS with mass-action kinetics the nonnegativity of all concentrations of all species for all finite times. They also proved the positiveness of the concentration of all reachable species. The set of reachable species is what is called closure in COT. The Volpert indices correspond to the indices k in the notation of the sets $\text{clos}_1^k(S)$, $i \in \mathbb{N}$, that we used in Definition 2.4.1 of this work. In Section 3.1.4 of this study we prove for more general kinetics that the set of species existent at a location of the domain at an arbitrary time immediately produces its closure. Furthermore, we complement the results from [62] in Section 3.1.5 by identifying those subsets of species, that persist for time approaching infinity. We show that they are special substructures of the underlying reaction networks of the RDS which we call DOs and define in Section 3.1.3. Note, that if the reaction network is not given, one can derive it from the RDS or the ODE system. This is exemplified in Section 2.3, Figure 2.1. More details about the relation between differential equations and their underlying reaction networks can be found in [87, 26].

3.1.2 Comparison of different concepts of persistence

Here we present two lemmas mentioned in Section 2.6. Lemma 3.1.3, already sketched in Equation 3.16, provides a comparison of our concept of persistence to a stronger and a weaker one. Lemma 3.1.2 is used to prove Lemma 3.1.3.

Lemma 3.1.2 (Equivalence criterion for the persistence of a species). *Given a solution c of a RDS with an underlying reaction network $(\mathcal{S}, \mathcal{R})$. A species $s_i \in \mathcal{S}$ with respect to c is persistent if and only if for all sequences $(t_j)_{j=1}^{\infty}$ of points in time*

$$\limsup_{j \rightarrow \infty} \frac{1}{t_{j+1} - t_j} \int_{t_j}^{t_{j+1}} \int_{x \in \Omega} c_i(x, t) dx dt > 0. \quad (3.17)$$

Proof. 1. First we assume that s_i is persistent with respect to c . From Lemma 3.1.1 follows that there is an $\varepsilon > 0$ such that $F(\{s_i\}^\varepsilon) > 0$ with respect to c and to all sequences $(t_j)_{j=1}^{\infty}$ of points in time. Thus,

$$\begin{aligned} & \limsup_{j \rightarrow \infty} \frac{1}{t_{j+1} - t_j} \int_{t_j}^{t_{j+1}} \int_{x \in \Omega} c_i(x, t) dx dt \\ & \geq \limsup_{j \rightarrow \infty} \frac{1}{t_{j+1} - t_j} \int_{t_j}^{t_{j+1}} \int_{x \in \Omega: c_i(x, t) > \varepsilon} \varepsilon dx dt \\ & = \varepsilon \cdot F(\{s_i\}^\varepsilon) \\ & > 0. \end{aligned}$$

2. Now we prove the other direction by contradiction. We assume, that Equation 3.17 holds true for all sequences $(t_j)_{j=1}^{\infty}$ of points in time and that s_i is not persistent with respect to c , that is (following Lemma 3.1.1), $F(\{s_i\}^\varepsilon) = 0$ for all sufficiently small $\varepsilon > 0$ and all sequences $(t_j)_{j=1}^{\infty}$ of points in time. Thus, for all sufficiently small $\varepsilon > 0$ holds

$$\begin{aligned} 0 & < \limsup_{j \rightarrow \infty} \frac{1}{t_{j+1} - t_j} \int_{t_j}^{t_{j+1}} \int_{x \in \Omega} c_i(x, t) dx dt \\ & = \limsup_{j \rightarrow \infty} \frac{1}{t_{j+1} - t_j} \int_{t_j}^{t_{j+1}} \left[\int_{x \in \Omega: c_i(x, t) \leq \varepsilon} c_i(x, t) dx \right. \\ & \quad \left. + \int_{x \in \Omega: c_i(x, t) > \varepsilon} c_i(x, t) dx \right] dt \\ & \leq \limsup_{j \rightarrow \infty} \frac{1}{t_{j+1} - t_j} \int_{t_j}^{t_{j+1}} \left[\varepsilon \cdot |\Omega| + K \int_{x \in \Omega: c_i(x, t) > \varepsilon} dx \right] dt \\ & = \varepsilon \cdot |\Omega| + K \cdot F(\{s_i\}^\varepsilon) \\ & = \varepsilon \cdot |\Omega| \\ & \xrightarrow{\varepsilon \rightarrow 0} 0, \end{aligned}$$

where $K \in \mathbb{R}_+$ is an upper boundary for $c_i(x, t)$, $x \in \Omega$, $t \geq 0$. This is a contradiction and thus the proof is completed. \square

Next we state the promised lemma ranking different grades of persistence of a species including the definition used in this work (see Definition 3.1.3).

Lemma 3.1.3 (Comparison of different grades of persistence). *Given a solution c of a RDS with an underlying reaction network $(\mathcal{S}, \mathcal{R})$ and an arbitrary species $s_i \in \mathcal{S}$. Then the following two conclusions hold true:*

$$1. \liminf_{t \rightarrow \infty} \int_{x \in \Omega} c_i(x, t) dx > 0 \quad \Rightarrow \quad s_i \text{ is persistent with respect to } c.$$

2. s_i is persistent with respect to c , $\Rightarrow \limsup_{t \rightarrow \infty} \int_{x \in \Omega} c_i(x, t) dx > 0$.

Proof. 1. We assume

$$\liminf_{t \rightarrow \infty} \int_{x \in \Omega} c_i(x, t) dx > 0. \quad (3.18)$$

So there is a time $T > 0$ such that

$$\int_{x \in \Omega} c_i(x, t) dx > \varepsilon. \quad (3.19)$$

for all $t > T$ and all sufficiently small $\varepsilon > 0$. Thus, for every sequence $(t_j)_{j=1}^{\infty}$ of points in time there is a natural number j_0 such that for all $j > j_0$ and all sufficiently small $\varepsilon > 0$

$$\frac{1}{t_{j+1} - t_j} \int_{t_j}^{t_{j+1}} \int_{x \in \Omega} c_i(x, t) dx dt > \frac{t_{j+1} - t_j}{t_{j+1} - t_j} \varepsilon = \varepsilon > 0. \quad (3.20)$$

With Lemma 3.1.1 we deduce that s_i is persistent.

2. We prove the equivalent statement that from

$$\limsup_{t \rightarrow \infty} \int_{x \in \Omega} c_i(x, t) dx = 0. \quad (3.21)$$

follows that s_i is not persistent. Thus we assume that Equation 3.21 holds true. Then for all $\delta_1 > 0$ there is a $T(\delta_1) > 0$ such that

$$\int_{x \in \Omega} c_s(x, t) dx < \delta_1 \quad (3.22)$$

for all $t > T(\delta_1)$. Then for all $\varepsilon > 0$

$$\int_{\{x \in \Omega: c_i(x, t) > \varepsilon\}} dx \xrightarrow{t \rightarrow \infty} 0. \quad (3.23)$$

We deduce that for all $\delta_2, \varepsilon > 0$ there is a $T(\delta_2, \varepsilon) > 0$ such that

$$\int_{\{x \in \Omega: c_i(x, t) > \varepsilon\}} dx < \delta_2 \quad (3.24)$$

for all $t > T(\delta_2, \varepsilon)$. Thus for all sequences $(t_j)_{j=1}^{\infty}$ of points in time and all $\delta_2, \varepsilon > 0$ there is a natural number $j(\delta_2, \varepsilon)$ such that

$$\int_{t_j}^{t_{j+1}} \int_{\{x \in \Omega: c_i(x, t) > \varepsilon\}} dx dt < (t_{j+1} - t_j) \delta_2 \quad (3.25)$$

for all $j > j(\delta_2, \varepsilon)$. Thus for all sequences $(t_j)_{j=1}^{\infty}$ of points in time

$$\limsup_{j \rightarrow \infty} \frac{1}{t_{j+1} - t_j} \int_{t_j}^{t_{j+1}} \int_{\{x \in \Omega: c_i(x, t) > \varepsilon\}} dx dt < \frac{t_{j+1} - t_j}{t_{j+1} - t_j} \delta_2 \quad (3.26)$$

for all $\delta_2, \varepsilon > 0$. By letting $\delta_2 \rightarrow 0$ we conclude

$$F(\{s_i\}^\varepsilon) = 0 \quad (3.27)$$

for all $\varepsilon > 0$, that is, s_i is not persistent. □

3.1.3 Distributed Organizations

In this subsection we first define DOs as a generalization of organizations and then compare these two terms. After proving that computing DOs is NP-hard, we prove that the set of all DOs of a reaction network forms a lattice.

A DO consists of one or more subsets of species that are each closed and together obey a generalized kind of self-maintenance. We now present a precise definition.

Definition 3.1.4 (Distributed organizations (DOs)). *Given a reaction network $(\mathcal{S}, \mathcal{R})$, a subset $D \subseteq \mathcal{S}$ is a DO if and only if there are $k, k \in \mathbb{N}$, different subsets $S_1, \dots, S_k \subseteq D$ with*

$$D = \cup_{i=1}^k S_i \quad (3.28)$$

such that

1. all $S_i, i = 1, \dots, k$, are closed;
2. there is a vector $\hat{v} \in \mathbb{R}_+^m, \hat{v} \geq 0$, such that

$$N\hat{v} \geq 0; \quad (3.29)$$

3. and there is a feasible flux $\hat{v}^i \in \mathbb{R}_+^m, \hat{v}^i \geq 0$, with respect to each subset $S_i, i = 1, \dots, k$, with

$$\hat{v} = \sum_{i=1}^k \hat{v}^i. \quad (3.30)$$

Collectively, we call the second and third items of the list above the self-maintenance property of a DO. We say "D is distributed to the S_i " or "the S_i are a distribution of D". When listing the elements of the subsets $S_i, i = 1, \dots, k$, of species, we use a special notation, for example, if D is distributed to $S_1 = \{s_1, s_2\}$ and $S_2 = \{s_1, s_3\}$, we write

$$D = S_1 \cup S_2 = \{s_1 s_2 | s_1 s_3\}. \quad (3.31)$$

Note that a species can be contained in several subsets $S_i, i = 1, \dots, k$, of a DO, and a DO can be empty. The next lemma elucidates the relation between organizations and DOs. The situation is illustrated in Figure 3.3.

Lemma 3.1.4 (Relation of organizations and DOs).

1. Every organization of a reaction network $(\mathcal{S}, \mathcal{R})$ is a DO of that reaction network.
2. Every DO of a reaction network $(\mathcal{S}, \mathcal{R})$ that has a distribution to a single subset that is $k = 1$ in Definition 3.1.4 is an organization.
3. There exist reaction networks that exhibit DOs that are not organizations.

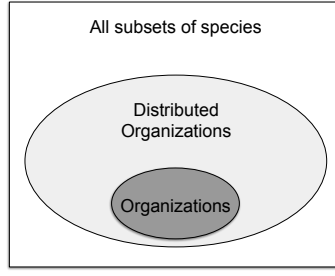


FIGURE 3.3: [76] Illustration of the relation between organizations and distributed organizations.

- Proof.*
1. Let O be an organization of a reaction network $(\mathcal{S}, \mathcal{R})$. Then O is a DO that is distributed to a single subset $S_1 = O$, since O is closed and, furthermore, self-maintaining both, in the way organizations are self-maintaining and in the way DOs are self-maintaining.
 2. This follows from the previous item.
 3. Let $\mathcal{S} \equiv \{s_1, s_2\}$ and $\mathcal{R} \equiv \{r_1 : s_1 + s_2 \rightarrow \emptyset\}$ be the set of species (resp., reactions) of the reaction network $(\mathcal{S}, \mathcal{R})$. Then $D \equiv \{s_1|s_2\}$ is a DO but not an organization. \square

Remark 3.1.3 (DOs not being organizations). *Assume a DO $D = \{S_1|S_2|\dots|S_k\}$ with $\hat{v} = \sum_{i=1}^k \hat{v}^i$ such that $N\hat{v} = 0$ and $\hat{v}^i, i = 1, \dots, k$, are feasible fluxes with respect to the subsets $S_i, i = 1, \dots, k$.*

If $\cup_{i=1}^k S_i$ is closed and self-maintaining, then D is an organization. This is especially the case if there is no reaction $r_j \in \mathcal{R}$ with $\text{supp}(r_j) \subseteq \cup_{i=1}^k S_i$ but $\text{supp}(r_j) \not\subseteq S_i$ for all $i = 1, \dots, k$, since in this case \hat{v} from above is a feasible flux with respect to $\cup_{i=1}^k S_i$ and $\cup_{i=1}^k S_i$ is closed because all the $S_i, i = 1, \dots, k$, are closed.

On the other hand, if there is a reaction $r_j \in \mathcal{R}$ with $\text{supp}(r_j) \subseteq \cup_{i=1}^k S_i$ but $\text{supp}(r_j) \not\subseteq S_i$ for all $i = 1, \dots, k$, then \hat{v} is not a feasible flux with respect to $\cup_{i=1}^k S_i$ since $\hat{v}_j = 0$. Such a reaction can

1. produce new species that are not contained in $\cup_{i=1}^k S_i$, and then $\cup_{i=1}^k S_i$ is not closed;
2. prevent $\cup_{i=1}^k S_i$ from being self-maintaining; or
3. do both.

In any of the cases 1–3 $\cup_{i=1}^k S_i$ is not an organization.

Corollary 3.1.1 (Complexity of the computation of DOs). *The computation of DOs is NP-hard.*

Proof. In [15] it was proven that deciding whether a given reaction network contains a reactive organization is NP-complete and thus that computing organizations is NP-hard. This was done by constructing a reaction network containing an organization such that finding that organization is equivalent to the 3-SAT problem. Since we know from Lemma 3.1.4 that every organization is a DO, the proof from [15] works for DOs too. \square

For more information about the complexity of relevant subsets of species in a reaction network the reader is referred to [98]. The next lemma is the first part of a sequence of statements culminating in a theorem about the lattice property of the set of DOs of a given reaction network.

Lemma 3.1.5 (Existence of a unique smallest organization). *For every reaction network $(\mathcal{S}, \mathcal{R})$ there is a unique smallest DO O_{min} , which is an organization. That is, O_{min} is a subset of any other DO of that reaction network. For any DO $D = \{S_1 | \dots | S_k\}$, O_{min} is even a subset of all S_i . Note, that O_{min} might be empty.*

Proof. We define

$$O_{min} \equiv \text{clos}(\emptyset); \quad (3.32)$$

then O_{min} is closed. Furthermore, since O_{min} is produced from the empty set \emptyset , it is a subset of all S_i , $i = 1, \dots, k$, for any DO $D = \{S_1 | \dots | S_k\}$. Thus, to prove that O_{min} is an organization, it remains to prove, that there is a feasible flux $\hat{v} \in \mathbb{R}_+^m$ with respect to O_{min} with $N\hat{v} \geq 0$. With $k_{min} \in \mathbb{N}_0$ from Definition 2.4.1, we define the vector $\hat{v}^{k_{min}} \in \mathbb{R}_+^m$ by

$$\hat{v}_j^{k_{min}} \begin{cases} = 1, & \text{iff } \text{supp}(r_j) \cap \text{clos}_1^{k_{min}}(\emptyset) \neq \emptyset, \\ = \lambda_{k_{min}, j}, & \text{iff } \text{supp}(r_j) \subseteq \text{clos}_1^{k_{min}-1}(\emptyset) \text{ and} \\ & a_{ij} = 0, b_{ij} > 0 \text{ for a species } s_i \in \text{clos}_1^{k_{min}} \setminus \text{clos}_1^{k_{min}-1} \\ = 0, & \text{otherwise,} \end{cases} \quad (3.33)$$

for $j = 1, \dots, m$, and by strictly positive real numbers $\lambda_{k_{min}, j}$, such that

$$(N\hat{v}^{k_{min}})_i \geq 0 \forall s_i \in \text{clos}_1^{k_{min}}(\emptyset) \setminus \text{clos}_1^{k_{min}-1}(\emptyset). \quad (3.34)$$

Then for k from $k_{min} - 1$ stepwise decreasing by 1 to $k = 1$, we construct the vectors $\hat{v}^k \equiv \hat{v}^{k+1} + \Delta\hat{v}^k \in \mathbb{R}_+^m$ by adding to \hat{v}^k the vector $\Delta\hat{v}^k$ defined by

$$\Delta\hat{v}_j^k = \begin{cases} 1, & \text{iff } \text{supp}(r_j) \subseteq \text{clos}_1^k(\emptyset) \text{ and} \\ & a_{ij} > 0 \text{ for all species } s_i \in \text{clos}_1^k \setminus \text{clos}_1^{k-1} \\ \lambda_{k, j}, & \text{iff } \text{supp}(r_j) \subseteq \text{clos}_1^{k-1}(\emptyset) \text{ and} \\ & a_{ij} = 0, b_{ij} > 0 \text{ for a species } s_i \in \text{clos}_1^k \setminus \text{clos}_1^{k-1} \\ 0, & \text{otherwise,} \end{cases} \quad (3.35)$$

for $j = 1, \dots, m$, and by strictly positive real numbers $\lambda_{k, j}$, such that

$$(N\hat{v}^k)_i \geq 0 \forall s_i \in \text{clos}_1^k(\emptyset) \setminus \text{clos}_1^{k-1}(\emptyset) \quad (3.36)$$

and so

$$(N\hat{v}^k)_i \geq 0 \forall s_i \in \text{clos}_1^{k_{min}}(\emptyset) \setminus \text{clos}_1^{k-1}(\emptyset). \quad (3.37)$$

Finally, by defining $\hat{v} \equiv \hat{v}^1$ we obtain a feasible flux with respect to $\text{clos}(\emptyset)$ such that

$$(N\hat{v}^k)_i \geq 0 \forall s_i \in \text{clos}(\emptyset), \quad (3.38)$$

that is, O_{min} is self-maintaining and thus an organization. \square

Note that this subsection and Section 2.5 are the only parts of this section where it is necessary to define self-maintenance of organizations and DOs by the inequality $N\hat{v} \geq 0$ instead of the equation $N\hat{v} = 0$. The rest of this section indeed still holds true if the inequality $N\hat{v} \geq 0$ in the definitions of organizations and DOs is replaced by the equation $N\hat{v} = 0$. Thus, all results of this section dealing with organizations or DOs with regard to the dynamics of RDSs are, strictly speaking, not formulated in their strongest possible forms.

Lemma 3.1.6 (Union of DOs). *Given a reaction network $(\mathcal{S}, \mathcal{R})$ and two DOs $D_1, D_2 \in \mathcal{S}$, the union $D_1 \cup D_2$ is also a DO.*

Proof. Let $D_1 = \{S_1 | \dots | S_k\}$ and $D_2 = \{T_1 | \dots | T_l\}$ be DOs with closed subsets $S_i, T_j \subseteq D_1, i = 1, \dots, k, j = 1, \dots, l$, of species and let their feasible fluxes be $\hat{v}^i, \hat{v}^j, i = 1, \dots, k, j = 1, \dots, l$, such that $N \sum_{i=1}^k \hat{v}^i = 0$ and $N \sum_{j=1}^l \hat{v}^j = 0$.

Then $D \equiv D_1 \cup D_2$ with the distribution $D \equiv \{S_1 | \dots | S_k | T_1 | \dots | T_l\}, i = 1, \dots, k, j = 1, \dots, l$, is a DO, since $N(\sum_{i=1}^k \hat{v}^i + \sum_{j=1}^l \hat{v}^j) = N \sum_{i=1}^k \hat{v}^i + N \sum_{j=1}^l \hat{v}^j = 0$. \square

Note that the union of two DOs as constructed in Lemma 3.1.6 is always a DO but not necessarily an organization. The next lemma complements Lemma 3.1.5.

Corollary 3.1.2 (Existence of a unique biggest DO). *Given a reaction network $(\mathcal{S}, \mathcal{R})$ and a subset $S \subseteq \mathcal{S}$ of species with $O_{min} \subseteq S$ for O_{min} from Lemma 3.1.5, the union*

$$D_{max}(S) \equiv \cup\{D \subseteq S : D \text{ is a DO}\} \quad (3.39)$$

of all DOs contained in S is the unique biggest DO contained in S in the sense that all other DOs contained in S are subsets of $D_{max}(S)$.

Proof. Let $S \subseteq \mathcal{S}$ be an arbitrary closed subset of species. It follows from Lemma 3.1.6 that $D_{max}(S)$ is a DO. From lemma 3.1.5 it follows that the union is never empty, since it always contains the smallest organization $O_{min} \equiv \text{clos}(\emptyset)$ of the reaction network. \square

Based on the previous results, the next theorem states the lattice property of the set of DOs of a reaction network.

Theorem 3.1.1 (Lattice property of DOs). *Given a reaction network $(\mathcal{S}, \mathcal{R})$ the set of its DOs forms a lattice.*

Proof. According to the subarea of mathematics called order theory, a lattice is a partially ordered set in which every two elements have a unique supremum and a unique infimum. Therefore, the set of DOs is a lattice if the following three conditions hold:

1. *Partial order of the set of DOs:* The subset relation for sets provides a partial order.
2. *Unique supremum:* Given two DOs $D_1, D_2 \subseteq \mathcal{S}$, following Lemma 3.1.6, a unique supremum is given by the set union

$$D_{sup} \equiv D_1 \cup D_2. \quad (3.40)$$

3. *Unique infimum:* Given two DOs $D_1, D_2 \subseteq \mathcal{S}$ of the reaction network we take the union of all DOs in $D_1 \cap D_2$ as the infimum, that is,

$$D_{inf} \equiv D_{max}(D_1 \cap D_2) = \cup\{D \subseteq D_1 \cap D_2 : D \text{ is a DO}\}. \quad (3.41)$$

The existence of D_{inf} follows from Corollary 3.1.2.

□

Summarizing, we visualize the previous statements in Figure 3.4. Note that besides the lattice of DOs, also the set of all subsets of species forms a lattice by taking set union and set intersection as supremum and infimum, respectively. Thus the lattice of DOs can be embedded as a subset into the lattice of all subsets of species. In contrast, the set of organizations and the set of all closed subsets of species are not lattices in general.

We derive Corollary 3.1.3 from Theorem 3.1.1.

Corollary 3.1.3 (Lattice criterion for DOs). *Given a reaction network $(\mathcal{S}, \mathcal{R})$, if the Hasse diagram of organizations is not a lattice, then there exists at least one DO that is not an organization.*

Proof. Since by Lemma 3.1.4 every organization is a DO, the set of organizations of the Hasse diagram must be a proper subset of the set of DOs if the Hasse diagram of organizations is not a lattice. □

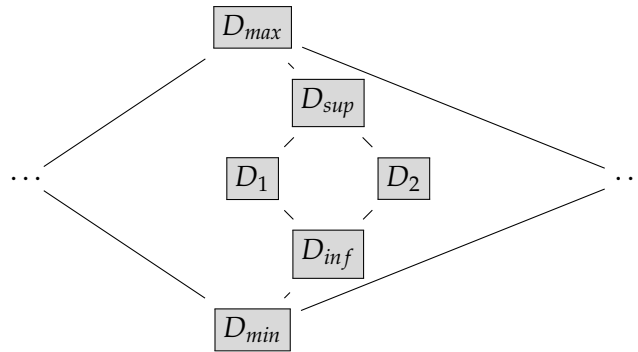


FIGURE 3.4: [76] Visualization of the lattice property of the set of DOs (that were proven in Theorem 3.1.1) of a given reaction network.

We conclude this subsection by providing an example reaction network, which is visualized in Figure 3.5 together with its lattice of DOs. The lattice contains five DOs that are all organizations. Note that the biggest DO $\mathcal{S} = \{s_1, s_2, s_3\}$ exhibits different distributions, for example, one for which it is distributed to only one subset \mathcal{S} of species and another for which it is distributed to two subsets $\mathcal{S}_1 = \{s_1, s_2\}$ and $\mathcal{S}_2 = \{s_2, s_3\}$ of species. But the two different distributions share the same total fluxes, since no reaction is deactivated by distributing the species.

3.1.4 The role closedness plays in the dynamics

In this subsection we first derive some statements about the effects of the diffusion term appearing in the RDS and prove the nonnegativity of any solution of a RDS. Then we show that for any time and any location the closure of the species existing there leads to the immediate production of the closure of these species. Finally we prove the first part of the main result of this work, that it, that a subset of species that is persistent with respect to a solution of an RDS is always closed.

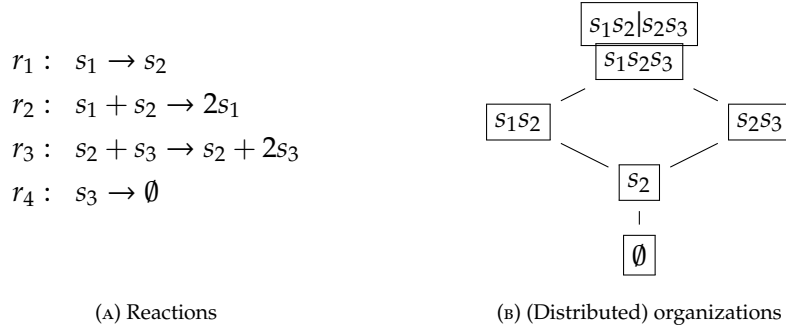


FIGURE 3.5: [76] An example reaction network pertaining to five different DOs. The vertical bar in the uppermost DO represents the fact that this DO can be distributed to two different subsets of species such that the species s_1 and s_3 are separated from each other.

Remark 3.1.4 (Nonnegative diffusion for concentration equal zero). *Given the solution c of an RDS with the underlying reaction network $(\mathcal{S}, \mathcal{R})$, a species $s_i \in \mathcal{S}$, a time $t_0 \geq 0$, and a location $x_0 \in \Omega$, the following conclusion holds:*

$$c_i(x_0, t_0) = 0 \text{ and } c_i(x, t_0) \geq 0 \forall x \neq x_0 \Rightarrow \frac{\partial^2 c_i}{\partial x^2}(x_0, t_0) \geq 0. \quad (3.42)$$

Proof. For readability we assume $\Omega \subseteq \mathbb{R}$, since the proof for $\Omega \subseteq \mathbb{R}^p$ for $p > 1$ can be deduced easily. Furthermore, we assume that $x_0 \in \Omega$ is an element of the interior of Ω , since in the case $x_0 \in \delta\Omega$, the proof holds for the one-sided derivatives too.

From $c_i(x_0, t_0) = 0$ and $c_i(x, t_0) \geq 0$ for all $x \neq x_0$ it follows that

$$\begin{aligned} \frac{\partial^2 c_i}{\partial x^2}(x_0, t_0) &= \lim_{h \rightarrow 0} \frac{c_i(x_0 + h, t_0) - 2c_i(x_0, t_0) + c_i(x_0 - h, t_0)}{h^2} \\ &= \lim_{h \rightarrow 0} \frac{c_i(x_0 + h, t_0) + c_i(x_0 - h, t_0)}{h^2} \geq 0. \end{aligned} \quad (3.43)$$

□

Now we prove the nonnegativity of the solutions of an RDS.

Lemma 3.1.7 (Nonnegativity of the solution of a RDS). *Given the solution c of an RDS with the underlying reaction network $(\mathcal{S}, \mathcal{R})$, c is nonnegative, that is,*

$$c_i(x, t) \geq 0 \quad \forall s_i \in \mathcal{S}, t \geq 0, x \in \Omega. \quad (3.44)$$

Proof. The proof is by contradiction. Therefore we assume that the supremum

$$\tilde{t} \equiv \sup\{t \geq 0 : c_i(x, t) \geq 0 \forall s_i \in \mathcal{S}, x \in \Omega\} \quad (3.45)$$

is finite, that is, $0 \leq \tilde{t} < \infty$. Since c is continuous, there is a location $\tilde{x} \in \Omega$ and an $i \in \{1, \dots, n\}$ such that for the concentration of the species $s_i \in \mathcal{S}$ it holds that

$$c_i(\tilde{x}, t) \begin{cases} \geq 0 : t \leq \tilde{t}, \\ = 0 : t = \tilde{t}, \\ < 0 : \text{for all sufficiently small } t > \tilde{t}. \end{cases} \quad (3.46)$$

and $c_i(x, \tilde{t}) \geq 0$ for all $x \in \Omega$. From Remark 3.1.4 it follows that $\frac{\partial^2 c_i}{\partial x^2}(\tilde{x}, \tilde{t}) \geq 0$, and thus

$$\begin{aligned} \frac{\partial c_i}{\partial t}(\tilde{x}, \tilde{t}) &= N \cdot v(c(\tilde{x}, \tilde{t})) + \frac{\partial^2 c_i}{\partial x^2}(\tilde{x}, \tilde{t}) \\ &\geq N \cdot v(c(\tilde{x}, \tilde{t})) \\ &\stackrel{c_i(\tilde{x}, \tilde{t})=0}{\geq} 0. \end{aligned} \tag{3.47}$$

The last inequality holds true, since when $c_i = 0$ there is no reaction that can consume the species s_i since $v(\cdot)$ is defined to be a flux vector function. The resulting inequality $\frac{\partial c_i}{\partial t}(\tilde{x}, \tilde{t}) \geq 0$ contradicts $c_i(\tilde{x}, t) < 0$ for all sufficiently small $t > \tilde{t}$, that is, the third case of 3.46. Thus the assumption is false and the solution of an RDS is nonnegative for all $t \geq 0$ and $x \in \Omega$ and all species. \square

From Lemma 3.1.7 and Remark 3.1.4 we easily derive the following corollary.

Corollary 3.1.4 (Nonnegative diffusion for concentration equal zero). *Given the solution c of an RDS with underlying reaction network $(\mathcal{S}, \mathcal{R})$, a species $s_i \in \mathcal{S}$, a time $t_0 \geq 0$, and a location $x_0 \in \Omega$, the following conclusion holds*

$$c_i(x_0, t_0) = 0 \Rightarrow \frac{\partial^2 c_i}{\partial x^2}(x_0, t_0) \geq 0. \tag{3.48}$$

Next we state another result about diffusion we use in this work.

Remark 3.1.5 (Integral over the divergence equals zero). *Given the solution c of an RDS with the underlying reaction network $(\mathcal{S}, \mathcal{R})$ and a time $t_0 \geq 0$, for every species $s_i \in \mathcal{S}$, $i = 1, \dots, n$, it holds that*

$$\int_{\Omega} \frac{\partial^2 c_i}{\partial x^2}(x, t_0) dx = 0. \tag{3.49}$$

Proof. From the divergence theorem, also referred to as Gauss's theorem we know that

$$\int_{\Omega} \frac{\partial^2 c_i}{\partial x^2}(x, t_0) dx = \int_{\partial\Omega} \frac{\partial c_i}{\partial \nu}(x, t_0) dx \tag{3.50}$$

and the term on the right-hand side of this equation equals zero, since we apply homogeneous Neumann boundary conditions (see Section 2.1). \square

From Remark 3.1.5 it follows that the diffusion does not change the total integral over the concentration values of the species, but, instead, the total concentration value of each species is determined solely by its interactions with the other species via the reactions. In Section 3.2 we outline exemplarily, how the set of reactions is to be modified according to the boundary conditions applied, to return the right set of organizations and DOs of the reaction network. For homogeneous Neumann boundary conditions we had seen, that the set of reactions needs not to be changed and this result is confirmed by Remark 3.1.5.

Next we state a lemma necessary to prove the two main results of this subsection about closedness.

Lemma 3.1.8 (Production of the closure). *Given a solution c of an RDS with underlying reaction network $(\mathcal{S}, \mathcal{R})$, a subset $S \subseteq \mathcal{S}$, a location $x_0 \in \Omega$, a time $t_0 > 0$, and an $\varepsilon > 0$ such that for all species $s_i \in S$ it holds that*

$$c_i(x_0, t_0) > \varepsilon, \quad (3.51)$$

then

$$c_j(x_0, t_0) > 0 \quad (3.52)$$

for all $s_j \in \text{clos}(S)$.

Proof. By assumption there is an $\varepsilon > 0$ with $c_i(x_0, t_0) > \varepsilon$ for every $s_i \in S$. We prove this by contradiction. To this end we assume that there is a species $s_j \in \text{clos}(S)$ with $c_j(x_0, t_0) = 0$. For readability we assume $s_j \in \text{clos}_1(S)$, since from this case the proof can easily be transferred to the cases $s_j \in \text{clos}_1^k(S)$, $k > 1$. From $s_j \in \text{clos}_1(S)$ it follows that there is a reaction $r_k \in \mathcal{R}$ with $\text{supp}(r_k) \subseteq S$, that produces s_j , that is, $a_{jk} = 0$ and $b_{jk} > 0$ and thus $n_{jk} > 0$. Due to the continuity of the involved functions, there is a $\delta > 0$ such that

- $f_+(c(x_0, t)) \equiv \sum_{k: n_{jk} > 0} n_{jk} \cdot v_k(c(x_0, t)) > \varepsilon/2$,
- $f_-(c(x_0, t)) \equiv \sum_{k: n_{jk} < 0} n_{jk} \cdot v_k(c(x_0, t)) < -\varepsilon/8$, and
- $d_j \frac{\partial^2 c_j}{\partial x^2}(x_0, t) > -\varepsilon/8$

for all $t \in (t_0 - \delta, t_0 + \delta)$. Thus, contrary to the assumption, we arrive at

$$c_j(x_0, t_0) = c_j(x_0, t_0 - \delta) + \int_{t_0 - \delta}^{t_0} f_+(c(x_0, t)) + f_-(c(x_0, t)) + d_j \frac{\partial^2 c_j}{\partial x^2}(x_0, t) dt > \delta \frac{\varepsilon}{4} > 0, \quad (3.53)$$

which finishes the proof. □

Lemma 3.1.8 allows for proving our first main result about closedness with regard to the solutions c of an RDS. For ODEs, it was already proven in Lemma 4 in [72].

Lemma 3.1.9 (Instant appearance of the closure). *Given the solution c of an RDS with an underlying reaction network $(\mathcal{S}, \mathcal{R})$ and a location $x \in \Omega$ the following hold:*

1. For all times $t > 0$, the set of species $\phi(c(x, t))$ with strictly positive concentration is closed.
2. For sufficiently small times $t > 0$, the set of species $\phi(c(x, t))$ with strictly positive concentration contains the closure of the set $\phi(c(x, 0))$ of species with initial concentration strictly positive, that is,

$$\phi(c(x, t)) \supseteq \text{clos}(\phi(c(x, 0))). \quad (3.54)$$

Proof. 1. The closedness of $\phi(c(x, t))$ for any $t > 0$ follows directly from lemma 3.1.8.

2. Because of the continuity of c with respect to t , we know that for sufficiently small times $t > 0$,

$$\phi(c(x, t)) \supseteq \phi(c(x, 0)), \quad (3.55)$$

and thus with Lemma 3.1.8 it follows that

$$\phi(c(x, t)) \supseteq \text{clos}(\phi(c(x, 0))). \quad (3.56)$$

□

We learn from Lemma 3.1.9 that the immediate production of the closure of an initially present but not closed set of species is an intrinsic phenomenon of all solutions of any RDS. In the following we focus on the dynamics in the long-run. We prove that a persistent subset $S \in P(c)$ of species is always closed. In the next subsection, to complement this result, we prove that the set $\Phi(c)$ of persistent species with respect to c always fulfills the self-maintenance property of a DO.

Lemma 3.1.10 (Persistent subsets of species are closed). *Given a solution c of an RDS with the underlying reaction network $(\mathcal{S}, \mathcal{R})$, every persistent subset $S \in P(c)$ of species is closed.*

Proof. We prove this by contradiction. Therefore we assume that there is a persistent subset $S \in P(c)$ of species that is not closed. From Lemma 3.1.8 it follows that for every $\varepsilon > 0$ there is a $\delta_0 > 0$ such that for all concentration vectors $c \in \mathbb{R}_+^n$ and all $\delta \in (0, \delta_0)$, $x \in \Omega$, $t \geq 0$, it holds that

$$c(x, t) \in S^\varepsilon \Rightarrow c(x, t) \notin S^{\varepsilon, \delta}. \quad (3.57)$$

Thus the set $\{(x, t) \in \Omega \times (0, \infty) : c(x, t) \in S^{\varepsilon, \delta}\}$ is empty for all $\varepsilon > 0$ and all sufficiently small $\delta > 0$, so the frequency $F(S^{\varepsilon, \delta})$ is zero and S is not persistent in contradiction to the assumptions of this lemma. □

3.1.5 DOs and persistence

In this subsection we state the second main result of this work, that is, that the set $\Phi(c)$ of persistent species with respect to a solution c is always a DO. After having shown the closedness of each element of $P(c)$ in the previous subsection, it remains to prove self-maintenance. We do this in two steps:

- First, in Lemma 3.1.11 we construct from the solution c of the RDS a total flux $\hat{v} \in \mathbb{R}_{\geq 0}^m$ with respect to c with $N \cdot \hat{v} \geq 0$.
- Then, in Lemma 3.1.12 we show that there is a feasible flux with respect to each of the persistent subsets $S \in P(c)$ of species and that the sum of these feasible fluxes equals the total flux \hat{v} constructed in Lemma 3.1.11.

Thereafter we transfer the result to initial value problems based on ODEs. Furthermore, given an organization, we present a way to construct an RDS with a (constant with respect to x) solution c such that the set $\Phi(c)$ of persistent species equals that organization.

Lemma 3.1.11 (Construction of a vector proving self-maintenance). *Given a solution c of an RDS with underlying reaction network $(\mathcal{S}, \mathcal{R})$, there is a sequence $(t_l)_{l=1}^\infty$ of points in time such that the total flux*

$$\hat{v} \equiv \lim_{l \rightarrow \infty} \frac{1}{t_{l+1} - t_l} \int_{t_l}^{t_{l+1}} \int_{x \in \Omega} v(c(x, t)) \, dx \, dt \in \mathbb{R}_{\geq 0}^m \quad (3.58)$$

with respect to c and $(t_l)_{l=1}^\infty$ fulfills

$$N \cdot \hat{v} \geq 0. \quad (3.59)$$

Proof. Since

$$c^\Omega(t) \equiv \int_{x \in \Omega} c(x, t) dx \quad (3.60)$$

is bounded by assumption, it has at least one accumulation point $\tilde{c} \in \mathbb{R}_+^n$. Thus there is a sequence $(t_j)_{j=1}^\infty$ of points in time such that

$$\lim_{j \rightarrow \infty} c^\Omega(t_j) = \tilde{c} \quad (3.61)$$

and so

$$\begin{aligned} 0 &\stackrel{(3.61)}{=} \lim_{j \rightarrow \infty} (c^\Omega(t_{j+1}) - c^\Omega(t_j)) \\ &\stackrel{(3.60)}{=} \lim_{j \rightarrow \infty} \left(\int_{x \in \Omega} c(x, t_{j+1}) dx - \int_{x \in \Omega} c(x, t_j) dx \right) \\ &= \lim_{j \rightarrow \infty} \int_{x \in \Omega} c(x, t_{j+1}) - c(x, t_j) dx \\ &= \lim_{j \rightarrow \infty} \int_{x \in \Omega} \int_{t_j}^{t_{j+1}} \dot{c}(x, t) dt dx \\ &\geq \lim_{j \rightarrow \infty} \frac{1}{t_{j+1} - t_j} \int_{x \in \Omega} \int_{t_j}^{t_{j+1}} \dot{c}(x, t) dt dx \\ &\stackrel{(2.7)}{=} \lim_{j \rightarrow \infty} \frac{1}{t_{j+1} - t_j} \int_{x \in \Omega} \int_{t_j}^{t_{j+1}} Nv(c(x, t)) + \frac{\partial^2 c(x, t)}{\partial x^2} \cdot (d_1, \dots, d_n)^T dt dx \\ &= \lim_{j \rightarrow \infty} \frac{1}{t_{j+1} - t_j} \left[\int_{x \in \Omega} \int_{t_j}^{t_{j+1}} Nv(c(x, t)) dt dx \right. \\ &\quad \left. + \int_{x \in \Omega} \int_{t_j}^{t_{j+1}} D \frac{\partial^2 c(x, t)}{\partial x^2} dt dx \right] \\ &= \lim_{j \rightarrow \infty} \frac{1}{t_{j+1} - t_j} \left[\int_{t_j}^{t_{j+1}} \int_{x \in \Omega} Nv(c(x, t)) dt dx \right. \\ &\quad \left. + \underbrace{\int_{t_j}^{t_{j+1}} \int_{x \in \Omega} \frac{\partial^2 c(x, t)}{\partial x^2} \cdot (d_1, \dots, d_n)^T dx dt}_{=0 \text{ (remark 3.1.5)}} \right] \\ &= \lim_{j \rightarrow \infty} \frac{1}{t_{j+1} - t_j} \left[\int_{t_j}^{t_{j+1}} \int_{x \in \Omega} Nv(c(x, t)) dt dx \right] \\ &= \lim_{j \rightarrow \infty} N \cdot \frac{1}{t_{j+1} - t_j} \left[\int_{t_j}^{t_{j+1}} \int_{x \in \Omega} v(c(x, t)) dt dx \right] \\ &= N \cdot \underbrace{\lim_{l \rightarrow \infty} \frac{1}{t_{l+1} - t_l} \int_{t_j}^{t_{j+1}} \int_{x \in \Omega} v(c(x, t)) dt dx}_{\equiv \hat{v}, \hat{v} \geq 0} \end{aligned}$$

where $D \in \mathbb{R}^{n \times n}$ denotes the Fickian diffusivity matrix, which in this work is assumed

to be a diagonal matrix containing the diffusion rates d_i , $i = 1, \dots, n$, on its diagonal. Thus there is a subsequence $(t_l)_{l=1}^\infty$ of $(t_j)_{j=1}^\infty$ such that the total flux

$$\hat{v} \equiv \lim_{l \rightarrow \infty} \frac{1}{t_{l+1} - t_l} \int_{t_l}^{t_{l+1}} \int_{x \in \Omega} v(c(x, t)) dt dx \quad (3.62)$$

with respect to c and $(t_l)_{l=1}^\infty$ exists, because the flux vector function $v(\cdot)$ is by assumption Lipschitz continuous on every bounded subset of \mathbb{R}_+^n , and c is bounded by assumption too, and thus $v(\cdot)$ is bounded for all $x \in \Omega$, $t \geq 0$. \square

Next we prove that the vector \hat{v} obtained in Lemma 3.1.11 can be written as a sum of feasible fluxes with respect to the persistent subsets of species.

Lemma 3.1.12 (Construction of a feasible flux (with respect to every persistent subset of species) summing up to \hat{v}). *Given the solution c of an RDS with underlying reaction network $(\mathcal{S}, \mathcal{R})$ and a vector $\hat{v} \in \mathbb{R}_+^m$ constructed as in Lemma 3.1.11, then there is a feasible flux \hat{v}^i with respect to each $S_i \in P(c)$, $i = 1, \dots, k$, such that*

$$\hat{v} = \lim_{l \rightarrow \infty} \frac{1}{t_{l+1} - t_l} \int_{t_l}^{t_{l+1}} \int_{x \in \Omega} v(c(x, t)) dt dx = \sum_{i=1}^k \hat{v}^i. \quad (3.63)$$

Proof. Let $r_j \in \mathcal{R}$ be an arbitrarily chosen reaction, and let $n(r_j)$ be the number of persistent subsets $S \in P(c)$ of species with $\text{support}(r_j) \subseteq S$. We can distinguish the following two alternative cases:

- $n(r_j) > 0$, and
- $n(r_j) = 0$.

We will prove that

$$n(r_j) > 0 \Leftrightarrow \hat{v}_j > 0 \quad (3.64)$$

by proving the following two conclusions

1. $n(r_j) > 0 \Rightarrow \hat{v}_j > 0$, and
2. $n(r_j) = 0 \Rightarrow \hat{v}_j = 0$.

Then, for each persistent subset $S_i \in P(c)$, $i = 1, \dots, k$, of species we construct the vector \hat{v}^i by defining

$$\hat{v}_j^i \equiv \begin{cases} \hat{v}_j / n(r_j), & \text{if } n(r_j) > 0 \text{ and } \text{support}(r_j) \subseteq S_i \\ 0, & \text{otherwise} \end{cases} \quad (3.65)$$

for all reactions $r_j \in \mathcal{R}$. Then each vector $\hat{v}^i \in \mathbb{R}_{\geq 0}^m$ is a feasible flux with respect to the corresponding persistent subset $S_i \in P(c)$, $i = 1, \dots, k$, of species and $\hat{v} = \sum_{i=1}^k \hat{v}^i$ as desired.

Now it only remains to prove the following two conclusions mentioned above:

1. $n(r_j) > 0 \Rightarrow \hat{v}_j > 0$.

If for a reaction $r_j \in \mathcal{R}$ it holds that $n(r_j) > 0$, then there is a persistent subset $\tilde{S} \in P(c)$ of species with $\text{support}(r_j) \subseteq \tilde{S}$. Thus for all sufficiently small $\varepsilon > 0$ it

holds that $F(\tilde{S}^\epsilon) > 0$, and according to Remark 3.1.1 there is a lower boundary $L(\epsilon) > 0$ for v_j such that

$$\begin{aligned}
 \hat{v}_j &\stackrel{(3.62)}{=} \lim_{l \rightarrow \infty} \frac{1}{t_{l+1} - t_l} \int_{t_l}^{t_{l+1}} \int_{x \in \Omega} v_j(c(x, t)) dt dx \\
 &\geq \lim_{l \rightarrow \infty} \frac{1}{t_{l+1} - t_l} \int_{t_l}^{t_{l+1}} \int_{\{x \in \Omega: c(x, t) \in \tilde{S}^\epsilon\}} v_j(c(x, t)) dt dx \\
 &\stackrel{\text{Remark 3.1.1}}{\geq} \lim_{l \rightarrow \infty} \frac{1}{t_{l+1} - t_l} \int_{t_l}^{t_{l+1}} \int_{\{x \in \Omega: c(x, t) \in \tilde{S}^\epsilon\}} L(\epsilon) dt dx \\
 &\stackrel{\text{Remark 3.1.1}}{\geq} L(\epsilon) \cdot \lim_{l \rightarrow \infty} \frac{1}{t_{l+1} - t_l} \int_{t_l}^{t_{l+1}} \int_{\{x \in \Omega: c(x, t) \in \tilde{S}^\epsilon\}} dt dx \\
 &= L(\epsilon) \cdot F(\tilde{S}^\epsilon) \\
 &> 0,
 \end{aligned} \tag{3.66}$$

where $(t_l)_{l=1}^\infty$ is a sequence of points in time from Lemma 3.1.11.

2. $\overline{n(r_j)} = 0 \Rightarrow \hat{v}_j = 0$.

We prove this by contradiction, that is, by showing that from $\hat{v}_j > 0$ it follows that $n(r_j) > 0$. Thus we assume $\hat{v}_j > 0$. For

$$K \equiv \sup\{v_j(c(x, t)) : t \geq 0, x \in \Omega\}, \tag{3.67}$$

$0 \leq K < \infty$ holds. Let $(t_l)_{l=1}^\infty$ be the sequence of points in time from Lemma 3.1.11. Then for all sufficiently small $\epsilon > 0$, from Remark 3.1.1 it follows that there is

an upper boundary $U(\varepsilon) > 0$ such that for every $\delta > 0$,

$$\begin{aligned}
0 &< \hat{v}_j \\
&\stackrel{(3.62)}{=} \lim_{l \rightarrow \infty} \frac{1}{t_{l+1} - t_l} \int_{t_l}^{t_{l+1}} \int_{x \in \Omega} v_j(c(x, t)) \, dx \, dt \\
&= \lim_{l \rightarrow \infty} \frac{1}{t_{l+1} - t_l} \int_{t_l}^{t_{l+1}} \left[\int_{\{x \in \Omega: c(x, t) \in \text{support}(r_j)^\varepsilon\}} v_j(c(x, t)) \, dx \right. \\
&\quad \left. + \int_{\{x \in \Omega: c(x, t) \notin \text{support}(r_j)^\varepsilon\}} v_j(c(x, t)) \, dx \right] dt \\
&\stackrel{(3.67), \text{Remark 3.1.1}}{\leq} \lim_{l \rightarrow \infty} \frac{1}{t_{l+1} - t_l} \left[\int_{t_l}^{t_{l+1}} \int_{\{x \in \Omega: c(x, t) \in \text{support}(r_j)^\varepsilon\}} K \, dx \, dt \right. \\
&\quad \left. + \int_{t_l}^{t_{l+1}} \int_{\{x \in \Omega: c(x, t) \notin \text{support}(r_j)^\varepsilon\}} U(\varepsilon) \, dx \, dt \right] \\
&= K \cdot \lim_{l \rightarrow \infty} \frac{1}{t_{l+1} - t_l} \int_{t_l}^{t_{l+1}} \int_{\{x \in \Omega: c(x, t) \in \text{support}(r_j)^\varepsilon\}} dx \, dt \\
&\quad + U(\varepsilon) \cdot \lim_{l \rightarrow \infty} \frac{1}{t_{l+1} - t_l} \int_{t_l}^{t_{l+1}} \int_{\{x \in \Omega: c(x, t) \notin \text{support}(r_j)^\varepsilon\}} dx \, dt \\
&\stackrel{\text{Remark 3.1.2}}{=} K \lim_{l \rightarrow \infty} \frac{1}{t_{l+1} - t_l} \int_{t_l}^{t_{l+1}} \sum_{S \supseteq \text{support}(r_j)} \int_{\{x \in \Omega: c(x, t) \in S^{\varepsilon, \delta}\}} dx \, dt \\
&\quad + U(\varepsilon) \lim_{l \rightarrow \infty} \frac{1}{t_{l+1} - t_l} \int_{t_l}^{t_{l+1}} \int_{\{x \in \Omega: c(x, t) \notin \text{support}(r_j)^\varepsilon\}} dx \, dt \\
&= K \cdot \sum_{S \supseteq \text{support}(r_j)} \lim_{l \rightarrow \infty} \frac{1}{t_{l+1} - t_l} \int_{t_l}^{t_{l+1}} \int_{\{x \in \Omega: c(x, t) \in S^{\varepsilon, \delta}\}} dx \, dt \\
&\quad + U(\varepsilon) \cdot \lim_{l \rightarrow \infty} \frac{1}{t_{l+1} - t_l} \int_{t_l}^{t_{l+1}} \int_{\{x \in \Omega: c(x, t) \notin \text{support}(r_j)^\varepsilon\}} dx \, dt \\
&= K \cdot \sum_{S \supseteq \text{support}(r_j)} F(S^{\varepsilon, \delta}) \\
&\quad + U(\varepsilon) \cdot \lim_{l \rightarrow \infty} \frac{1}{t_{l+1} - t_l} \int_{t_l}^{t_{l+1}} \int_{\{x \in \Omega: c(x, t) \notin \text{support}(r_j)^\varepsilon\}} dx \, dt \tag{B.68}
\end{aligned}$$

By letting $\varepsilon \rightarrow 0$ we get

$$\begin{aligned}
0 &< \lim_{\varepsilon \rightarrow 0} \left[K \cdot \sum_{S \supseteq \text{support}(r_j)} F(S^{\varepsilon, \delta}) \right. \\
&\quad \left. + U(\varepsilon) \cdot \lim_{l \rightarrow \infty} \frac{1}{t_{l+1} - t_l} \int_{t_l}^{t_{l+1}} \int_{\{x \in \Omega: c(x, t) \notin \text{support}(r_j)^\varepsilon\}} dx \, dt \right] \\
&\stackrel{\text{Remark 3.1.1}}{=} \lim_{\varepsilon \rightarrow 0} \left[K \cdot \sum_{S \supseteq \text{support}(r_j)} F(S^{\varepsilon, \delta}) \right] \\
&= K \cdot \sum_{S \supseteq \text{support}(r_j)} \lim_{\varepsilon \rightarrow 0} F(S^{\varepsilon, \delta}) \tag{3.69}
\end{aligned}$$

for every $\delta > 0$. Thus from Definition 3.1.3 it follows that at least one subset S of species with $S \supseteq \text{support}(r_j)$ is persistent with respect to c , that is, $S \in P(c)$. This means $n(r_j) \geq 1 > 0$ in contradiction to the assumption.

This completes the proof of Lemma 3.1.12. □

Note that in Equation 3.65 we did not construct the vectors $\hat{\nu}^i$ such that they necessarily represent the frequency of their appearance in the solution c of the RDS. Rather we only considered whether or not their components are zero. Putting Lemma 3.1.10, Lemma 3.1.11, and Lemma 3.1.12 together, we are able to state the second main result of this paper.

Theorem 3.1.2 (The set of persistent species is a DO). *Given the solution c of an RDS with an underlying reaction network, the set $\Phi(c)$ of persistent species is a DO.*

Remark 3.1.6 (Unbounded solutions). *Note that this work does not examine unbounded solutions c to RDSs. A simple example might shed some light onto the consequences of this. Let $(\mathcal{S}, \mathcal{R}) \equiv (\{s_1\}, \{r_1 : \emptyset \rightarrow s_1\})$ be a reaction network. It exhibits only one DO, that is, the organization $O \equiv \{s_1\}$. For every solution c of any RDS with the same underlying reaction network $(\mathcal{S}, \mathcal{R})$ it holds that $\lim_{t \rightarrow \infty} c_1(x, t) = \infty$ for all $x \in \Omega$. Even though this long-term behavior seems to be captured by the organization O , strictly speaking, the theory developed in this work does not apply to this case, and even the usage of the term "persistence" as defined here is not allowed in this case unless a thorough study for the case of unbounded solutions is made.*

The next corollary is some kind of counterpart to Theorem 3.1.2.

Corollary 3.1.5 (Equivalence of organizations and persistent subsets). *Given a reaction network $(\mathcal{S}, \mathcal{R})$ and a subset $S \subseteq \mathcal{S}$ of species, then the following two statements are equivalent:*

1. *There is an RDS with an underlying reaction network $(\mathcal{S}, \mathcal{R})$ with a constant solution $c(x, t) = c \in \mathbb{R}_+^n$ for all $x \in \Omega$, $t \geq 0$, and $P(c) = \{S\}$.*
2. *S is an organization and there is a feasible flux $\hat{\nu}$ with respect to S such that $N\hat{\nu} = 0$.*

Proof. We prove the two directions of the equivalence separately.

- 1. \Rightarrow 2.

From statement 1 it follows that by Theorem 3.1.2 that S is a DO. Since S is distributed to only one subset of species, that is, to S itself, from the second part of Lemma 3.1.4 it follows that S is an organization. Since statement 1 provides a fixed-point solution, for every sequence of points in time the total flux $\hat{\nu}$ constructed as in Equation 3.62 fulfills $N\hat{\nu} = 0$.

- 2. \Rightarrow 1.

Let S be an organization with $\hat{\nu} \in \mathbb{R}_+^m$ a feasible flux with respect to S fulfilling $N \cdot \hat{\nu} = 0$. We construct an RDS with the underlying reaction network $(\mathcal{S}, \mathcal{R})$ such that for its solution c it holds that $P(c) = \{S\}$, that is, S is the only persistent subset with respect to c . We set the diffusion rates of all species to zero and choose the domain $\Omega = [0, 1] \subseteq \mathbb{R}$. We set the initial conditions

$$c_i^0(x) = \begin{cases} 1, & \text{iff } s_i \in S, \\ 0, & \text{otherwise.} \end{cases} \quad (3.70)$$

for all species $s_i \in \mathcal{S}$, $i = 1, \dots, n$, and all $x \in \Omega$. For the flux vector function $v(\cdot)$ we choose mass-action kinetics. For all reactions $r_j \in \mathcal{R}$, $j = 1, \dots, m$, we set the reaction constants

$$k_j \equiv \hat{v}_j. \quad (3.71)$$

Then for all times $t \geq 0$ and all $x \in \Omega$,

$$v(c(x, t)) = \hat{v} \quad (3.72)$$

holds, and thus

$$\dot{c}(x, t) = N\hat{v} = 0. \quad (3.73)$$

□

It might be possible (but it is more difficult) to prove that Corollary 3.1.5 holds also for DOs and not just for organizations. There are dynamical systems with a spatial domain for which the proof of Corollary 3.1.5 for DOs should be easier, for example, the patch models defined in [2], which are systems of ODEs with a discrete spatial domain. Given a DO distributed to subsets S_i , $i = 1, \dots, k$, of species, such a system could be designed containing k patches such that in each patch exactly one of the S_i , $i = 1, \dots, k$, is present as a fixed point, and the exchange of species between different patches is adjusted properly.

As a special case, Theorem 3.1.2 is applicable to ODE systems which do not have any space dimension and thus no diffusion.

Remark 3.1.7 (ODE systems as a special case). *Given an initial value problem*

$$\dot{c}(t) = N \cdot v(c(t)), \quad c(0) = c^0 \quad (3.74)$$

with an underlying reaction network as outlined in the introduction, one can transfer the whole of this work to that problem by neglecting all aspects concerning the space variable x , for example, integration with respect to x .

3.1.6 Analysis of a DO lattices

In this subsection we bring together the two main results of this work, Theorem 3.1.1 (the set of DOs of a given reaction network forms a lattice) and Theorem 3.1.2 (the set of persistent species with respect to every bounded solution being a DO). That is, we show how to interpret a single DO lattice with regard to persistence. As for the Hasse diagram of organizations, analyzing a single lattice of DOs of a given reaction network can reveal much information about the behavior of the solutions of RDSs with that underlying reaction network.

For example, the smallest DO of a lattice, which following Lemma 3.1.5 is a unique organization, tells us which species persist in every solution. Furthermore, if a subset of species does not appear in the lattice of DOs, following Theorem 3.1.2 it cannot appear as a set of persistent species with respect to any solution, since if it could, it would be a DO. So it is easy to check from the lattice of DOs whether, for example, the whole set of species \mathcal{S} can persist in any solution, because if so, then it appears as a DO at the top of the lattice.

Given two DOs D_1 and D_2 , it is interesting, for example for interpretation of ecological systems, to study the DOs that contain both these DOs. Doing so reveals,

under which circumstances both DOs can coexist. The question of whether or not $D_1 \cup D_2$ is an organization tells us something about the possible modes of coexistence of D_1 and D_2 . If $D_1 \cup D_2$ is an organization, all species can persist when mixed together. If not, they can only coexist when separated properly. Also it is interesting to analyze those DOs that contain more species than $D_1 \cup D_2$, because these species allow for the coexistence of D_1 and D_2 distributed either to different subsets of species or to the same.

Now, instead of subsets of species, let us consider a single species. If a species does not appear in any of the DOs of a lattice, it will not persist with respect to any solution of any RDS with the underlying reaction network, which the lattice of DOs was derived from. On the other hand, if a species appears in all DOs of a lattice, then it will persist with respect to every solution of every RDS with the respective reaction network.

Using the lattice of DOs one can distinguish different degrees of persistence of a subset or a single species with regard to the reaction network (not with respect to a single solution of an RDS). In this sense, for example, a species is more persistent the further down it appears in the lattice and thus is an element of more DOs. Of all DOs that contain a given species, the one occupying the lowest position in the lattice determines which of the considered species definitely needs to persist. By discussing our third example model in Section 3.1.10 below we will learn more about such dependencies of species with regard to their persistence.

Contrary to dependency, if two species are elements of two different DOs that are not linked by a vertical chain of interlaced DOs in the lattice, then these species exhibit some sort of independence with regard to their persistence. Generally, the more vertical levels a lattice pertains to between its lowest and its highest DO, the more complex it is with regard to persistence.

For a solution c of an RDS, the dynamical changes of the set of species existent at any time t can be visualized within the lattice by arrows between different subsets of species indicating, which species are newly created (according to Lemma 3.1.9) or which go extinct due to missing self-maintenance. In Figure 3.6 we have exemplified this. Note that, as in Figure 3.6, it might be advantageous to augment the lattice of DOs by further sets of relevance, for example, important transient sets of species, which following Lemma 3.1.9 are initial sets of species and their closures. In Section 3.3 we provide an example simulation for an Influenza A virus infection dynamics model from [37] where we juxtaposed the diagram with the courses of the concentrations of the species from an ODE simulation (Figure 3.27) and the respective movement in the Hasse diagram of organizations of the underlying reaction network (Figure 3.26b).

3.1.7 Comparisons and hierarchies of several models using their signature

Above we have shown that computing the lattice of DOs allows for some sort of overall steady-state analysis of the whole set of possible solutions on the level of species. In Section 3.3 we use the lattices of organizations of different in-host Influenza A virus infection dynamics models based on ODEs to compare these models and to put them into a hierarchy revealing different degrees of complexity and different types of overall dynamic behavior.

In Section 3.4 we compute the lattices of DOs of different SARS-CoV-2 infection dynamics models including not only in-host but also host-to-host models and one mixed model. Furthermore we did not restrict that work to ODE models but included PDE models as well proving the universality of our approach that is due to the fact

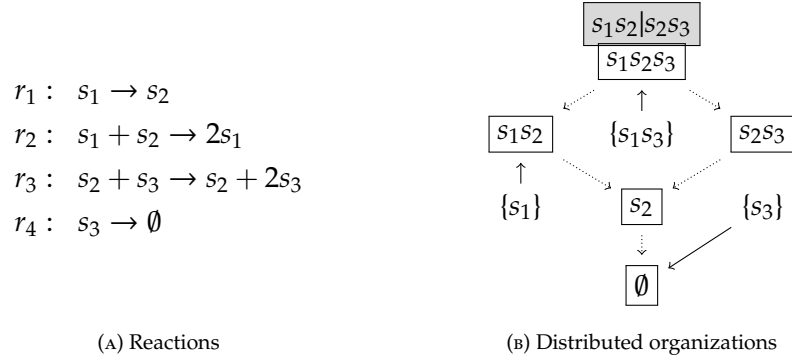


FIGURE 3.6: [76] An example reaction network (left) with the lattice of all subsets of species (right). Those subsets in the boxes are DOs. From each subset that is not a DO, a solid arrow points towards the DO that will be approached initially by any solution starting with that subset of species. More precisely, $\{s_3\}$ goes extinct since it is not self-maintaining, and both $\{s_1\}$ and $\{s_1, s_3\}$ will produce their closures $\{s_1, s_2\}$ (resp., $\{s_1, s_2, s_2\}$). Further possible movements from the DOs downward leading to one of their subsets are depicted by dotted arrows.

that it relies solely on the underlying reaction network of the models. We found DOs that were not organizations proving the purpose of this work from another perspective. Besides some similarities, the DO lattices showed significant differences which resulted in contradictory conclusions about their long-term behavior. Even though those models are mostly intended to capture only the quantitative aspect of a special subset of solutions, such conflicts regarding their overall qualitative dynamics can be interpreted as showing a weak point in such modeling. Finally, in Section 3.4, by using the lattice of DOs we also put the Influenza A and SARS-CoV-2 infection dynamics models into one common hierarchy, revealing not only some of their similarities but also their differences, for example, the lower complexity of the SARS-CoV-2 infection dynamics models.

3.1.8 Example I

Figure 3.7a exhibits the PDEs of an RDS that pertains to a solution for which a simulation result is shown in Figure 3.8. In Figure 3.7b the reactions of the underlying reaction network are shown. Note that these reactions can be derived easily from the PDEs by writing the part related to the reactions in the form $N \cdot v(c)$ and obeying the fact that v is a flux vector function. In Section 2.3 an example of this procedure is described. Figure 3.7c shows the lattice of DOs of the reaction network of Example I. Now, we want to retrace the simulation results illustrated in Figure 3.8. Since the species s_2 and s_3 do not diffuse we can take a fixed location $x \in \Omega$ and analyze for it the ODE system

$$\frac{\partial c_2(t)}{\partial t} = -c_2(t)c_3(t) \quad (3.75)$$

$$\frac{\partial c_3(t)}{\partial t} = -c_2(t)c_3(t) \quad (3.76)$$

governing the concentrations $c_2(t) = c_2(x, t)$ (resp., $c_3(t) = c_3(x, t)$) of s_2 and s_3 at this location x . Then one of the following three cases occurs.

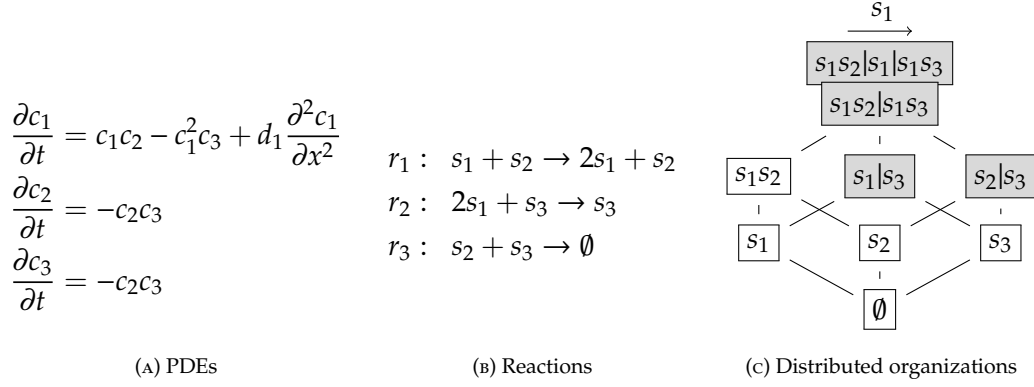


FIGURE 3.7: [76] PDEs, reactions and lattice of DOs of Example I. Unshaded boxes indicate organizations. Shaded boxes indicate DOs that are not organizations. Note that the Hasse diagram of organizations in this case is not a lattice. From Corollary 3.1.3 we know that there must be at least one DO (which is not an organization) containing the union of $\{s_1, s_2\}$, $\{s_2\}$ and $\{s_3\}$. For this example we have three DOs that are not organizations, one of which contains all species. For that DO we depicted two different distributions one upon the other. The lower one represents to the two subsets $\{s_1, s_2\}$ and $\{s_1, s_3\}$ which appear as persistent subsets of species in the simulation shown in Figure 3.8. There are feasible fluxes $\hat{v}^1 = (2, 0, 0)^T$ for $\{s_1, s_2\}$ and $\hat{v}^2 = (0, 1, 0)^T$ for $\{s_1, s_3\}$ for example proving the self-maintenance for the DO \mathcal{S} . It is also possible to calculate a total flux from the simulation numerically. The horizontal arrow symbolizes the necessary flow of the species s_1 from the subset $\{s_1, s_2\}$, where it is overproduced, to the subset $\{s_1, s_3\}$, where it is reduced. That flow is enabled by diffusion which does not have any preferred direction.

1. *Case I:* If $c_2(0) < c_3(0)$, then c_2 will tend towards zero and $c_3(t)$ towards the strictly positive value $c_3(0) - c_2(0)$ in the long-run, with both converging from above.
2. *Case II:* If, conversely, $c_2(0) > c_3(0)$, then $c_3(t)$ tends towards zero and $c_2(t)$ towards the strictly positive value $c_2(0) - c_3(0)$.
3. *Case III:* If $c_2^0 = c_3^0$, then c_2 and c_3 equally tend towards zero in the long-run.

The previously analyzed dynamics of the concentrations of s_2 and s_3 is independent of that of the concentration of c_1 . With the initial conditions used in this example (see the caption of Figure 3.8) the system finally reaches a steady state with

- species s_2 only existing in the interval $[-2; 0) \subseteq \Omega$,
- species s_3 only existing in the interval $(0; 2] \subseteq \Omega$, and
- species s_1 existing in the whole domain, keeping the balance between its overproduction catalyzed by s_2 and its consumption catalyzed by s_3 .

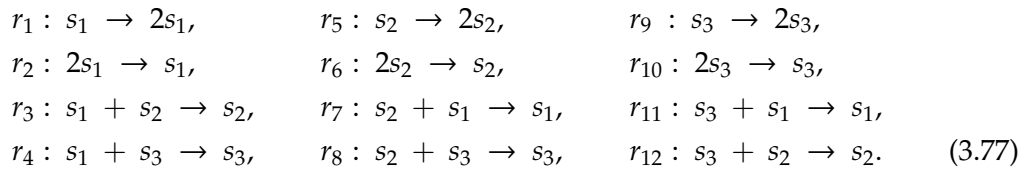
Thus the observed coexistence of all three species, which is impossible at any single location, is reached by the spatial separation of the two persistent subsets $\{s_1, s_2\}$ and $\{s_1, s_3\}$, which keep the overall concentration of s_1 in balance by their complementary action on it. Note that even though the subset $\{s_1\}$ exists in the long-run at the singular location $x = 0$, it is not persistent with regard to Definition 3.1.3 since the frequency of occurrence of its respective (ε, δ) -neighborhoods tends towards zero as $\delta \rightarrow 0$.

In the next subsection we present a simulation where the persistent subsets are not separated spatially but with respect to time, that is, they disappear and reappear forever.

In Section 3.2 we will modify Example I to show how knowledge about the diffusion of the species and their boundary conditions can be used to modify the underlying reaction network such that all persistent subsets of species are captured by DOs.

3.1.9 Example II

Our second example is adapted from an initial value problem based on a ODE system from Neumann and Schuster [69] which we extended towards an RDS by adding a spatial dimension x and using constant concentration values with regard to x for each species. It resembles many situations from game theory (for example, the rock-paper-scissors game or the prisoner's dilemma with three participants) and biology (for example, the coexistence of different strains of bacteria, such as *E. coli*, competing for nutrition, intoxicating, invading, and resisting one another). The underlying reaction network of Example II has three species s_1 , s_2 , and s_3 and 12 reactions:



Each species self-replicates (r_1, r_5, r_9). So every subset of species is an organization. Every species decays spontaneously (r_2, r_6, r_{10}). Furthermore each species can reduce any other ($r_3, r_4, r_7, r_8, r_{11}, r_{12}$). The dynamics of the species' concentration values in the domain $\Omega = [0; 2]$ is described by the PDEs

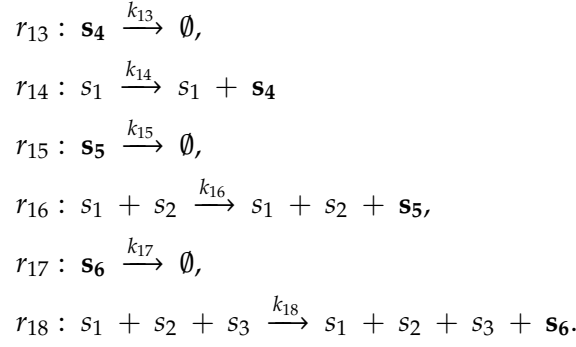
$$\begin{aligned}
 \dot{c}_1 &= \alpha c_1 - \kappa_1 c_1^2 - \mu c_1 c_2 - \mu c_1 c_3 + d_1 \frac{\partial^2 c_1}{\partial x^2}, \\
 \dot{c}_2 &= \beta c_2 - \kappa_2 c_2^2 - (\mu + \gamma) c_2 c_1 - \mu c_2 c_3 + d_2 \frac{\partial^2 c_2}{\partial x^2}, \\
 \dot{c}_3 &= \epsilon c_3 - \kappa_3 c_3^2 - \mu c_3 c_1 - \mu c_3 c_2 + d_3 \frac{\partial^2 c_3}{\partial x^2}.
 \end{aligned} \tag{3.78}$$

Figure 3.9 shows the results of a simulation for the reaction constants $\alpha = 1.156, \beta = 2, \epsilon = 1, \kappa_1 = 2, \kappa_2 = 1.75, \kappa_3 = 0.844$, and $\mu = 1, \gamma = 4.6$, with the diffusion rates $d_1 = d_3 = 0.1$ and $d_2 = 0.2$ and the initial conditions $c_1(0, x) = 0.1, c_2(0, x) = 0.64, c_3(0, x) = 0.31, x \in \Omega$. Figure 3.10 shows the lattice of all subsets of species of the reaction network. All of them are organizations. From [69] we know that the instances of the subsets of species with exactly one species are fixed points and thus their retention time gets longer and longer towards infinity with every passage of the trajectory. Thus they are persistent of course. The retention times of the subsets of species containing exactly two species converge towards strictly positive but finite values and so are persistent too. Nevertheless, the set \mathcal{S} containing all species is not persistent. Thus for this example all species are persistent and the limit superior of them is strictly positive, but the limit inferior equals zero. This is consistent with lemma 3.1.3 in the supplementary material, which states that a strictly positive limit inferior of the concentration values of a species is sufficient for its persistence and

this, in turn, is sufficient for a strictly positive limit superior of the concentration values.

3.1.10 Example III

Here we augment Example II by adding three further species s_4, s_5 and s_6 . Each of these species is involved in two reactions, an outflow reaction reducing the species and a reaction producing the species out of a subset of the set $\{s_1, s_2, s_3\}$,



None of these reactions affects the concentrations of any of the species s_1, s_2 , and s_3 . Also there is no mutual influence among s_4, s_5 and s_6 . Contrary to Example II, the lattice of DOs does not contain all subsets of species since some of them are not closed, for example, the subset $\{s_1\}$. Other subsets are no longer organizations but are still DOs, for example, $\{s_1, s_2\}$.

The dynamics of the concentration values of s_4 to s_6 is determined by the PDEs

$$\begin{aligned}
 \dot{c}_4 &= k_{14}c_1 - k_{13}c_4 + d_4 \frac{\partial^2 c_4}{\partial x^2}, \\
 \dot{c}_5 &= k_{16}c_1c_2 - k_{15}c_5 + d_5 \frac{\partial^2 c_5}{\partial x^2}. \\
 \dot{c}_6 &= k_{18}c_1c_2c_3 - k_{17}c_6 + d_5 \frac{\partial^2 c_6}{\partial x^2}.
 \end{aligned} \tag{3.79}$$

In this example we choose for s_1 to s_3 the same PDEs, reaction constants and initial conditions as in Example II. So we get the same simulation results (see Figure 3.9), that is, a periodic alternate appearing, disappearing, and reappearing of the species $s_1 - s_3$, where each is persistent even though together they do not form a persistent subset.

With the reaction constants $k_{13} = \dots = k_{18} = 0.05$, the homogeneous initial conditions $c_4(x, 0) = c_5(x, 0) = c_6(x, 0) = 0.1, x \in \Omega$, and some arbitrary diffusion constant, we arrive at the simulation result for $c_4 - c_6$ shown in Figure 3.11. The courses of the concentrations $c_1 - c_3$ are the same as in Example II. All species $s_4 - s_6$ are reduced by outflow reactions (r_{13}, r_{15}, r_{17}). For s_4 and s_5 this reduction is compensated by the reactions r_{14} (resp., r_{16}) in the sense that s_4 and s_5 are persistent. For s_6 the reduction by its outflow reaction r_{17} cannot be compensated by reaction r_{18} , that is, s_6 is not persistent but goes extinct in the long-run. The reason for this is that, contrary to r_{14} and r_{16} , the support of r_{18} is not a subset of any persistent subset of species. Figure 3.12 shows for Example II and Example III the sequences of persistent subsets of species traversed repeatedly in the long-run.

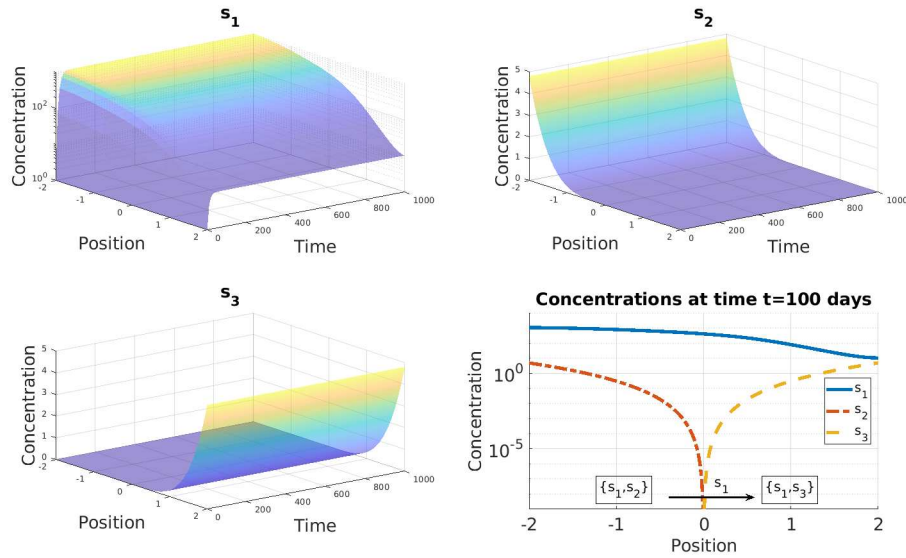


FIGURE 3.8: [76] Simulation result of Example I (see PDEs in Figure 3.7a) performed with MATLAB R2019a function `pdepe`. Note that we applied a logarithmic scale for the diagrams the upper left and in the lower right. The initial conditions are as follows: $c_1^0(x) = 1$ for $x \in \Omega$; $c_2^0(x) = 0.3x^4$ for $x < 0$ and $c_2^0(x) = 0$ for $x \geq 0$; and $c_3^0(x) = 0.3x^4$ for $x \geq 0$ and $c_3^0(x) = 0$ for $x < 0$. The diffusion rates are $d_1 = 5$, $d_2 = d_3 = 0$, that is, only species s_1 diffuses. By the initial conditions, the domain $\Omega = [-2; 2]$ is divided into left and right regions which initially overlap, but the overlap is deleted by the reaction between the two competing species s_2 and s_3 in distinct parts of the domain. Thus, as time approaches infinity, only the species s_1 mediates between the left and right parts of the domain, where each of the two persistent subsets of species persists. In the left part $[-2; 0)$ the species s_1 is overproduced whereas in the right part $(0; 2]$ it is consumed. Altogether diffusion is responsible for the shift of s_1 from the left to the right part of the domain thus maintains the balance of the total concentration of s_1 . Only species s_1 as an intermediary exists in both parts of the domain. The simulation of the solution c of this RDS shows that all three species are persistent and there are two persistent subsets $\{s_1, s_2\}$ and $\{s_1, s_3\}$. From the results of this paper it follows that the set $\Phi(c) = \{s_1, s_2, s_3\}$ of persistent species is a DO and we find from the simulation that it is distributed spatially to the two subsets $\{s_1, s_2\}$ and $\{s_1, s_3\}$.

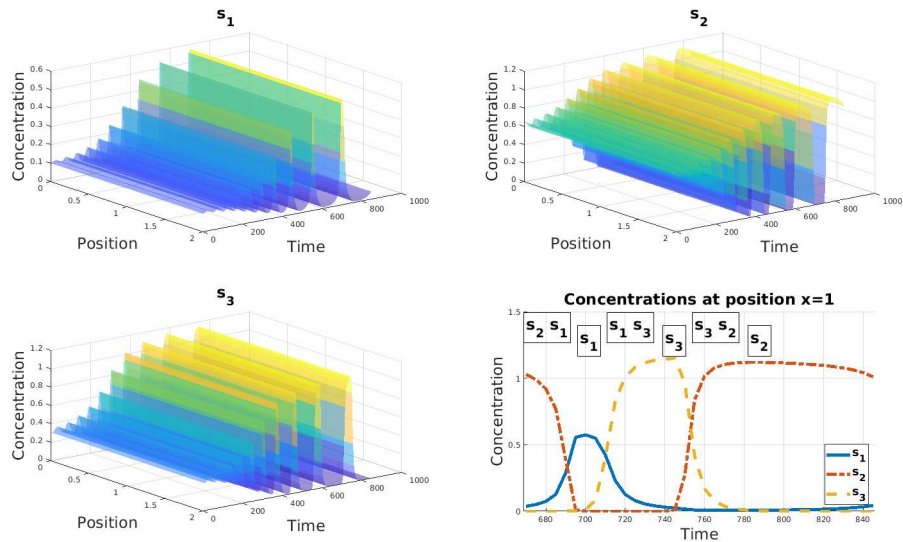


FIGURE 3.9: [76] Simulation result of Example II (see PDEs (3.78)) performed with MATLAB R2019a function `pdepe`. The periodicity (with increasing period) of the dynamic behavior is visible. From the lower right diagram it can be seen how the concentration values periodically approach different subsets of species depicted at the top. Those are the persistent subsets of species, that is, $\{s_1\}$, $\{s_1, s_3\}$, $\{s_3\}$, $\{s_3, s_2\}$, $\{s_2\}$, and $\{s_2, s_1\}$. The periodic behavior continues infinitely beyond the time span captured in the diagrams.

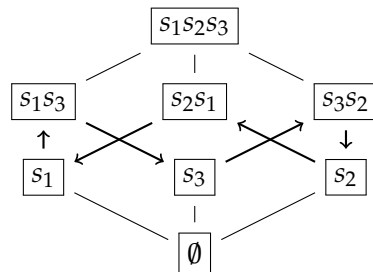


FIGURE 3.10: [76] All subsets of species of the reaction network of Example II are organizations. The arrows indicate the movement that is approached by the trajectory in the long-run.

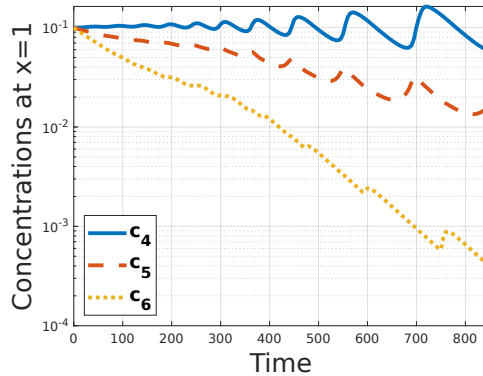
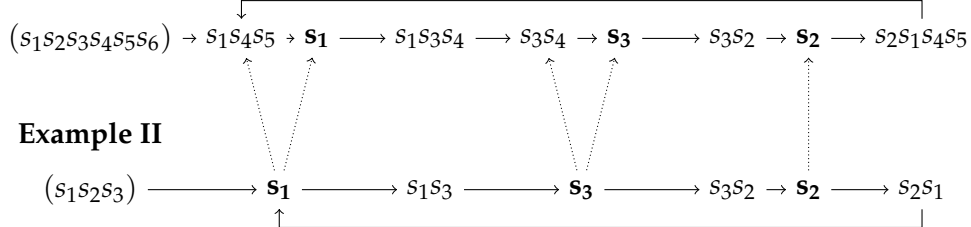


FIGURE 3.11: [76] Simulation result for species $s_4, s_5,$ and s_6 of Example III (see PDEs (3.79)) performed with MATLAB R2019a function `pdepe`. s_4 and s_5 are persistent, whereas s_6 does not persist. The reaction constant values are $k_{13} = \dots = k_{18} = 0.05$, and the homogeneous initial conditions are $c_4(x, 0) = c_5(x, 0) = c_6(x, 0) = 0.1, x \in \Omega$.

Example III



Example II



FIGURE 3.12: [76] The sequences of persistent subsets of species in the order they are periodically approached in the long-run. Shown in brackets are subsets of species referring to the initial conditions. Printed in bold are subsets of species with retention times approaching infinity as $t \rightarrow \infty$. The retention times of the other subsets converge towards finite values. Dotted lines indicate how the infinitely growing time periods of Example II each split into two time periods in Example III. Note that for Example III the transition from $\{s_1, s_4, s_5\}$ to $\{s_1\}$ might pass either the subset $\{s_1, s_4\}$ or $\{s_1, s_5\}$ depending on which of the species s_4 and s_5 vanishes more rapidly. Note that, consistent with the results of this paper, for both examples either of the persistent subsets of species of the illustrated sequences is closed and, together as DOs, they are self-maintaining.

3.2 Organizations in Reaction-Diffusion Systems: Effects of Diffusion and Boundary Conditions

We exemplify how diffusion and especially boundary conditions (BCs) influence the long-term behaviour of reaction-diffusion systems and how the reaction network can be changed accordingly to still exhibit the DOs representing all the possibly persistent sets of species. In Section 3.1 we only applied homogeneous Neumann BCs. Now we incorporate further types of BCs. See Figure 3.13 for an overview of some frequently used BCs, namely Neumann BCs and Dirichlet BCs.

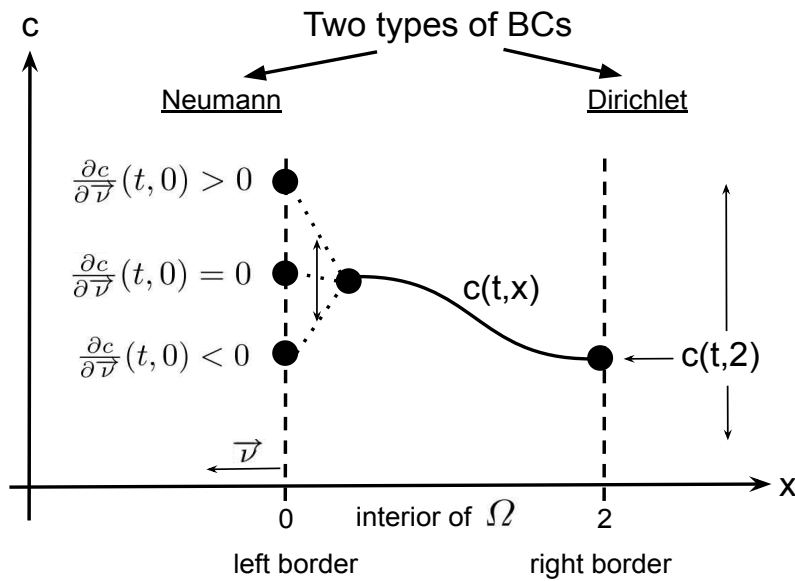


FIGURE 3.13: [74] Illustration of the two main types of BCs for an example domain $\Omega = [0; 2]$: Neumann BC shown at the left boundary $x = 0$ and Dirichlet BC at the right boundary $x = 2$.

For Neumann BCs the derivative $\frac{\partial c}{\partial \nu}(x, t)$ of the concentration with respect to the outward normal vector ν is fixed and for Dirichlet BCs the concentration values $c(x, t)$ are fixed for every $x \in \partial\Omega, t \geq 0$.

The following three Examples Ia, Ib, and Ic are modifications of Example I from Section 3.1.8. See Figure 3.14 to recapitulate the reactions and the lattice of DOs of Example I.

3.2.1 Example Ia

Here we modify Example I by deleting species s_2 completely from the initial state and compensate the lost production of s_1 by changing its BC at the left border of the domain to positive Dirichlet BC. See Figure 3.15 for simulation results. The simulations reveal the DO $\{s_1|s_1, s_3\}$ as the set of persistent species on hand. The DO $\{s_1|s_1, s_3\}$ was not a DO of the reaction network from Example I. But the modified reaction network, which is augmented by an inflow reaction $\emptyset \rightarrow s_1$, exhibits this DO (see Figure 3.16).

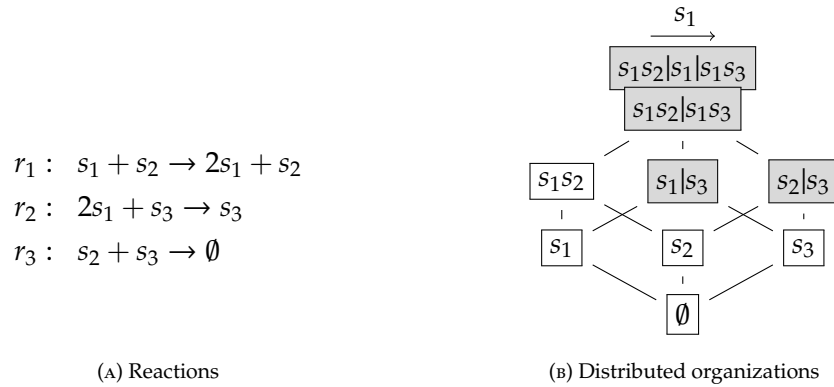


FIGURE 3.14: [76] Reactions and lattice of DOs of Example I. Subfigure (B): Unshaded boxes indicate organizations. Shaded boxes indicate DOs that are not organizations. The horizontal arrow on the top symbolizes the flow of the species s_1 from the subset $\{s_1, s_2\}$, where it is overproduced, to the subset $\{s_1, s_3\}$, where it is reduced. That flow is enabled by diffusion.

3.2.2 Example Ib

Here we modify Example I by allowing all species to diffuse and applying positive Dirichlet BC to s_2 at the left border of the domain and to s_3 at the right border of the domain. See Figure 3.17 for simulation results and Figure 3.18 for the modified reaction network and the respective lattice of DOs.

3.2.3 Example Ic

Here we modify Example I such that all species diffuse, s_2 is deleted from the initial state completely, and a positive Dirichlet BC for s_1 compensates for the missing replication of s_1 by s_2 . See Figure 3.19 for simulation results. The modified reaction network as well as the according lattice of DOs for Example Ic is shown in Figure 3.20.

3.2.4 Summary

In this section we have exemplified how the theory about DOs from Section 3.1 can be extended towards incorporating different boundary conditions. When ignoring BCs or applying homogeneous Neumann BCs solely, the four Examples I, Ia, Ib and Ic all have the same underlying reaction network and thus the same lattice of DOs, namely the one from Example I (see Figure 3.14a). But since the reaction network from Example I does not contain all the different sets of persistent species for the Examples Ia, Ib, and Ic, it is clear, that it is not appropriate to use it to study persistence when different BCs are applied. Nevertheless, for each of the three Examples Ia, Ib and Ic we have shown, that the reaction network can be modified such that it exhibits the right DOs, that is, all the possibly persistent subsets of species. The modifications consisted in adding new inflow reactions to the reaction networks.

We expect that finding appropriate modifications of the reaction network is not so straightforward and unambiguous for all BC as it might seem. Especially when having non-diffusing species it could be helpful to include "virtual" species to incorporate BCs. Such species do not change their own concentration values. But they represent compartments of the domain where the BCs influence the concentrations of

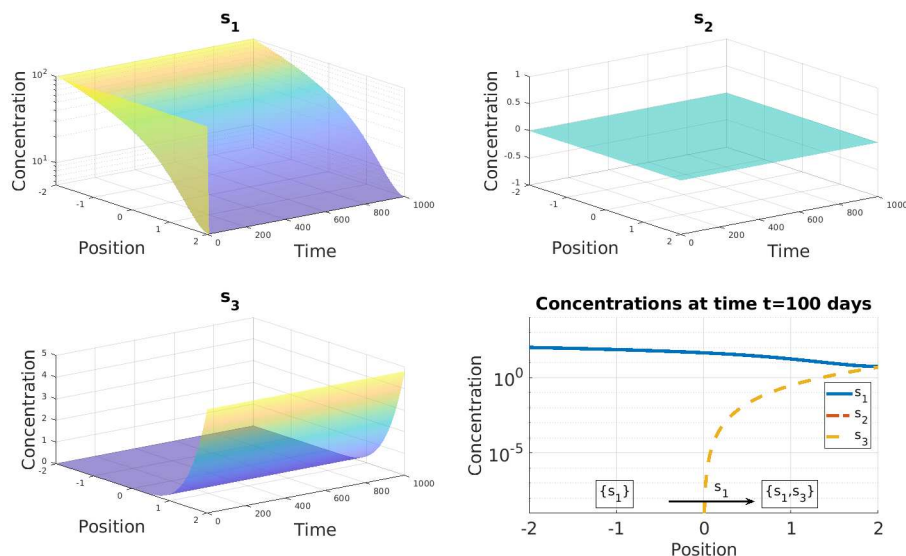


FIGURE 3.15: Simulation result of Example Ia (see PDEs (3.78) from Example I) performed with Matlab R2019a method 'pdepe'. Compared to Example I we made three changes: First, we raised the initial concentration of species s_1 from 1 to 100, that is, $c_1(x, 0) = 100$, $x \in \Omega$. Second, we applied positive Dirichlet BCs to s_1 at the left border, that is, $c_1(-2, t) = 100$, $t \geq 0$. Third, we deleted s_2 from the initial state, that is, $c_2(x, 0) = 0$, $x \in \Omega$. Since s_2 is not present at any point of the domain for all times, s_1 can not be produced with the help of s_2 anymore. But we see that this is compensated by the positive Dirichlet BC of s_1 resulting in almost the same concentration of s_1 in the long-run as it was the case for Example I in Section 3.1.8. As the set of persistent species we find $\{s_1|s_1, s_3\}$ in this simulation, which is a DO of the DO lattice derived from the reaction network of this example, which in turn was modified appropriately to incorporate the positive Dirichlet BC for s_1 (see Figure 3.16). Through diffusion the species s_1 is transferred from the left border of the domain, where it is produced, to the right half of the domain, where it is consumed to due its interaction with s_3 .

the "non-virtual" species. And via "virtual" reactions those "virtual" species influence the "non-virtual" species according to the BCs at hand. A systematic analysis of this topic is still pending.

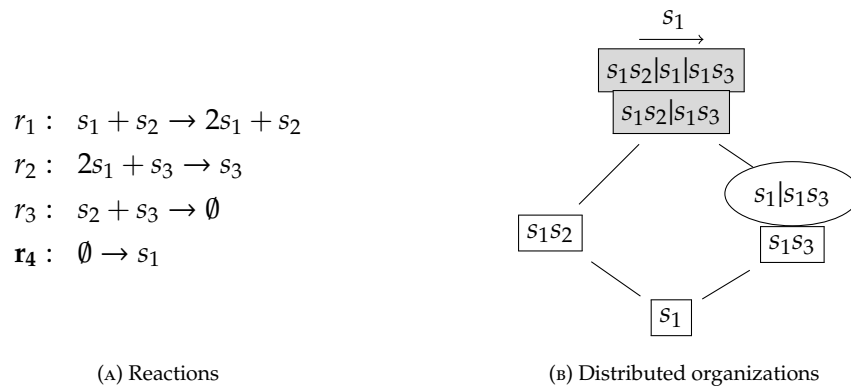


FIGURE 3.16: Modified reaction network (r_4 is added to incorporate the positive Dirichlet BC for s_1) and lattice of DOs of Example Ia. Those boxes with gray background mark DOs that are not organizations. The set of persistent species of the simulation of Example Ia is $\{s_1|s_1s_3\}$, which is marked by an ellipse on the right side of the lattice of DOs. The set $\{s_1s_3\}$ was not a DO for Example I. Its appearance is due to the changed BC of the species s_1 . Note that we did not illustrate all of the possible distributions of the DOs but only those we are interested in for now. For example we did not visualize $\{s_1|s_2\}$ in the lattice of DOs.

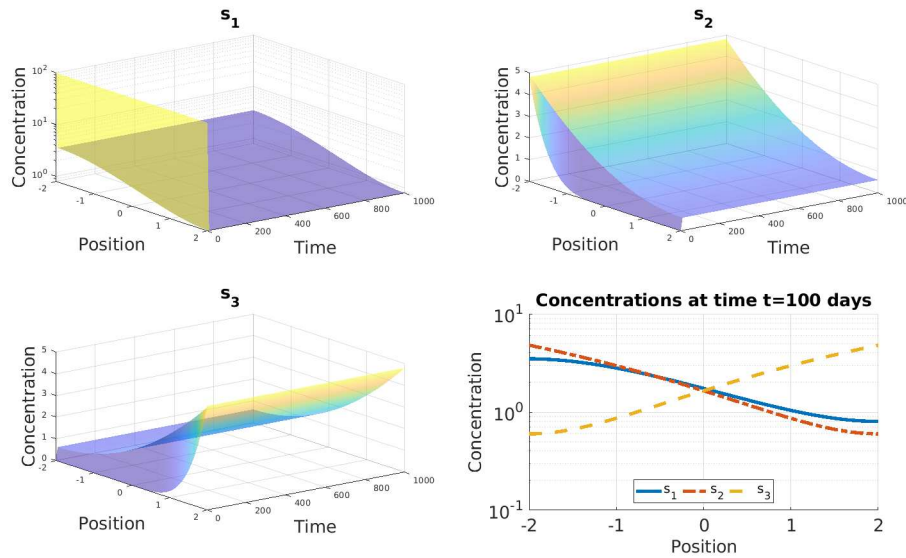


FIGURE 3.17: Simulation result of Example Ib (see PDEs (3.78) from Example I) performed with Matlab R2019a method 'pdepe'. Compared to Example I from Section 3.1.8 we made the following changes: First, as for Example Ia, we raised the initial concentration of species s_1 from 1 to 100, that is, $c_1(x, 0) = 100$, $x \in \Omega$. Second, we applied positive Dirichlet BCs to s_2 at the left border, that is, $c_2(-2, t) = 4.8$, $t \geq 0$, and to s_3 at the right border, that is, $c_3(2, t) = 4.8$, $t \geq 0$. Third, we applied positive diffusion to all species, that is, $d_1 = d_2 = d_3 = 5$. The set of persistent species contains all three species. It is an organization of the modified reaction network shown in Figure 3.18. The mutual destruction of the diffusing species s_2 and s_3 is compensated by their inflows due to their positive Dirichlet BCs. Due to the diffusion there is not any distribution of the species.

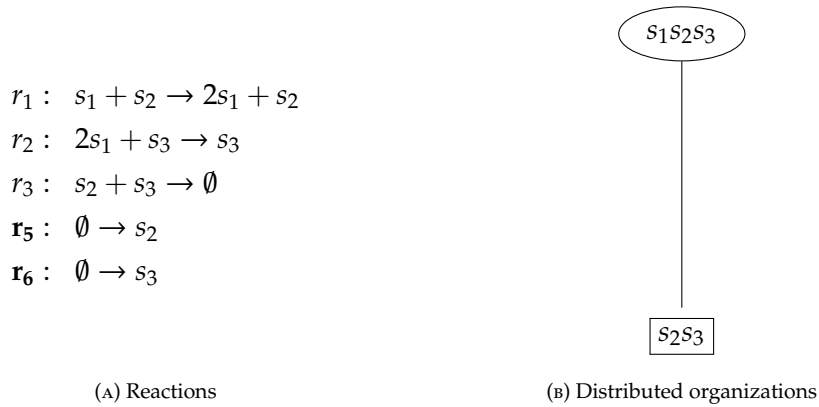


FIGURE 3.18: Modified reaction network (r_5 and r_6 are added to incorporate the positive Dirichlet BC for s_2 resp. s_3) and lattice of DOs of Example Ib. Note, that all depicted DOs are organizations here. Marked by an ellipse: the set $\{s_1, s_2, s_3\}$ of persistent species exhibited by the simulations of Example Ib. This set is an organization of the modified reaction network, but for the reaction network of Example I it existed only as a DO.

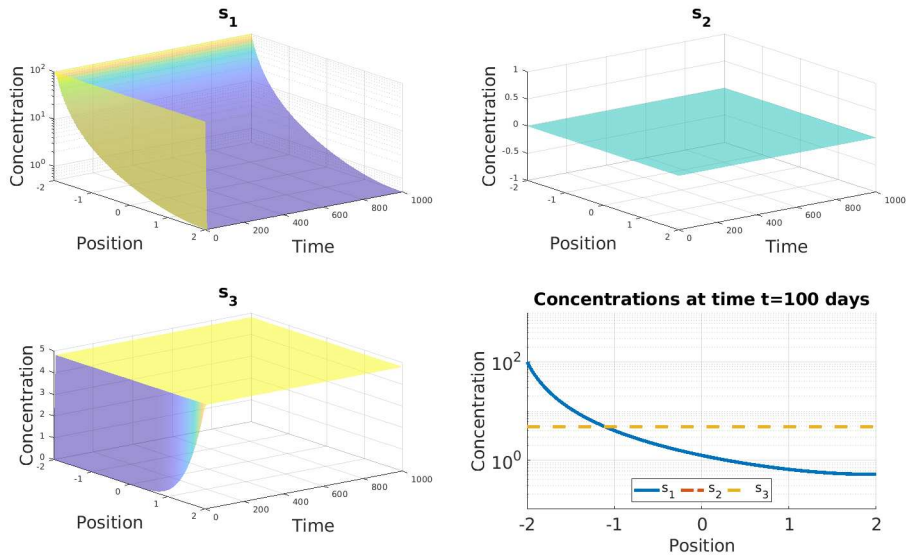


FIGURE 3.19: Simulation result of Example Ic (see PDEs (3.78)) performed with Matlab R2019a method 'pdepe'. Compared to Example I in Section 3.1.8 we only made the following changes: First, as in Example Ia and Ib, we raised the initial concentration of species s_1 from 1 to 100, that is, $c_1(x, 0) = 100$, $x \in \Omega$. Second, as in Example Ib, all species diffuse, that is, $d_1 = d_2 = d_3 = 5$. Third, as in Example Ia, we deleted s_2 from the initial state, that is, $c_2(x, 0) = 0$, $x \in \Omega$. Fourth, as in Example Ia, we applied positive Dirichlet BC to s_1 at the left border, that is, $c_1(-2, t) = 100$, $t \geq 0$. This compensates for the missing replication of s_1 catalyzed by s_2 . The set of persistent species is the organization $\{s_1, s_3\}$.

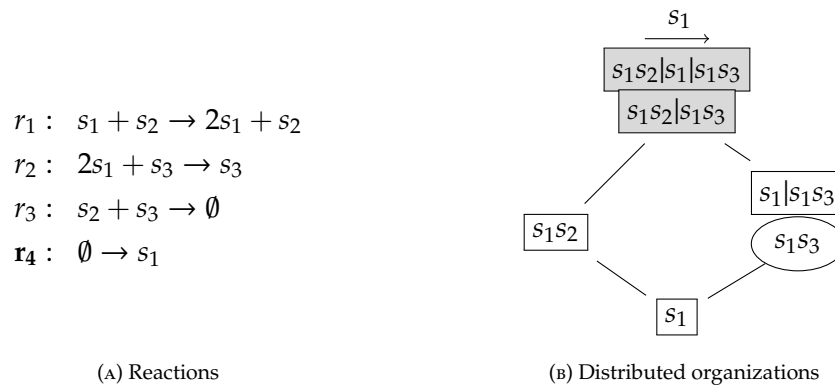


FIGURE 3.20: Modified reaction network (r_4 is added to incorporate the positive Dirichlet BC for s_1) and lattice of DOs of Example Ia. Boxes with white background mark DOs which exist as organizations too. Those boxes with gray background mark DOs that are not organizations. Since the reaction network equals that from Example Ia the lattices of DOs is the same. But here the simulation results exhibited the organization $\{s_1, s_3\}$ as the set of persistent species (marked by an ellipse) and not $\{s_1|s_1, s_3\}$ which was the set of persistent species in Example Ia.

3.3 Structure and Hierarchy of Influenza A Virus Infection Models

In the literature, there exist several mathematical models of IAV dynamics that are derived from experimental data, reviewed in Refs. [84, 9, 21, 11]. These models differ in their complexity, e.g., the number of reactions and the number of species, depending on the available experimental data used for parameter fitting and questions to be answered. For example, models can include eclipse phases, an innate immune response, or an adaptive immune response. We now present the full analysis of twelve influenza models of IAV dynamics, with up to 15 variables (species) and 45 reactions (cf. Table 3.1 for an overview at the end). Note that we refer to a model by the first author's name of the respective publication. Furthermore, note that for our analysis we abstract from kinetic details, that is, the organizations are independent of particular settings of parameter values.

Models

To illustrate our method, we follow a basic ODE model of influenza dynamics, namely the target cell limited model by Baccam *et al.* [5], called Baccam Model in the following. The Baccam Model is based on *in vivo* experimental data and contains three variables: the number of susceptible and uninfected target (epithelial) cells T , the number of infected cells I , and the number of infectious-viral titer V . The dynamical behavior of the variables is given by the ODEs shown in Figure 3.21a. That is, target cells become infected and thus converted to infected cells at a rate βTV , infected cells die spontaneously at rate δI , virus proliferates at a rate pI and dies at a rate cV . The parameters β , δ , p and c are, as usual, positive real numbers (cf. [5] for actual values).

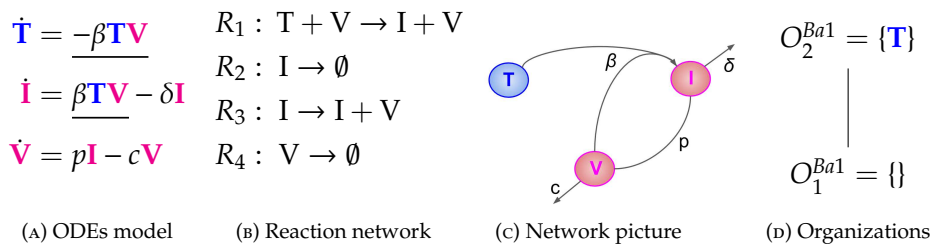


FIGURE 3.21: [75] The **Baccam Model** [5] with 3 variables: uninfected (susceptible) target cells (**T**), infected cells (**I**) and infectious-viral titer (**V**).

The models by Miao *et al.* [61] are designed to fit experimental *in vivo* data from mice [21, 11]. The first one ([61], Equation (1)) depends on measured time-series. The second one ([61], Equation (2)) is a simplified version of the first one, neglecting the terms depending on those time-series and still leading to a good fit within the first 5 days after infection [61]. Thus, we analyze this second model (Miao Model).

Compared to the basic Baccam Model, the Miao Model (Figure 3.22a) has the same three variables (named differently) and one additional reaction, $E_P \rightarrow 2E_P$. This reaction represents the self-replication of target cells E_P taking place at a rate $\rho_E E_P$. The full set of reactions can be found in the Appendix (Figure A.2).

In the lattice of organizations (Figure 3.22b) a new "full" organization O_3^M appears, which contains all three species. Thus organization O_3^M reflects the slight difference

between the two models: in the Baccam Model uninfected target cells T are only the susceptible ones and can not increase in number, but in the Miao Model uninfected cells E_P are reproduced repeatedly by the organism. Thus, in the Baccam Model infection is limited inherently by the limited number of uninfected target cells, while in the Miao Model the limitation of an infection in time and number of infected cells and viruses depends on other mechanisms.

$$\begin{aligned}
 \dot{\mathbf{E}}_P &= \rho_E \mathbf{E}_P - \beta_\alpha \mathbf{E}_P \mathbf{V} & O_3^M &= \{\text{all species}\} = \{\mathbf{E}_P, \mathbf{E}_P^*, \mathbf{V}\} \\
 \dot{\mathbf{E}}_P^* &= \beta_\alpha \mathbf{E}_P \mathbf{V} - \delta_{E^*} \mathbf{E}_P^* & O_2^M &= \{\mathbf{E}_P\} \\
 \dot{\mathbf{V}} &= \pi_\alpha \mathbf{E}_P^* - c_V \mathbf{V} & O_1^M &= \{\}
 \end{aligned}$$

(A) ODE model (B) Diagram of organizations

FIGURE 3.22: [75] The **Miao Model** [61] with 4 variables: uninfected target cells (\mathbf{E}_P), productively infected cells (\mathbf{E}_P^*) and free infectious influenza viruses (\mathbf{V}).

The Baccam II Model [5, 86] contains one more species than the Baccam Model presented in the methods section above. That is, there are now *two* types of infected cells: those which do not yet produce viruses I_1 and those which actively produce viruses I_2 . In addition, there is only one new reaction, which transforms infected cells of type I_1 into type I_2 at rate kI_1 (Figure 3.23a). But the lattice of organizations remains the same when compared with the basic Baccam Model [5].

$$\begin{aligned}
 \dot{\mathbf{T}} &= -\beta \mathbf{T} \mathbf{V} & O_2^{Ba2} &= \{\mathbf{T}\} \\
 \dot{\mathbf{I}}_1 &= \beta \mathbf{T} \mathbf{V} - k \mathbf{I}_1 & O_1^{Ba2} &= \{\} \\
 \dot{\mathbf{I}}_2 &= k \mathbf{I}_1 - \delta \mathbf{I}_2 \\
 \dot{\mathbf{V}} &= p \mathbf{I}_2 - c \mathbf{V}
 \end{aligned}$$

(A) ODE model (B) Lattice of organizations

FIGURE 3.23: [75] The **Baccam II Model** [5] with delayed virus production and 4 variables: uninfected (susceptible) target cells (\mathbf{T}), infected cells not yet producing virus (\mathbf{I}_1), infected cells actively producing virus (\mathbf{I}_2) and infectious-viral titer (\mathbf{V}).

The Pawelek Model [70] contains 11 parameters and was designed to fit *in vivo* experimental data of horses [21, 11]. The model has 5 variables and 9 reactions. Like the basic Baccam Model it contains uninfected target cells (T), infected cells (I), and viruses (V). Furthermore there are two new species: interferon (F) and uninfected cells that are refractory to infections (R), because of the antiviral effect induced by interferon.

Investigating the reaction network (Figure A.4 in the Appendix) derived from the differential equations (Figure 3.24a) we can see that like in the basic Baccam Model self-replication of uninfected cells T is missing. But due to the two new species R and F we have five new reactions, which are neither included in the Baccam Model nor

in the Miao Model. One of these five reactions is the spontaneous decay of interferon F at a rate dF . The other four new reactions describe interactions between different species:

- The rate term ϕFT represents the transformation of uninfected target cells to refractory cells catalysed by interferon.
- The reverse shift back from refractory to simple uninfected cells is represented by the term ρR .
- Furthermore infected cells are deleted by the action of interferon at a rate κIF .
- Interferon is produced in presence of infected cells at a rate qI .

Even though we have more species and more reactions we get the same small pattern of organizations as in the basic Baccam Model (Figure 3.24b). Both models have in common that there is no self-replication of target cells. This might be one reason for the missing of other and bigger organizations which could contain species related to infection and/or immune response. This in turn means that like the Baccam Model this model implicitly treats infections and immune responses as phenomena that can only appear in a limited (transient) time span. The lattice of organizations (Figure 3.24b) tells us that the system necessarily tends towards a state of healthiness, which is represented by the organizations $O_1^P = \{\}$ and $O_2^P = \{T\}$, showing absence of infection and immune response.

$\begin{aligned} \dot{T} &= -\underline{\beta VT} - \phi FT + \rho R \\ \dot{I} &= \underline{\beta VT} - \delta I - \kappa IF \\ \dot{R} &= \phi FT - \rho R \\ \dot{V} &= pI - cV \\ \dot{F} &= qI - dF \end{aligned}$	$O_2^P = \{T\}$ $ $ $O_1^P = \{\}$
(A) ODE model	(B) lattice of organizations

FIGURE 3.24: [75] The Pawelek Model [70] with 5 variables: (uninfected) target cells (T), productively infected cells (I), uninfected cells refractory to infections (R), free viruses (V) and interferon (F).

The Smith Model [85] contains 15 parameters and compared to experimental *in vivo* data from mice. It has 5 variables and 12 reactions. Like in the previous models we have susceptible target cells (T) and viruses (V). Note that T is only consumed in this model but not produced. Contrarily to previous models we have two kinds of infected cells (I_1 and I_2) here as well as bacteria (P). Bacteria P represent *bacterial co-infection* during or after virus infection. Infection is modeled as a transformation of susceptible target cells T into infected cells I_1 catalyzed by viruses V (see underlined terms in Figure 3.25a). Infected cells I_1 in turn spontaneously transform into I_2 at rate kI_1 . Only infected cells I_2 produce viruses V at a rate pI_2 . Furthermore, infected cells I_2 produce viruses V together with bacteria P . Bacteria P are self-replicating (rate term rP). Viruses V are the only species influencing bacteria P .

Figure 3.25b shows the lattice of organizations. The smallest one is the empty set. The biggest one is O_4^{Sm} , which contains susceptible target cells T and bacteria P .

It represents an organism without viral but with bacterial infection. Between those two extreme organizations we find $O_2^{Sm} = \{\mathbf{T}\}$ and $O_3^{Sm} = \{\mathbf{P}\}$. Thus O_2^{Sm} represents the healthy organism without any infection. $O_3^{Sm} = \{\mathbf{P}\}$ could mark the state after a viral-bacterial co-infection: After viral infection and because of the death of all target cells as well as all viruses only bacteria remain.

$$\dot{\mathbf{T}} = -\beta\mathbf{T}\mathbf{V}$$

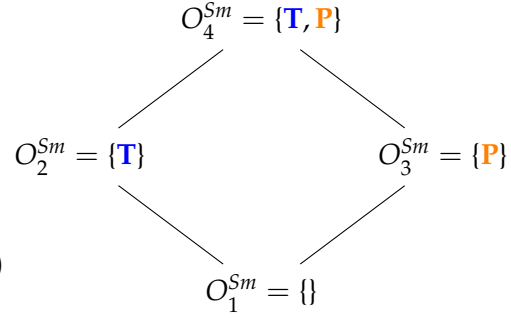
$$\dot{\mathbf{I}}_1 = \beta\mathbf{T}\mathbf{V} - k\mathbf{I}_1 - \mu\mathbf{P}\mathbf{I}_1$$

$$\dot{\mathbf{I}}_2 = k\mathbf{I}_1 - \delta\mathbf{I}_2 - \mu\mathbf{P}\mathbf{I}_2$$

$$\dot{\mathbf{V}} = p\mathbf{I}_2(1 + \mathbf{P}^Z) - c\mathbf{V}$$

$$\dot{\mathbf{P}} = r\mathbf{P}\left(1 - \frac{\mathbf{P}}{K_P(1 + \psi\mathbf{V})}\right) - \gamma_{M_A}n^2 \frac{M_A}{\mathbf{P}^2 + n^2M_A} M_A^* \mathbf{P} \left(1 - \frac{\phi\mathbf{V}}{K_{PV} + \mathbf{V}}\right)$$

(A) ODE model



(B) lattice of organizations

FIGURE 3.25: [75] The **Smith Model** [85] with 5 variables: susceptible target cells (\mathbf{T}), two classes of infected cells (\mathbf{I}_1 and \mathbf{I}_2), free viruses (\mathbf{V}), and bacteria (\mathbf{P}).

The Handel Model [37] contains 8 parameters and was designed to fit experimental *in vivo* data from mice [21, 11, 36]. It has 7 variables (see Figure 3.26) only 12 reactions (see Figure 3.26a):

- *Infection* is catalyzed by viruses V and transforms uninfected cells U to latently infected cells E and viruses V are consumed thereby. Latently infected cells E transform into infected cells I autonomously, which in turn transform into dead cells D autonomously too. Finally, the transformation of dead cells D into non-infected cells U closes the *circle*.
- The *remaining three species* V, F and X form an almost totally separate *subsystem* since the only interaction with the four species from the "circle" mentioned above is the catalysis of the infection by viruses V .
- The *interactions within the subsystem* $\{V, F, X\}$ consisting of viruses V and immune responses F and X are as follows:
 - viruses V catalyze the proliferation of F and X . In the Hernandez model proliferation of interferon F is catalyzed by infected cells instead of viruses.
 - There is no direct interaction between innate immune response F and adaptive immune response X .
 - The adaptive immune response X deletes viruses directly. Innate immune response F inhibits the self-replication of the viruses which is represented by the denominator of the fraction $\frac{p\mathbf{I}}{1 + \kappa\mathbf{F}}$. We ignore the inhibition, because whether the rate is zero or not is independent of F .

The lattice in Figure 3.26b shows five organizations. For the first time it contains the empty set as well as the set of all species at the same time. Between these extremes we

find $O_2^{Ha} = \{\mathbf{U}\}$ representing the healthy organism. The Baccam, Miao, and Pawelek models exhibit the same organization. Structurally the lattice of the Handel Model is very similar to that of the Smith Model (Figure 3.25b). The first reveals an autonomy of the adaptive immune response X whereas the latter does this same for bacteria P .

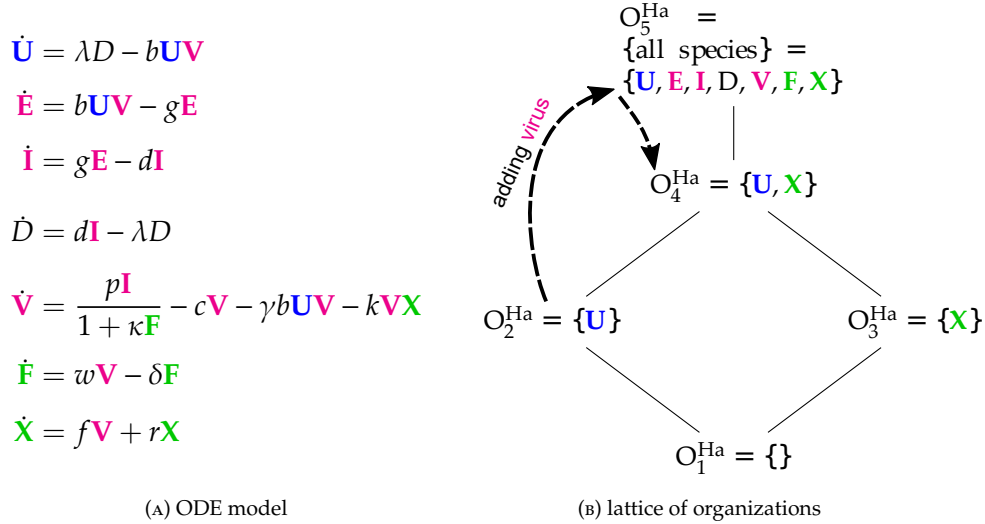


FIGURE 3.26: [75] The **Handel model** [37] with 7 variables: uninfected cells (\mathbf{U}), latently infected cells (\mathbf{E}), productively infected cells (\mathbf{I}), dead cells (\mathbf{D}), free viruses (\mathbf{V}), innate immune response (\mathbf{F}) and adaptive immune response (\mathbf{X}). The dotted arrows denote the projection of the dynamics shown in Figure 3.27

For the Handel Model we perform dynamical simulation in order to show how the organizational hierarchy helps also to understand transient short-term behavior. We start at $t = -20d$ with an uninfected state, i.e., $7 \cdot 10^9$ uninfected cells. After 20 days, at $t = 0$, we add 10^4 virus particles. The resulting seven-dimensional trajectory in state space is shown in Figure 3.27. Projecting this trajectory to organizations results in a more abstract view of the dynamics, shown as dashed curved arrow in Figure 3.26b. The system starts in organization O_2^{Ha} (uninfected organization), moves after adding virus particles at $t = 0$ into organization O_5^{Ha} (infected organization with immune response), and drops after 37 days into organization O_4^{Ha} (immune response active, virus absent).

The projection of a state x to an organization O follows the procedure suggested by Dittrich and Speroni d.F. [19]: First, we generate a set S of those species whose concentration is greater than a particular threshold (here: $10^0 = 1$). Then we generate the closure of this set by adding all species that can be produced from the set. Finally, we take the largest organization O that is a subset of that closure. For example: At $t = 0$ by adding viruses to the system we have $S = \{U, V\}$, whose closure is the set of all species, which is also an organization, here; thus the state at $t = 0$ is projected to organization O_5^{Ha} . At $t = 60d$, we have $S = \{U, X, D\}$, whose closure is again $\{U, X, D\}$ and the largest organization contained is $O_4^{Ha} = \{U, X\}$. So, as can be seen in Figure 3.27, the system state is projected to organization O_4^{Ha} , in which it stays for $t > 37d$.

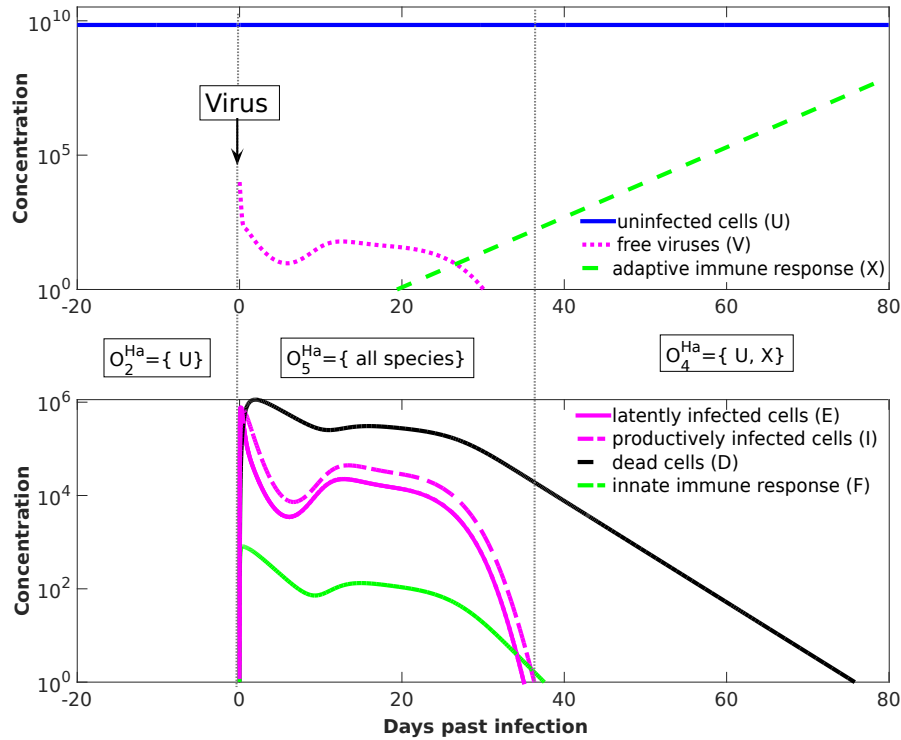


FIGURE 3.27: [75] Temporal dynamics of the Handel model. By projecting the 7-dimensional trajectory to organizations (dotted arrows in Figure 3.26b) we find three phases: (Phase 1) Until day number 0 there are solely $7 \cdot 10^9$ uninfected cells \mathbf{U} in the system represented by the organization $O_2^{Ha} = \{\mathbf{U}\}$. (Phase 2) At day 0 **infection** is simulated by adding $V(0) = 10^4$ virus particles to the system. The resulting state $\{\mathbf{U}, \mathbf{V}\}$ is projected to organization O_5^{Ha} (all species). (Phase 3) Lastly, at day $t=37$ d past infection the system settles in the final organization, namely $O_4^{Ha} = \{\mathbf{U}, \mathbf{X}\}$, which is generated by the set $\{\mathbf{U}, \mathbf{X}, \mathbf{D}\}$ (see text). The values of the model parameters are (from [37]): $\lambda = 0.25$, $b = 2.1 \cdot 10^{-7}$, $g = 4$, $d = 2$, $p = 5 \cdot 10^{-2}$, $\kappa = 1.8 \cdot 10^{-2}$, $c = 10$, $\gamma = 7.5 \cdot 10^{-4}$, $k = 1.8$, $w = 1$, $\delta = 0.4$, $f = 2.7 \cdot 10^{-6}$, and $r = 0.3$. Note that the number of uninfected cells \mathbf{U} is not constant after infection as it may seem from the figure. In fact, after infection the number of uninfected cells first decreases and then rises again [37].

The 13 parameters of the Hernandez Model [40] were fitted to data from many different sources. The model contains 7 variables and 16 reactions (see Figure 3.28). The species refer to viruses (V), interferon (F) and natural killer cells (K) as well as four types of respiratory tract epithelial cells: healthy/uninfected (U_H), partially infected (U_E), infected (U_I) and resistant to infection (U_R). Compared to the Pawelek Model there are two qualitatively new species: partially infected cells U_E and killers K .

Next we state some remarks about the reactions:

- There is an *infection* reaction catalyzed by viruses like in all previous models but with one difference: during infection, healthy cells U_H first transform to *partially infected* cells U_E and only after that they transform spontaneously to infected cells U_I at a rate $k_e U_E$.
- *Interferon* catalyzes the transformation of healthy cells to resistant cells U_R , like in the Pawelek Model. But in the Pawelek Model interferon removes infected

cells. Here, interferon's production is catalyzed by infected cells U_I at a rate $a_I U_I$. There is no further influence of interferon on any other species.

- Infected cells are removed by natural *killers* K , which also delete partially infected cells in this model. The production of *killers* K is catalyzed by infected cells U_I at a rate $\Phi_K U_I$.
- Note that here we have an constant *inflow of healthy cells* U_H at a rate S_H (first differential equation). Thus healthy cells cannot converge to zero.

The lattice of organizations consists only of two organization (Figure 3.28b). For the first time the empty set is not an organization, because the empty set is not closed due to a constant inflow of healthy cells U_H and killers K , represented by the reaction $\emptyset \rightarrow U_H$ and $\emptyset \rightarrow K$, respectively. The smallest organization $O_1^{He} = \{U_H, K\}$ can be regarded as a state of healthiness. Contrarily the second organization O_2^{He} contains all species (as in the Miao Model) and therefore can be interpreted as the infected organism exhibiting immune response to infection.

$\begin{aligned} \dot{U}_H &= S_H - k_I U_H V - k_R U_H F - \delta_H U_H \\ \dot{U}_E &= k_I U_H V - k_E U_E - q_K U_E K \\ \dot{U}_I &= k_E U_E - \delta_I U_I - q_K U_I K \\ \dot{U}_R &= k_R U_H F - \delta_R U_R \\ \dot{V} &= \rho_V U_I - \delta_V V \\ \dot{F} &= a_I U_I - \delta_F F \\ \dot{K} &= S_K + \Phi_K U_I - \delta_K K \end{aligned}$ <p style="text-align: center;">(A) ODE model</p>	$\begin{aligned} O_2^{He} &= \\ \{all\ species\} &= \\ \{U_H, U_E, U_I, U_R, V, F, K\} & \\ & \Bigg \\ O_1^{He} &= \{U_H, K\} \end{aligned}$ <p style="text-align: center;">(B) lattice of organizations</p>
---	---

FIGURE 3.28: [75] The **Hernandez Model** [40] with 7 variables: healthy cells (U_H), partially infected cell (U_E), infected cells (U_I), cells resistant to infection (U_R), virus particles (V), interferon (F) and natural killers (K).

The Cao Model [13] consists of 20 parameters and has been derived by referring to experimental data from ferrets. The model has 7 variables and 26 reactions. Like in most of the previous models we have (uninfected) target cells (T), infected cells (I), viruses (V), resistant cells (R), and interferon (F). Furthermore there are B cells B and antibodies A .

According to the ODE shown in Figure 3.29a B cells are only influenced by viruses: viruses support the production of B cells (rate term $m_1 V$) but the more B cells are present the more of them are destroyed by viruses again (term: $m_1 V B$). B cells influence only one other species namely antibodies B , which they produce. Antibodies A influence only one other species, namely viruses, which are destroyed by this reaction at rate $\mu V A$. Antibodies in turn are influenced by B cells positively and by viruses negatively.

There are three organizations in this model (Figure 3.29b): the empty set, the healthy organism without any infection and without any immune response ($O_2^C = \{T\}$) and the organization O_3^C containing all species.

$$\begin{aligned}
\dot{\mathbf{T}} &= g(\mathbf{T} + \mathbf{R})\left(1 - \frac{\mathbf{T} + \mathbf{R} + \mathbf{I}}{C_t}\right) - \beta' \mathbf{V}\mathbf{T} + \rho \mathbf{R} - \phi \mathbf{F}\mathbf{T} \\
\dot{\mathbf{I}} &= \beta' \mathbf{V}\mathbf{T} - \delta \mathbf{I} - \kappa \mathbf{I}\mathbf{F} \\
\dot{\mathbf{V}} &= \frac{p \mathbf{I}}{1 + s \mathbf{F}} - c \mathbf{V} - \mu \mathbf{V}\mathbf{A} - \beta \mathbf{V}\mathbf{T} \\
\dot{\mathbf{R}} &= \phi \mathbf{F}\mathbf{T} - \rho \mathbf{R} - \xi \mathbf{R} \\
\dot{\mathbf{F}} &= q \mathbf{I} - d \mathbf{F} \\
\dot{\mathbf{B}} &= m_1 \mathbf{V}(1 - \mathbf{B}) - m_2 \mathbf{B} \\
\dot{\mathbf{A}} &= m_3 \mathbf{B} - r \mathbf{A} - \mu' \mathbf{V}\mathbf{A}
\end{aligned}$$

(A) ODE model

$$\begin{aligned}
O_3^C &= \\
\{\text{all species}\} &= \\
\{\mathbf{T}, \mathbf{I}, \mathbf{V}, \mathbf{R}, \mathbf{F}, \mathbf{B}, \mathbf{A}\} & \\
& \quad | \\
O_2^C &= \{\mathbf{T}\} \\
& \quad | \\
O_1^C &= \{\}
\end{aligned}$$

(B) Lattice of organizations

FIGURE 3.29: [75] The **Cao Model** [13] with 7 variables: target cells (**T**), infected cells (**I**), viruses (**V**), resistant cells (**R**), interferon (**F**), B cells (**B**), and antibodies (**A**).

The Saenz Model [80] requires 12 parameters and was designed to fit experimental *in vivo* data from horses [21, 11]. The model contains 8 variables and 12 reactions (Figure 3.30a). There are no adaptive immune response, no dead cells, and no natural killer cells. However, the model contains viruses V and interferon F . There is an eclipse phase (E_1 and E_2) here as well as prerefractory and refractory cells. In particular, epithelial cells are represented by six species: susceptible (T), eclipse phases (E_1 and E_2), infectious (I), prerefractory (W), and refractory (R). Thus the new features are the inclusion of two eclipse phases and three steps for the transformation of uninfected cells to refractory cells.

The lattice of organizations is composed by four organizations: $O_1^{Sa} = \{\}$: the empty set; $O_2^{Sa} = \{\mathbf{T}\}$: representing a healthy organism; $O_3^{Sa} = \{\mathbf{R}\}$: there is no consuming reaction for refractory cells R ; $O_4^{Sa} = \{\mathbf{T}, \mathbf{R}\}$: also representing a healthy organism that contains refractory cells maybe as remains of a previous infection.

The lattice is very similar to that from of the Handel Model. There are only two differences:

- The "full" organization is missing here. For sure, one of the reasons is that there is no reaction producing susceptible cells T . Thus, when viruses V or interferon F are present susceptible cells T can not survive and the "full" organization neither.
- Adaptive immune response is replaced by refractory cells in the organizations here.

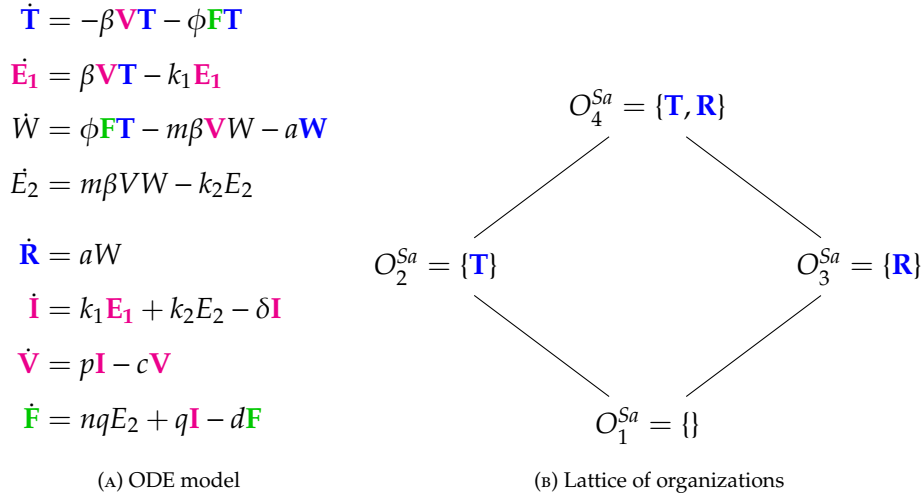


FIGURE 3.30: [75] The **Saenz Model** [80] with 8 variables: Epithelial cells in one of the states: susceptible (**T**), eclipse phase (**E₁** and **E₂**), prerefractory (**W**), refractory (**R**) and infectious (**I**). The further variables are: virus cells (**V**) and interferon (**F**).

The Hancioglu Model [34] contains 11 variables and 35 reactions. It has not been mathematically fitted to data, but has been designed to meet specific general criteria [21, 11]. The ODEs (Figure 3.31a) describe the dynamics of the following 10 species: viruses (**V**), healthy cells (**H**), infected cells (**I**), interferon (**F**) and resistant cells (**R**). The remaining species are new: antigen presenting cells (**M**), effector cells (**E**), plasma cells (**P**) antibodies (**A**) and antigenic distance (**S**). There are no species for an eclipse phase in this model.

Looking at the reaction network (Figure A.8) we can see again a reaction for *infection*, i.e., the transformation of healthy cells **H** into infected cells **I** catalyzed by viruses **V** at a rate $\gamma_{HV}VH$ (single underlined in Figure 3.31a). Furthermore, *interferon* **F** is produced catalytically by antigen presenting **M** and infected cells **I**, decays spontaneously at a rate a_FF , and is additionally removed when converting healthy cells **H** into resistant cells **R** by the reaction $H + F \rightarrow R$ at rate $b_{HF}FH$ (double underlined in Figure 3.31a).

The Hancioglu Model has four organizations (Figure 3.31b):

- O_1^{Hcg} and O_3^{Hcg} contain only species responsible for the *immune response* and neither healthy cells nor species representing infection. Thus, these two organizations are practically not realistic.
- O_2^{Hcg} represents the healthy state of the organism.
- O_4^{Hcg} , which contains all species, represents the infected organism with immune response.

$$\dot{\mathbf{H}} = b_{HD}D(\mathbf{H} + \mathbf{R}) + a_R\mathbf{R} - \gamma_{HV}\mathbf{V}\mathbf{H} - b_{HF}\mathbf{F}\mathbf{H}$$

$$\dot{\mathbf{I}} = \gamma_{HV}\mathbf{V}\mathbf{H} - b_{IE}\mathbf{E}\mathbf{I} - a_I\mathbf{I}$$

$$\dot{\mathbf{V}} = \gamma_V\mathbf{I} - \gamma_{VA}S\mathbf{A}\mathbf{V} - \gamma_{VH}\mathbf{H}\mathbf{V} - \alpha_V\mathbf{V} - \frac{a_{V1}\mathbf{V}}{1 + a_{V2}\mathbf{V}}$$

$$\dot{\mathbf{R}} = b_{HF}\mathbf{F}\mathbf{H} - a_R\mathbf{R}$$

$$\dot{M} = (b_{MD}D + b_{MV}\mathbf{V})(1 - M) - a_MM$$

$$\dot{\mathbf{F}} = b_FM + c_F\mathbf{I} - b_{FH}\mathbf{H}\mathbf{F} - a_F\mathbf{F}$$

$$\dot{\mathbf{E}} = b_{EM}M\mathbf{E} - b_{EI}\mathbf{I}\mathbf{E} + a_E(1 - \mathbf{E})$$

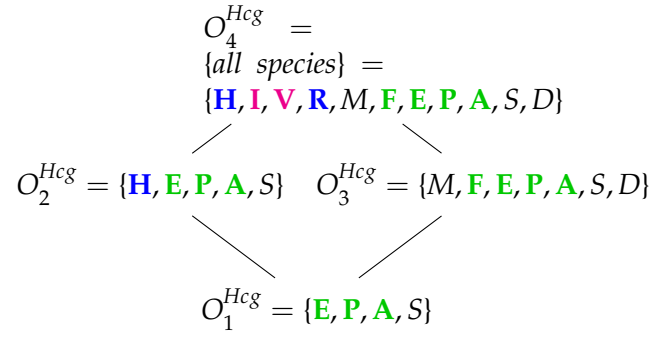
$$\dot{\mathbf{P}} = b_{PM}M\mathbf{P} + a_P(1 - \mathbf{P})$$

$$\dot{\mathbf{A}} = b_A\mathbf{P} - \gamma_{AV}S\mathbf{A}\mathbf{V} - a_A\mathbf{A}$$

$$\dot{S} = r\mathbf{P}(1 - S)$$

$$\dot{D} = -b_{HD}D\mathbf{H} - b_{HD}D\mathbf{R} + b_{IE}\mathbf{E}\mathbf{I} + a_I\mathbf{I}$$

(A) ODE model



(B) Lattice of organizations

FIGURE 3.31: [75] The **Hancioglu Model** [34] with 11 variables: viral load (\mathbf{V}), healthy cells (\mathbf{H}), infected cells (\mathbf{I}), antigen presenting cells (M), interferon (\mathbf{F}), resistant cells (\mathbf{R}), effector cells (\mathbf{E}), plasma cells (\mathbf{P}), antibodies (\mathbf{A}), antigenic distance (S) and dead cells (D).

The Bocharov Model [10] contains 49 parameters and was designed to fit experimental *in vivo* data from humans [21, 11]. It includes 11 variables and 35 reactions (Figure A.9). Only here and in the Lee Model (below) we have differential equations with *delay*, i.e., some rates depend on variable values from the past (Figure 3.32a). Because the delay does not matter in a steady-state, we can also neglect the delay when analyzing the chemical organizations of a delay differential equation model.

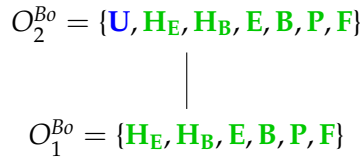
Note that this is by far the oldest model analyzed here. The names of the variables are a bit particular when compared to those of the previously analyzed models. As in all the other models we have viruses V_f and infected cells C . Furthermore, there are destroyed epithelial cells m as in the Handel Model. All other species belong to the immune response. Note that only in this model there is no state variable for uninfected, healthy cells. Bocharov *et al.* represent these healthy cells implicitly by subtracting the amounts of infected-cells C and destroyed epithelial cells m from the initial total amount of target epithelial cells C^* . Since all the other models analyzed here have a related variable, we inserted the variable $U = C^* - C - m$ for uninfected cells together with its ODE to make the model comparable to the others.

Due to the fact that the majority of the species belongs to the immune response this is the case for most of the reactions too. These species of the immune response form exactly the organization O_1^{Bo} , only macrophages M_V are missing.

Similarly to the Hancioglu model the smallest organization O_1^{Bo} is an organization with immune response but without infection (C, V_f). There is only one further organization that contains only one more species than O_1^{Bo} namely uninfected cells U . This organization we already found in three of the previous models. However, for the first time there is no bigger organization in this model. Thus, virus infection is necessarily transient.

$$\begin{aligned}
\dot{\mathbf{V}}_f &= \nu \mathbf{C} + nb_{CE} \mathbf{C} \mathbf{E} - \gamma_{VF} \mathbf{V}_f \mathbf{F} - \gamma_{VM} \mathbf{V}_f - \gamma_{VC} \mathbf{V}_f \mathbf{U} \\
\dot{\mathbf{C}} &= \sigma \mathbf{V}_f \mathbf{U} - b_{CE} \mathbf{C} \mathbf{E} - b_m \mathbf{C} \\
\dot{m} &= b_{CE} \mathbf{C} \mathbf{E} + b_m \mathbf{C} - \alpha_m m \\
\dot{\mathbf{M}}_V &= \gamma_{MV} M^* \mathbf{V}_f - \alpha_M \mathbf{M}_V \\
\dot{\mathbf{H}}_E &= b_H^E \left[\left(1 - \frac{m}{C^*}\right) \rho_H^E \mathbf{M}_V (t - \tau_H^E) \mathbf{H}_E (t - \tau_H^E) - \mathbf{M}_V \mathbf{H}_E \right] - b_P^{H_E} \mathbf{M}_V \mathbf{H}_E \mathbf{E} + \alpha_H^E (H_E^* - \mathbf{H}_E) \\
\dot{\mathbf{H}}_B &= b_H^B \left[\left(1 - \frac{m}{C^*}\right) \rho_H^B \mathbf{M}_V (t - \tau_H^B) \mathbf{H}_B (t - \tau_H^B) - \mathbf{M}_V \mathbf{H}_B \right] - b_P^{H_B} \mathbf{M}_V \mathbf{H}_B \mathbf{B} + \alpha_H^B (H_B^* - \mathbf{H}_B) \\
\dot{\mathbf{E}} &= b_P^E \left[\left(1 - \frac{m}{C^*}\right) \rho_E \mathbf{M}_V ((t - \tau_E)) \mathbf{H}_E (t - \tau_E) \mathbf{E} (t - \tau_E) - \mathbf{M}_V \mathbf{H}_E \mathbf{E} \right] - b_{EC} \mathbf{C}_V \mathbf{E} + \alpha_E (E^* - \mathbf{E}) \\
\dot{\mathbf{B}} &= b_P^B \left[\left(1 - \frac{m}{C^*}\right) \rho_B \mathbf{M}_V (t - \tau_B) \mathbf{H}_B (t - \tau_B) \mathbf{B} (t - \tau_B) - \mathbf{M}_V \mathbf{H}_B \mathbf{B} \right] + \alpha_E (B^* - \mathbf{B}) \\
\dot{\mathbf{P}} &= b_P^P \left(1 - \frac{m}{C^*}\right) \rho_P \mathbf{M}_V (t - \tau^P) \mathbf{H}_B (t - \tau_P) \mathbf{B} (t - \tau_P) + \alpha_P (P^* - P) \\
\dot{\mathbf{F}} &= \rho_F \mathbf{P} - \gamma_{FV} \mathbf{F} \mathbf{V}_f - \alpha_F \mathbf{F} \\
\dot{\mathbf{U}} &= \frac{d}{dt} (C^* - \mathbf{C} - m) = -\sigma \mathbf{V}_f \mathbf{U} + \alpha_m m
\end{aligned}$$

(A) ODE model



(B) Hasse diagram of organizations

FIGURE 3.32: [75] The **Bocharov Model** [10] with 10 variables: infective IAV particles (\mathbf{V}_f), IAV-infected cells (\mathbf{C}), destroyed epithelial cells (m), stimulated macrophages (\mathbf{M}_V), activated helper T cells providing proliferation of cytotoxic T cells (\mathbf{H}_E), activated helper T cells providing proliferation and differentiation of B cells B (\mathbf{H}_B), activated CTL (\mathbf{E}), B cells (\mathbf{B}), plasma cells (\mathbf{P}), antibodies to IAV (\mathbf{F}), and uninfected epithelial cells (\mathbf{U}). Note that, for clarity, we have added \mathbf{U} as a state variable, which is only implicitly represented as $\mathbf{U} = C^* - \mathbf{C} - m$ in the original model by Bocharov *et al.*

The Lee Model [58] is the most complex model considered here. It contains 48 parameters and was designed with respect to experimental *in vivo* data from mice [21, 11]. It has 15 variables and 37 reactions (Figure A.10). Like in the Bocharov Model, Lee *et al.* apply delay differential equations.

Note that this model is the only one analyzed here that distinguishes between *lung compartment* and *lymphatic compartment*. There is one species representing uninfected (healthy) cells \mathbf{E}_p and three species for modelling *infection*: \mathbf{E}_p^* , \mathbf{D}^* and viruses \mathbf{V} . The remaining species belong to the *immune response*, colored black when naive to infection, while colored green when activated for infection.

Note that we write a species in the *organizations* in Figure 3.34 in bold text, if it is

"new", that is, not contained in neither of its subset organizations. The Hasse diagram contains 8 organizations. The smallest one is $O_1^L = \{\mathbf{E}_P, \mathbf{D}, H_N, T_N, B_N\}$ and contains exactly the uninfected cells as well as the naive part of the immune response. The biggest organization contains all species. Between these two "extreme" organizations are 6 further organizations containing different parts of the activated part of the immune response.

$$\begin{aligned}
\dot{\mathbf{E}}_P &= \delta_E(E_0 - \mathbf{E}_P) - \beta_E \mathbf{E}_P \mathbf{V} \\
\dot{\mathbf{E}}_P^* &= \beta_E \mathbf{E}_P \mathbf{V} - k_E \mathbf{E}_P^* \gamma \mathbf{T}_E(t - \tau_T) - \delta_{E^*} \mathbf{E}_P^* \\
\dot{\mathbf{V}} &= \pi_V \mathbf{E}_P^* - c_V \mathbf{V} - k_V \mathbf{V} \mathbf{A}(t) \\
\dot{\mathbf{D}} &= \delta_D(D_0 - \mathbf{D}) - \beta_D \mathbf{D} \mathbf{V} \\
\dot{\mathbf{D}}^* &= \beta_D \mathbf{D} \mathbf{V} - \delta_{D^*} \mathbf{D}^* \\
\dot{\mathbf{D}}_M &= k_D \mathbf{D}^*(t - \tau_D) - \delta_{D_M} \mathbf{D}_M \\
\dot{H}_N &= \delta_{H_N}(H_{N0} - H_N) - \pi_{H1} \frac{\mathbf{D}_M}{\mathbf{D}_M + \pi_{H2}} H_N \\
\dot{H}_E &= \pi_{H1} \frac{\mathbf{D}_M}{\mathbf{D}_M + \pi_{H2}} H_N + \rho_{H1} \frac{\mathbf{D}_M}{\mathbf{D}_M + \rho_{H2}} H_E - \delta_{H1} \frac{\mathbf{D}_M}{\mathbf{D}_M + \delta_{H2}} H_E \\
\dot{T}_N &= \delta_{T_N}(T_{N0} - T_N) - \pi_{T1} \frac{\mathbf{D}_M}{\mathbf{D}_M + \pi_{T2}} T_N \\
\dot{T}_E &= \pi_{T1} \frac{\mathbf{D}_M}{\mathbf{D}_M + \pi_{T2}} H_N + \rho_{T1} \frac{\mathbf{D}_M}{\mathbf{D}_M + \rho_{T2}} T_E - \delta_{T1} \frac{\mathbf{D}_M}{\mathbf{D}_M + \delta_{T2}} T_E \\
\dot{B}_N &= \delta_B(B_{N0} - B_N) - \pi_{B1} \frac{\mathbf{D}_M}{\mathbf{D}_M + \pi_{B2}} B_N \\
\dot{B}_A &= \pi_{B1} \frac{\mathbf{D}_M}{\mathbf{D}_M + \pi_{B2}} B_N + \rho_{B1} \frac{\mathbf{D}_M + h H_E}{\mathbf{D}_M + h H_E + \rho_{B2}} B_A - \delta_{B_A} B_A - \pi_S B_A - \pi_L H_E B_A \\
\dot{P}_S &= \pi_S B_A - \delta_S P_S \\
\dot{P}_L &= \pi_L H_E B_A - \delta_L P_L \\
\dot{A} &= \pi_{A_S} P_S + \pi - AL P_L - \delta_A A
\end{aligned}$$

FIGURE 3.33: [75] ODEs of the **Lee model** [58] which contains 15 variables: uninfected epithelial cells (\mathbf{E}_P), infected epithelial cells (\mathbf{E}_P^*), virus titer (EID_{50}/ml) (\mathbf{V}), immature dendritic cells (\mathbf{D}), virus-loaded dendritic cells (\mathbf{D}^*), mature dendritic cells (\mathbf{D}_M), naive CD4+ T cells (H_N), effector CD4+ T cells (H_E), naive CD8+ T cells (T_N), effector CD8+ T cells (T_E), naive B cells (B_N), activated B cells (B_A), short-lived plasma (antibody-secreting) B cells (P_S), long-lived plasma (antibody-secreting) B cells (P_L) and antiviral antibody titer (A). Note that here we have colored green only those species representing the **immune system when activated**.

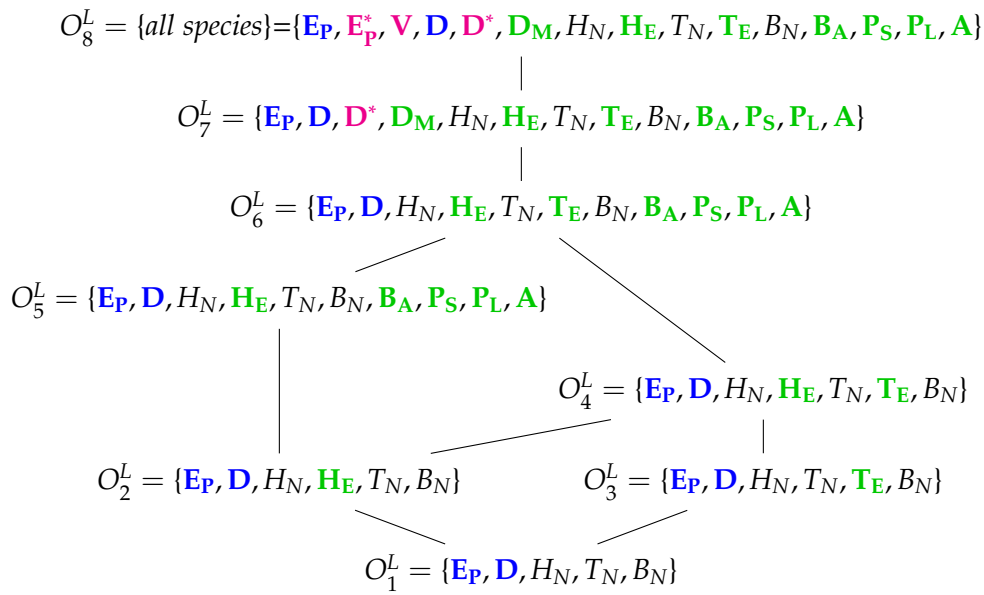


FIGURE 3.34: [75] Hasse diagram of organizations of the **Lee model** [58].

Hierarchy of influenza A virus models

In order to construct a hierarchical map of all investigated models, we characterize a model by a signature of organizations, which is a set of organization types. For example, the signature of the Handel Model (Figure 3.26b) is the set $\{\emptyset, \mathbf{X}, \mathbf{X}, \mathbf{XX}, \mathbf{XXX}\}$. An organization type like \mathbf{XX} means that there is at least one organization that contains uninfected (target) cells (\mathbf{X}) and species of the active immune response (\mathbf{X}). The signatures of all are models is shown in Table 3.1.

Model	Number of variables	Number of reactions	Number of organizations	Organizations & Signature
Baccam [5] 2006	3	4	2	$O_1^{Ba1} = \emptyset$ O_2^{Ba1} X
Miao [61] 2010	3	5	3	$O_1^M = \emptyset$ O_2^M X O_3^M X X
Baccam II [5] 2006	4	5	2	$O_1^{Ba2} = \emptyset$ O_2^{Ba2} X
Pawelek [70] 2012	5	9	2	$O_1^P = \emptyset$ O_2^P X
Smith [85] 2016	5	12	4	$O_1^{Sm} = \emptyset$ O_2^{Sm} X O_3^{Sm} X O_4^{Sm} X X
Handel [37] 2010	7	12	5	$O_1^{Ha} = \emptyset$ O_2^{Ha} X O_3^{Ha} X O_4^{Ha} X X $O_5^{Ha} = \{all\}$ X X X
Hernandez [40] 2012	7	16	2	$O_1^{He} = \emptyset$ X X $O_2^{He} = \{all\}$ X X X
Cao [13] 2015	7	26	3	$O_1^C = \emptyset$ O_2^C X $O_3^C = \{all\}$ X X X
Saenz [80] 2010	8	12	4	$O_1^{Sa} = \emptyset$ $O_2^{Sa}, O_3^{Sa}, O_4^{Sa}$ X
Bocharov [10] 1994	10	45	2	$O_1^{Bo} = \emptyset$ X O_2^{Bo} X X
Hancioglu [34] 2007	11	35	4	O_1^{Hcg}, O_3^{Hcg} X O_2^{Hcg} X X $O_4^{Hcg} = \{all\}$ X X X
Lee [58] 2009	15	37	8	$O_1^L = \emptyset$ X $O_2^L, O_3^L, O_4^L, O_5^L, O_6^L$ X X $O_7^L, O_8^L = \{all\}$ X X X

TABLE 3.1: [75] Overview of all models and organization types contained. An organization type like **XX** denotes the type of species contained in an organization, according to our coloring scheme. The set of organization types of a model is called its signature.

Note that we ignore species colored black. We include the empty set \emptyset , because

this distinguishes models without any inflow from those that possess an inflow of some species. Now we can obtain a partial order among models by defining that a model A is smaller or equal to another model B ($A \leq B$), if the signature of A is a subset of the signature of model B. For example, the Hernandez Model is smaller than the Lee Model, because $\{XX, XXX\} \subseteq \{X, XX, XXX\}$. This partial order among models leads to a hierarchical map of models, which is visualized by a Hasse-diagram in Figure 3.35. Note that a model A that is smaller than a model B according to this partial order can possess more species and reactions than B.

In Figure 3.35 we can see that all models have organizations with uninfected, healthy cells (X). There are models that furthermore have infection (X) and/or immune response (X) in their organizations. There are exactly two models (Hancioglu and Hernandez Model) with immune response in all their organizations which means that these models implicitly assume immune response to be active all the time. Among the models neglecting immune response are those which have infection (Miao Model) or bacteria (X) (Smith Model) in their organizations and also those that do not (Baccam and Baccam II Model). For models involving immune response the situation is more complex. There are those that only have healthy cells in their organizations (Pawelek and Saenz Models). This means that these models implicitly exclude infection and immune response from the long run and thus treat them as transient phenomena a priori. The Bocharov Model is the only one that exhibits only healthy cells and immune response in its organizations but no infection. The remaining five models include all kinds of species (except for bacteria of course) in their organizations.

By looking at the hierarchy of models it becomes evident that there is space for more models. Above the Smith and Handel Model there could be one in which virus infection as well as bacterial coinfection can be simultaneously persistent ("fully persistent models" denotes such hypothetical models in Figure 3.35). Another extreme case would be a "fully-transient model" in which we have only transient dynamics and all species would finally tend to zero. Such a model would be the smallest one in our partial order of models (Figure 3.35).

The derived hierarchical map of models might be used to choose the most appropriate model for a particular domain and data set: The model should contain at least one organization for each set of species that were experimentally observed to survive in the long run. If there are several models with such organizations the one with the smallest organizations might be chosen to provide maximum efficiency in modeling. Table 3.1 as well as Figure 3.35 might guide the selection process, complementing established quantitative selection methods, such as those using the area under the viral load curve [14].

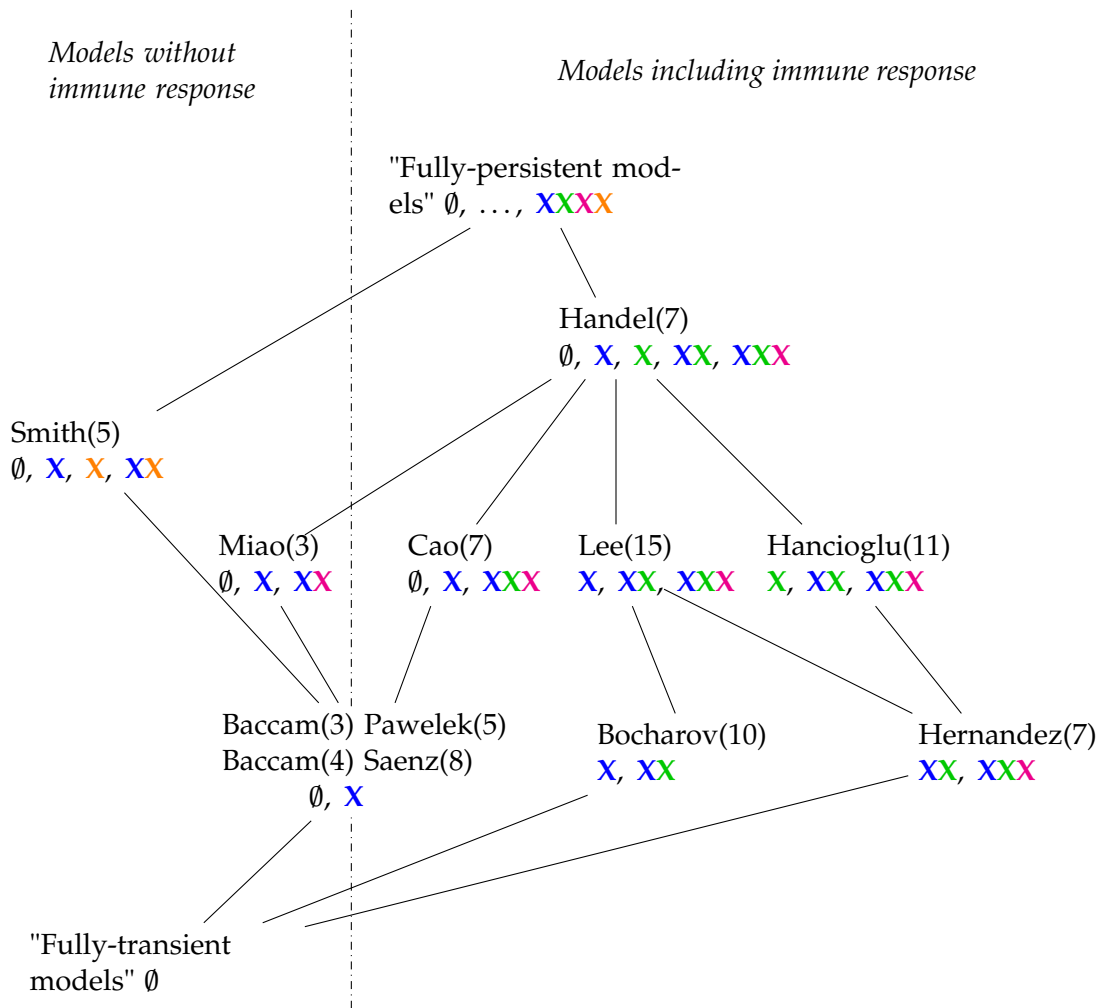


FIGURE 3.35: [75] Hasse-diagram of the hierarchy of IAV models with respect to their long-term behaviour. In brackets () we added the number of species of each model. Underneath (marked by colors) the kinds of species contained in the organizations belonging to each model. The meaning of the 4 colors is as follows: Species belonging to the healthy state of the organism are colored blue, those belonging to the immune response are colored green, those belonging to infection like infected cells and viruses are colored magenta, and bacteria from bacterial co-infection are colored orange. Horizontally the diagram consists of four lines. The models in the lowest line contain organizations with exactly two different kinds of species (colors) (including the empty set). In the second line above there are three different combinations of species (colors) to be found in each model. There is only one model in each of the highest two lines: The Smith model [84] is the only one with bacteria and contains four different combinations of colors. In the Handel Model there are even five different combinations of colors out of $2^4 = 16$ possible combinations.

3.4 Structure and Hierarchy of SARS-Cov-2 Virus Infection Models

We provide a list of the models analyzed in this section in Table 3.2.

Model Type	ODE	PDE
In-host	[94] ^{CoV} Vargas-I : $\mathbf{V}_g, \mathbf{V}_d$	[91] Bocharov-I: \mathbf{v}
	[94] ^{CoV} Vargas-II : \mathbf{V}, \mathbf{T}	[91] Bocharov-II: \mathbf{v}, \mathbf{c}
	[1] ^{CoV} Abuin : $\mathbf{U}, \mathbf{I}, \mathbf{V}$	
	[90] ^{CoV} Su : $\mathbf{H}, \mathbf{V}_b, \mathbf{m}, \mathbf{P}, \mathbf{S}, \mathbf{In}, \mathbf{V}$	
Host-to-host	[68] ^{CoV} Nesteruk : $\mathbf{S}, \mathbf{I}, \mathbf{R}$	[30] Fitzgibbon-I: ρ
	[100] ^{CoV} Wu : $\mathbf{S}, \mathbf{E}, \mathbf{I}, \mathbf{R}$	[30] Fitzgibbon-II: \mathbf{S}, \mathbf{I}
	[6] ^{CoV} Bai : $\mathbf{S}, \mathbf{E}, \mathbf{I}, \mathbf{R}, \mathbf{D}$	
Linked	[3] Almcocera: In-Host: \mathbf{V}, \mathbf{E} ; Linked: $\mathbf{V}, \mathbf{E}, \mathbf{S}, \mathbf{I}$	–

TABLE 3.2: [73] Overview of all models analyzed in this work each named by its first author and followed by the names of the variables used in the models. By clicking on the model names or the model types (left) you are directed to the part of this work where the respective model is analyzed. The model names tagged with ^{CoV}() in the beginning are explicitly for SARS-CoV-2 infection whereas the others are designed for viral infections in general. All models except for the two models from Bocharov and Almcocera (both published in 2018) were published in 2020.

In the following we present the respective ODEs and PDEs and the lattices of organizations of the models from Table 3.2. The reactions that we derive from the models are listed in Appendix B. We will start with the models basing on ODEs. These models, be they in-host or host-to-host models, were constructed especially for modeling the SARS-CoV-2 infection dynamics. After having analyzed the ODE models, we did the same for the PDE models. Note, that the latter were not solely built to model SARS-CoV-2 infection but rather viral infection dynamics in general. Finally, we analyze one ODE model (the Almcocera model [3, 11]) linking an in-host scenario (the example model from the Introduction) with a host-to-host scenario of virus infection dynamics. In four organizations (contained in the Vargas-II, Su and Almcocera Models) species can be distinguished marked by a bar | in the lattice of DOs. This property can only be captured by DOs but not by organizations.

In-Host Models

Here we firstly present four in-host ODE models with increasing numbers of species (see Figures 3.36 to 3.39). These models describe the spread of the infection within a host, in this case humans. All models contain a virus species but the models differ in terms of the identity of the species.



FIGURE 3.36: [73] The Vargas-I Model [94, 99] with two variables: Exponential growth viruses ($\mathbf{V}_{\mathbf{g}}$) and decay of viruses ($\mathbf{V}_{\mathbf{d}}$). There are two organizations: the empty set and the single species set $\{\mathbf{V}_{\mathbf{g}}\}$. The set of all species is not an organization since $\mathbf{V}_{\mathbf{d}}$ decays but is not produced by any reaction. The signature of this model is: \emptyset, \mathbf{X} .

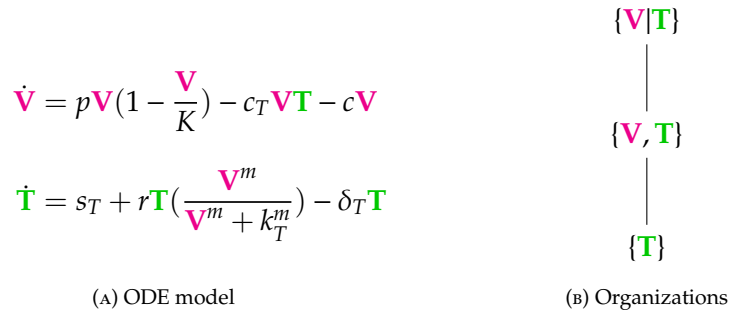


FIGURE 3.37: [73] The Vargas-II Model [94, 11, 3] with two variables: viruses \mathbf{V} and T-cells \mathbf{T} , and two organizations: $\{\mathbf{V}, \mathbf{T}\}$ and $\{\mathbf{T}\}$. The empty set is not an organization for this model since T has an inflow reaction with reaction constant s_T and thus does not go extinct. The organization $\{\mathbf{V}, \mathbf{T}\}$ exists also as distributed organization $\{\mathbf{V}|\mathbf{T}\}$. So, if \mathbf{V} and \mathbf{T} are separated the two reactions with reaction constants c_T and r are inactive, but this does neither destroy the self-maintenance nor the closedness. The signature of this model is: \mathbf{X}, \mathbf{XX} . Note that, by replacing \mathbf{T} by \mathbf{E} in this model, we get almost the same reactions and the same stoichiometric matrix as for the in-host Almcocera Model we introduced in the Materials and Methods Section ??.

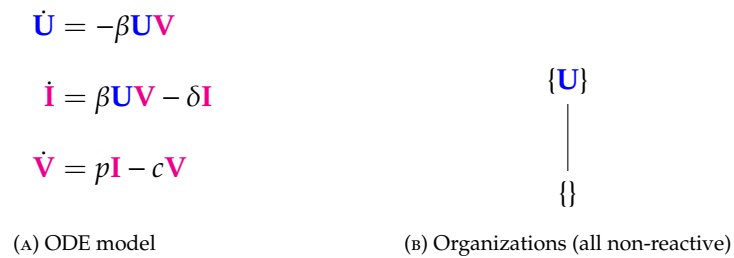


FIGURE 3.38: [73] The Abuin Model [1, 94, 41, 71, 16] with three variables: susceptible host cells \mathbf{U} , infected host cells \mathbf{I} , and viral particles \mathbf{V} . There are two organizations: the empty set $\{\}$ and $\{\mathbf{U}\}$. None of them includes an active reaction; thus we say, that they are “non-reactive”. Note that for this model, a principal part of the infection dynamics, concerning \mathbf{I} and \mathbf{V} , does not take place within an organization. Thus, from the role organizations play in the long-run of dynamical systems [72, 55] we know that this model induces a vanishing of \mathbf{I} and \mathbf{V} in the long run. The signature of this model is: \emptyset, \mathbf{X} .

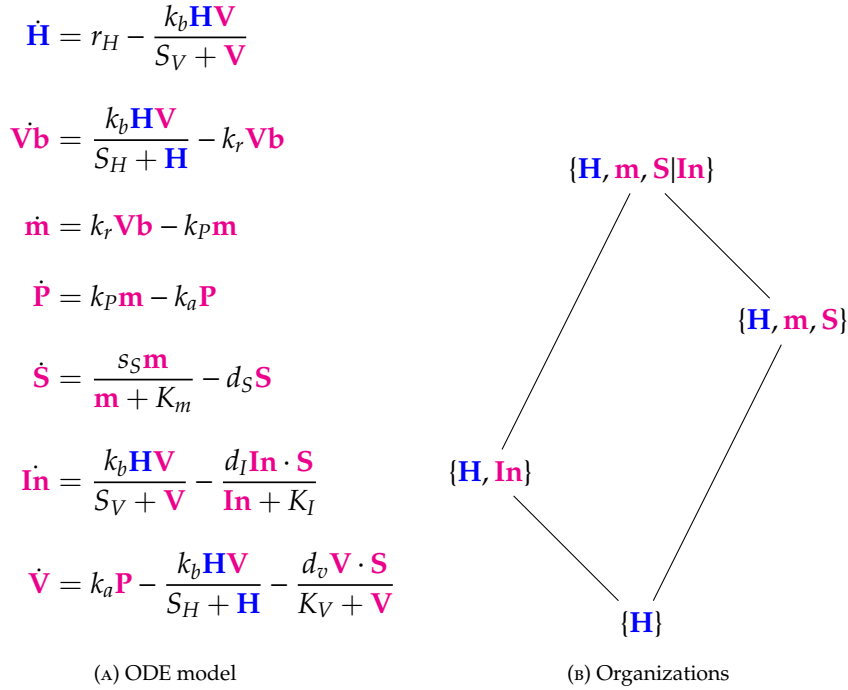


FIGURE 3.39: [73] The Su Model [90] with 7 variables: healthy cells \mathbf{H} , bound virus \mathbf{Vb} , RNA genome \mathbf{m} , proteins and replicated RNA packaged together in cytoplasm \mathbf{P} , cytokines stimulating inflammatory responses \mathbf{S} , infected cells \mathbf{In} , coronavirus \mathbf{V} . Here we have three organizations and one distributed organization $\{\mathbf{H}, \mathbf{m}, \mathbf{S}|\mathbf{In}\}$ that is not an organization. So, the species \mathbf{H} , \mathbf{m} , \mathbf{S} , and \mathbf{In} can only survive together, if \mathbf{S} and \mathbf{In} are separated. This deactivates the reaction with the reaction constant d_I and thus \mathbf{In} is able to persist. The signature of this model is: \mathbf{X}, \mathbf{XX} .

Now we analyze two in-host PDE models (see Figures 3.40, 3.41). Contrary to ODE models they are able to deal with spatial inhomogeneities of viral infection processes in the host. They were designed for general viral infections. Thus it is recommended for future SARS-CoV-2 infection dynamics modeling to adapt these models to capture the specifics of this new virus.

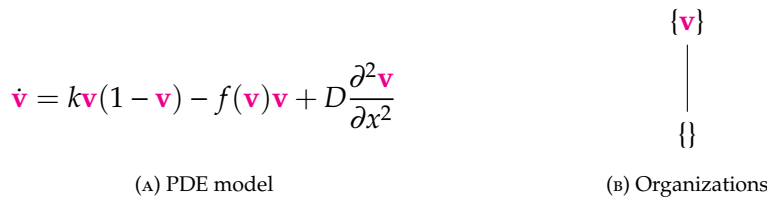
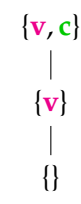


FIGURE 3.40: [73] The Bocharov-I Model [91] with one variable: the virus concentration \mathbf{v} . There are no boundary conditions specified. Thus, we assume Neumann boundary conditions for simplicity and in the style of the other PDE models analyzed in this work. There is the maximum number of two organizations for a model with one species here. This represents all possible long-term dynamics of the infection, i.e., its persistence as well as its extinction. The signature of this model is: \emptyset, \mathbf{X} .

$$\begin{aligned} \dot{\mathbf{v}} &= k\mathbf{v}(1 - \mathbf{v}) - \mathbf{c}\mathbf{v} + D_1 \frac{\partial^2 \mathbf{v}}{\partial x^2} \\ \dot{\mathbf{c}} &= \phi(\mathbf{v})\mathbf{c}(1 - \mathbf{c}) - \psi(\mathbf{v})\mathbf{c} + D_2 \frac{\partial^2 \mathbf{c}}{\partial x^2} \end{aligned}$$

(A) PDE model



(B) Organizations

FIGURE 3.41: [73] The Bocharov-II Model [94] from the year 2018 with two variables: the virus concentration \mathbf{v} and immune cell concentration \mathbf{c} . The functions $\phi(\mathbf{v})$ and $\psi(\mathbf{v})$ are assumed to be strictly positive if and only if $\mathbf{v} > 0$. As for the Bocharov-I Model (see Figure 3.40) we assume Neumann boundary conditions. There are three organizations. Only one subset of species is not an organization, i.e., the set $\{\mathbf{c}\}$. Thus the model provides a relatively big variety of possible long-term behaviors. The signature of this model is: $\emptyset, \mathbf{X}, \mathbf{XX}$.

Within the set of in-host models we observe a principal difference between the Abuin Model and the other models: The Abuin model does not have an organization with regard to the viral species causing the infection. Thus the Abuin model implicitly assumes the vanishing of the infection over time. The other models do not share this property and thus contain no assumptions regarding viral persistence, which may confer an advantage to these models since it is unclear what the extent of SARS-CoV-2 persistence is. The Su Model exhibits the most complex lattice of organizations. This is the model with the biggest number of species and the only model that explicitly focuses on the genetic aspects of SARS-CoV-2 infection dynamics. Interestingly the Su Model has a distributed organization that is not an organization. This emphasizes the role of the distribution of the species in space or time. Since the Su Model only has ODEs that do not allow for modeling spatial inhomogeneities this is an indication that adapting this model to PDEs may improve the model quality.

Host-To-Host Models

In this section we first analyze three different host-to-host ODE models describing SARS-CoV-2 infection as it spreads in a human population from one individual to the next (see Figure 3.42 to 3.44). Thus these models have three host species in common: susceptible, uninfected individuals (**S**) and infected individuals (**I**).

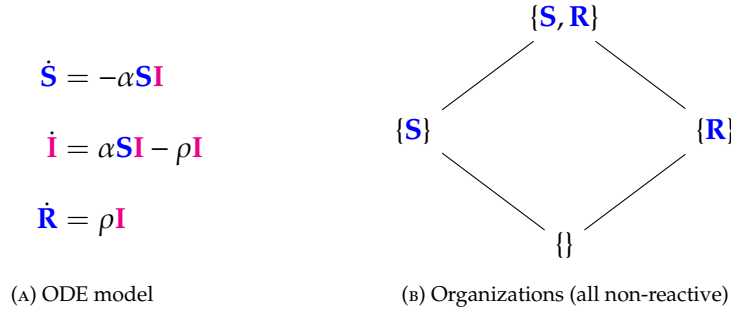


FIGURE 3.42: [73] The Nesteruk Model [68, 66, 7] with 3 variables (SIR): the number of susceptible persons **S**, infected (sick and infection-spreading) persons **I**, and removed (sum of isolated, recovered, and dead) persons **R**. There are four organizations that only contain healthy individuals. None of them contains infected individuals and all are non-reactive, i.e., no reaction is active for these organizations. Thus, as for the in-host Abuin Model from the previous section, the whole infection dynamics takes place outside the organizations. This model inherently assumes that all infected individuals **I** will vanish finally. The signature of this model is: $\emptyset, \underline{\mathbf{X}}$.

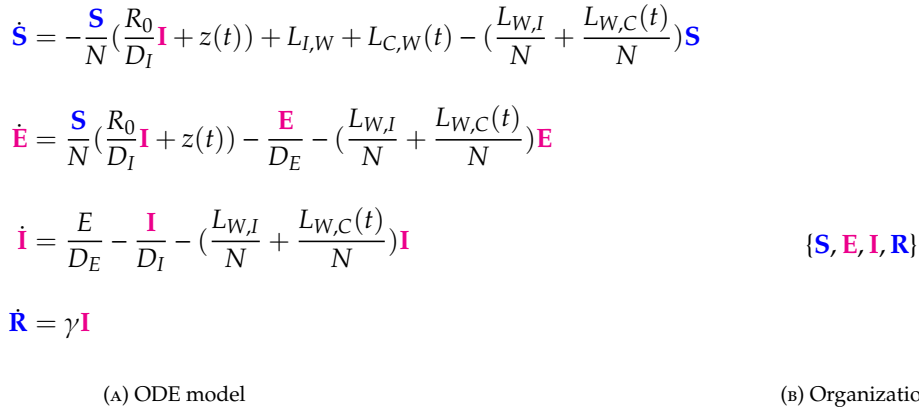


FIGURE 3.43: [73] The Wu Model [100](a SEIR model) with 4 variables: the number of susceptible **S**, latent **E**, infectious **I**, and removed **R** individuals, and only one organization: $\{\mathbf{S}, \mathbf{E}, \mathbf{I}, \mathbf{R}\}$, that contains all species. Thus this model implicitly assumes the infection to persist forever once it occurs which is a totally contrary assumption compared to the models assuming the vanishing of infection in the like the previously analyzed Nesteruk model. The signature of this model is: $\underline{\mathbf{X}\mathbf{X}}$.

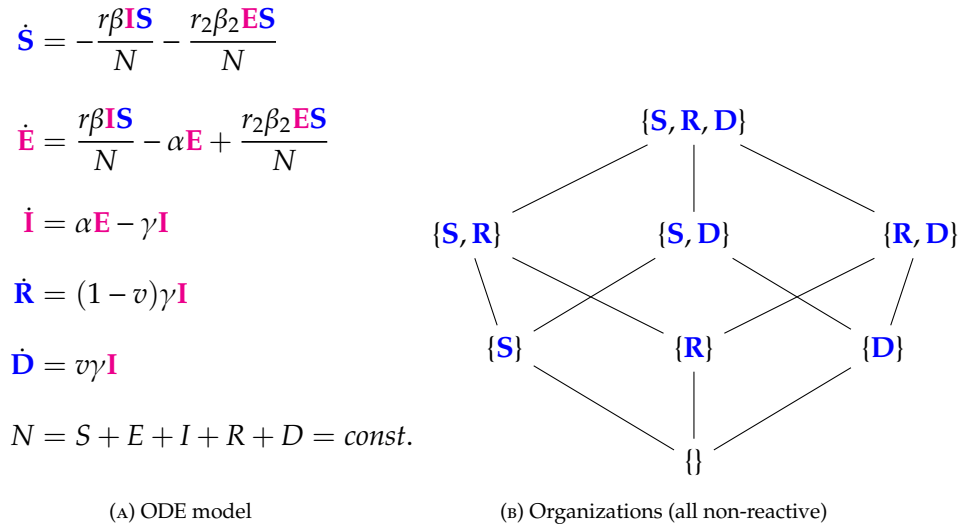


FIGURE 3.44: [73] The Bai Model [6, 97, 83] with 5 variables (SEIRD): the number of susceptible **S**, exposed **E**, infected **I**, recovered **R**, and dead **D** individuals. This model has a similar structure in terms of organizations to the Nesteruk model: there is no organization containing species representing the infection. Thus infection is implicitly assumed to vanish in the long-term. The remaining multitude of organizations exists simply due to the fact that recovered individuals **R** and dead individuals **D** can be combined arbitrarily with each other and with susceptible individuals **S** to form organizations. The signature of this model is: \emptyset, \underline{X} .

The host-to-host PDE models we subsequently analyzed (see Figures 3.45 and 3.46) have thus far only been applied to general viral infections. Because of the importance of the spatial dimension in SARS-CoV-2 transmissions, through interventions such as social distancing, it is pertinent to apply this approach to the current outbreak.

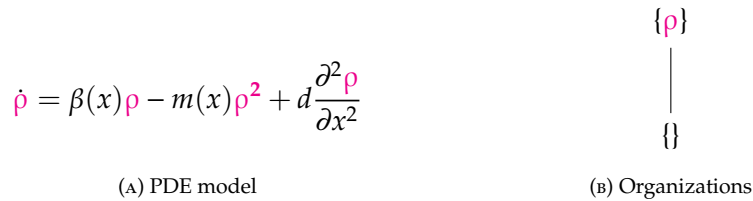


FIGURE 3.45: [73] The Fitzgibbon-I Model [30] with one variable ρ representing the current strength of the infection. ρ obeys Neumann boundary conditions. The reaction network structure of this model is almost equal to that of the in-host PDE Bocharov-I model (see Figure 3.40) from the previous section. Thus there is the maximum number of two organizations. All long-term dynamics of the infection, i.e., its persistence as well as its extinction, are possible. The signature of this model is: \emptyset, \underline{X} .

$$\begin{aligned} \dot{\mathbf{S}} &= -\sigma(x) \frac{\mathbf{I}^p}{1 + \kappa(x)\mathbf{I}^p} \mathbf{S} \\ \dot{\mathbf{I}} &= \sigma(x) \frac{\mathbf{I}^p}{1 + \kappa(x)\mathbf{I}^p} \mathbf{S} - \lambda \mathbf{I} + d \frac{\partial^2 \mathbf{I}}{\partial x^2} \end{aligned}$$

(A) PDE model

(B) Organizations

FIGURE 3.46: [73] The Fitzgibbon-II Model [30] with two variables: susceptible individuals $\mathbf{S}(t)$ and infected individuals $\mathbf{I}(x, t)$. Note that only the infected individuals \mathbf{I} are modeled dependent not only of time but also of space. It follows Neumann boundary condition. As for the Nesteruk Model and the Bai Model we here have no organization with any species representing the infection. Thus this model implies the infection to go extinct. The signature of this model is: \emptyset, \mathbf{X} .

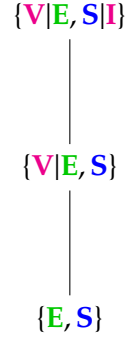
The Wu Model and the Fitzgibbon-I Model are the only ones that cover the infection dynamics on the level of organizations. However the Nesteruk Model, the Bai Model, and the Fitzgibbon-II Model have solely organizations without species representing infection. Thus these latter (three) models implicitly assume a vanishing of the infection in the long-term. It is currently unclear whether this assumption is justified for SARS-CoV-2.

A Linked In-Host/Host-To-Host Model

Here we analyze a model that we called “linked model” (see Figure 3.47) as it includes in-host as well as host-to-host dynamics, both described by ODEs. This model is designed for viral infections in general and its application to SARS-CoV-2 was deemed of interest because of its bigger focus compared to the previous models. For the analysis of the in-host part of the model we refer the reader to Figure 2.1. In the following we analyzed the linked model, where the in-host model is incorporated into a host-to-host model.

$$\begin{aligned} \dot{\mathbf{V}} &= p\mathbf{V} - p\frac{\mathbf{V}^2}{K_V} - c_V\mathbf{E}\mathbf{V} \\ \dot{\mathbf{E}} &= N_E - \delta_E\mathbf{E} + \frac{r\mathbf{V}}{\mathbf{V} + K_E}\mathbf{E} \\ \dot{\mathbf{S}} &= N_S - \delta_S\mathbf{S} - \frac{r_W\mathbf{V}}{\mathbf{V} + K_W}\mathbf{S}\mathbf{I} \\ \dot{\mathbf{I}} &= \frac{r_W\mathbf{V}}{\mathbf{V} + K_W}\mathbf{S}\mathbf{I} - \delta_I\mathbf{I} \end{aligned}$$

(A) Linked ODE model



(B) Organizations

FIGURE 3.47: [73] The linked Almcera Model [3, 4] has the two variables of the in-host model above (see Figure 2.1), i.e., viruses (\mathbf{V}) and T-cells (\mathbf{E}), plus two further variables: susceptible (\mathbf{S}) and infected (\mathbf{I}) individuals. Note that viruses \mathbf{V} as a part of the in-host model influence the host-to-host dynamics via the reaction with reaction constant r_W . There are three organizations: All of them contain \mathbf{E} and \mathbf{S} , since they are produced by the two inflow reactions with the reaction constants N_E and N_S , respectively. If \mathbf{V} is added to $\{\mathbf{E}, \mathbf{S}\}$, we get the organization $\{\mathbf{V}, \mathbf{E}, \mathbf{S}\}$ that can exist as a distributed organization by separation of \mathbf{V} and \mathbf{E} in the same way as it was the case for the in-host model (see Figure 2.1). If, furthermore, \mathbf{I} is added, then we get the full organization where still \mathbf{V} and \mathbf{E} can be separated, but \mathbf{I} must not be separated from \mathbf{V} and \mathbf{S} since then it could not regenerate via the reaction with the reaction constant r_W . Interestingly, in all the organizations of this model in-host species are mixed with host-to-host species. We find that in the long-term the species representing healthy, uninfected hosts, i.e., \mathbf{E} and \mathbf{S} always persist. Contrarily, \mathbf{V} and \mathbf{I} might persist too, but might also go extinct. If this is the case for the virus \mathbf{V} than also the infected individuals \mathbf{I} go extinct. This must not be the case the other way around. Lastly, the COT analysis shows that the model assumes that the T-cells \mathbf{E} can exist independently of the virus, but infected individuals can only exist persistently if in contact with healthy individuals \mathbf{S} and viruses \mathbf{V} . The signature of this model is: $\emptyset, \underline{\mathbf{X}}$. The signature of this model is: $\underline{\mathbf{XX}}, \underline{\mathbf{XXX}}, \underline{\mathbf{XXXX}}$.

Hierarchy of Models

In this section, we present the hierarchies of all models. First, we show the hierarchy of SARS-CoV-2 models (see Figure 3.48) and then the merged hierarchy of SARS-CoV-2 in addition to IAV models (see Figure 3.49).

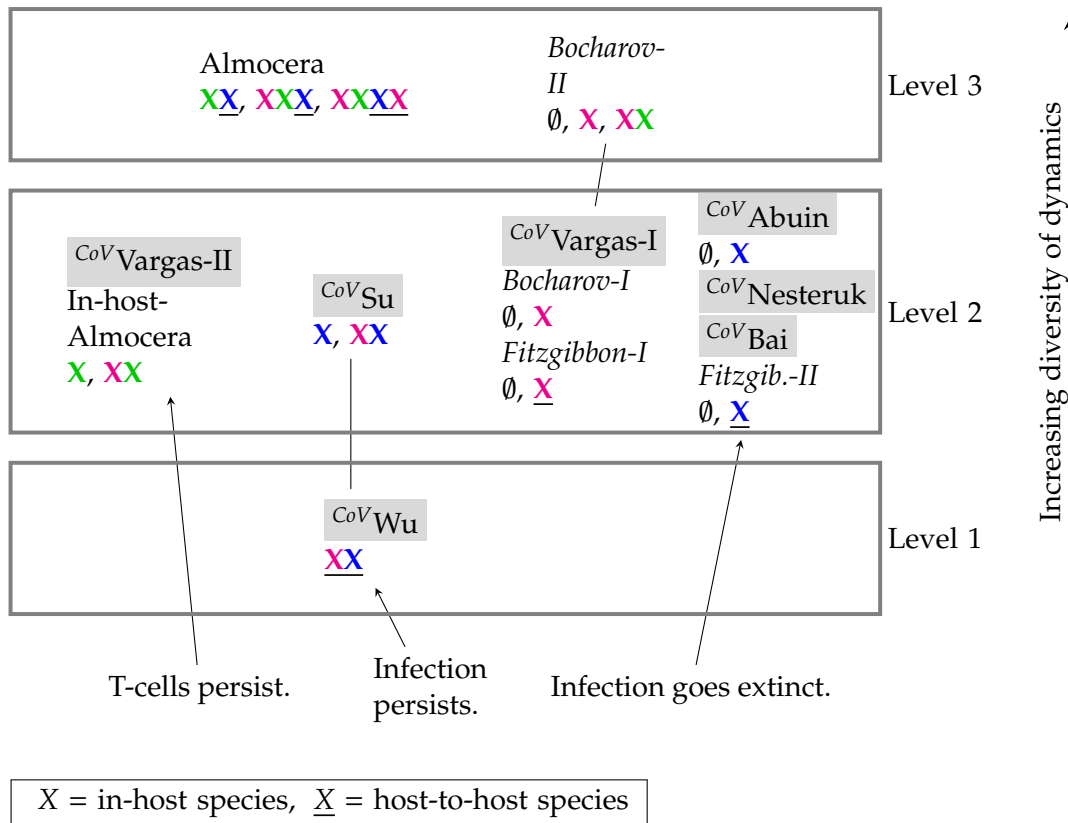
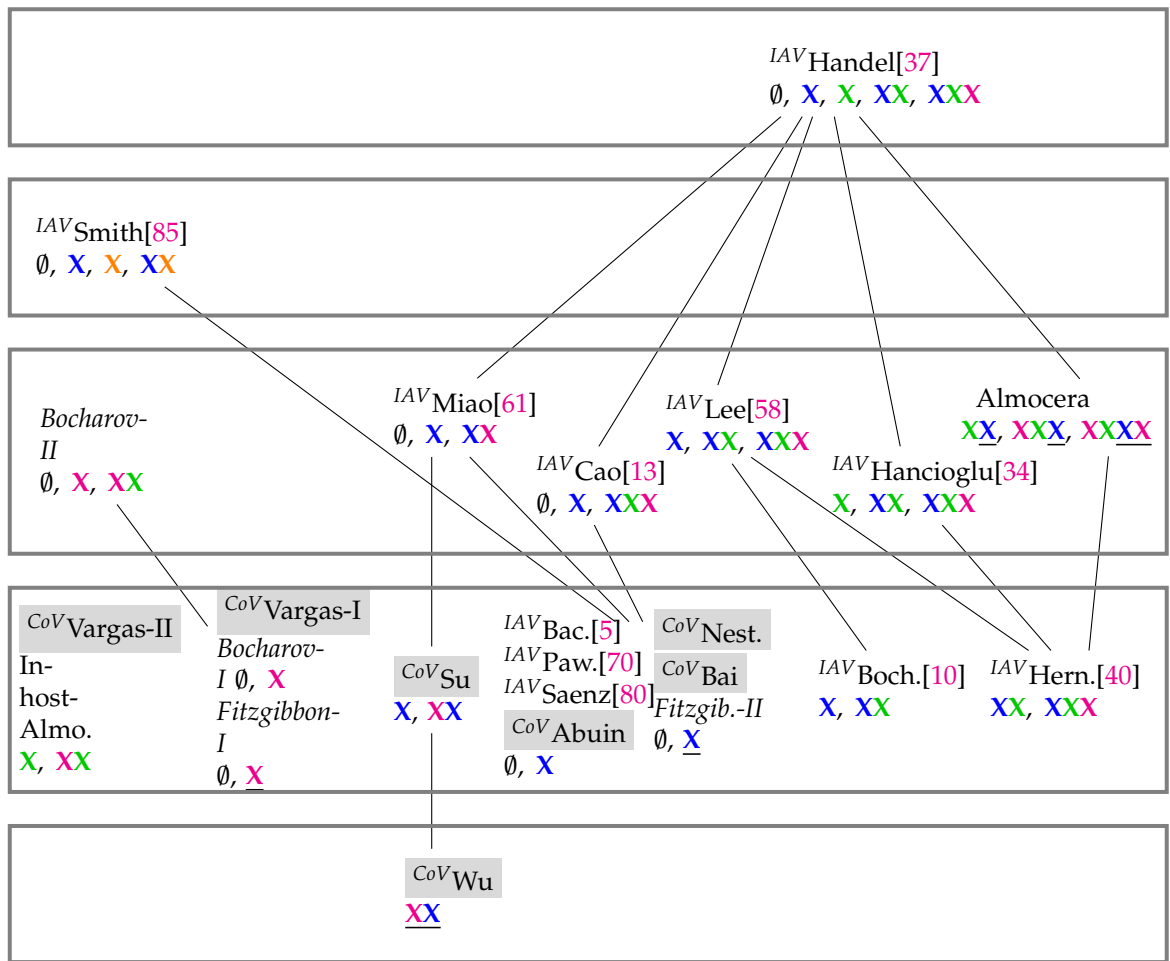


FIGURE 3.48: [73] Hierarchy of SARS-CoV-2 models (tagged with $CoV()$) and general virus models with respect to their long-term behavior identified by their signature. There are three different levels of increasing signatures. The higher the position of a model in the hierarchy the more diverse is its potential dynamical behavior. By clicking on the model names you are directed to the respective part of this work where the model is analyzed. PDE model names are written in italic.



X = in-host species, \underline{X} = host-to-host species

FIGURE 3.49: [73] Merged Hasse diagram of hierarchy of SARS-CoV-2 (tagged with $\text{CoV}()$), IAV models (tagged with $\text{IAV}()$), and general virus models. They are positioned at five different levels according to the size of their signatures. The higher the level of a model, the bigger is the number of components of its signature and thus the diversity of its potential dynamical behavior. By clicking on the model names you are directed to the respective part of this work where the models are analyzed. PDE model names are written in italic. Note, that contrary to many Influenza A infection models (third level and above) all SARS-CoV-2 infection models are on the second level (counted from bottom to top) and thus have a maximum number of two different species in their signature. This means that they are less complex in terms of their organizations than most of the Influenza A infection models. Note that the Smith Influenza A model is the only one that considers co-infection by bacteria X . For more information about the COT analysis of the Influenza A infection models see [75].

Chapter 4

Conclusions

In the first section of the Results, distributed organizations (DOs) were defined generalizing the concept of organizations from Chemical Organization Theory (COT). A DO consists of one or more closed subsets of species which complement one another to achieve self-maintenance as a whole. As one main result it was proven that the set of persistent species of every bounded solution of a reaction-diffusion system is always a DO. Here it is important to notice that DOs are computed solely from the reaction network underlying the reaction-diffusion system and thus do not depend on simulations of the dynamics of the system. The second main result was that the set of DOs of a given reaction network always forms a lattice. Thus the loss of information by abstracting away from the concrete dynamical behavior of one special RDS is accompanied by an increase of symmetry exhibited by the lattice of DOs.

The lattice of DOs does not depend on initial conditions or reaction constants but only on the reaction network. In the second section of the Results we have shown how to incorporate different boundary conditions into the reaction network. The lattice of DOs of a reaction network provides an overview of all potentially persistent subsets of species, which could persist by applying appropriate initial conditions and reaction constants. This in turn allows for comparing different reaction-diffusion systems or ODE systems in terms of persistence by comparing their lattices of DOs.

In the third and fourth section of the Results, this was done for several virus infection dynamics models of Influenza A as well as SARS-Cov-2. It was shown that our approach is able to combine not only models of different viruses but also of different types like ODE models and PDE models as well as in-host and host-to-host models (see Figure 3.48). In total, 24 models were analyzed by first identifying their underlying reaction networks and computing their lattices of DOs. Then these lattices were compressed to signatures by assigning a meaning (uninfected, infected, immune response) to each species of the models. Finally comparing these signatures by putting them into hierarchies allowed for comparing the models.

Thus, for each analyzed model a qualitative description of all possible long-term dynamics was obtained. That is, sets of species that can persist (organizations) and sets of species that can definitely not persist were distinguished. It stands out, that the hierarchy maps of models contain various empty territories, suggesting space for potential future models. For example there is no fully persistent and no fully transient model in the hierarchy map of Influenza A models (see Figure 3.35) There are a number of similarities among the models, for instance, the Abuin, Nesteruk, and Bai model are all in the same group regarding their organizations. Nevertheless, we also found a surprisingly high diversity of models with respect to their long-term qualitative behavior (Figure 3.48). Interestingly, there is only a small overlap between SARS-CoV-2 and Influenza A models. Compared to the Influenza A models the SARS-CoV-2 models appear to be simpler (mostly level 2 in Figure 3.48) and thus display a simpler hierarchy, that is, with only one inclusion relation between the Wu

and the Su model (Figure 3.49). It turned out, that the number of species (variables) of a model not necessarily correlates with the diversity of the potentially persistent species of a model. To see this, one can compare two Influenza A models (see Table 3.1), for example, the Handel Model has 7 species and the Saenz Model has 7 species and both models have 12 reactions each. But despite their similarity in terms of their number of species their signatures are very different: whereas the Handel Model exhibits five different types of organizations in its signature, the Saenz Model has only two. A lot of further differences were found. For example, among the SARS-Cov-2 models, there is only one, the Wu Model, which implies the unconditional persistence of infected cells. In stark contrast with this, three host-to-host (Nesteruk, Bai, Fitzgibbon-II) and one in-host model (Abuin) imply the definite extinction of any infection in the long-term. Such observations indicate, that COT can serve as a beneficial instrument supporting further development of virus infection dynamics models. This holds true also for other areas where modeling bases on reaction networks.

4.1 Future work

The first part of this work leaves several possibilities for extension: If nonnegativity of the solutions of the RDS (see lemma 3.1.7) can be proven for non-diagonal Fickian diffusivity matrices D , then our results hold true also in the case of cross-diffusion as described by [92]. Other types of dynamical systems derived from reaction networks can be considered, like the patch systems [2], which are connected ODE systems existing on a discrete domain, or stochastic reaction systems [65, 38]. As shown in section 3.2, our approach can also be extended to RDS with other boundary conditions than the homogeneous Neumann BCs considered here, for example, by modifying the reaction network (see also [74]). A systematic study of this area is still pending. Furthermore, this work did not consider unbounded solutions. The problem with unbounded solutions is that the concept of feasibility of flux vectors breaks down since, for example, a reaction can be active even though one of its reactants has a concentration value approaching zero. Summarizing, our work about DOs establishes a new field of research to be further-developed, which lies in the intersection of stability analyses, bifurcation theory, etc. An algorithm to compute all DOs of a given reaction network and an implementation as an online tool are in preparation.

The method of model structure analysis and comparison presented in the third and fourth section of the Results can help to select the right model for a particular situation, to relate other models to the present ones, to obtain an overview of the potential long-term dynamics of complex models, and to support model development, for example, by providing a rapid consistency check. Within the class of SARS-Cov-2 models there are three that exhibit organizations, for which the species can be distributed. It is an open question, whether this is represented by experimental data. We propose to find out whether it would be appropriate to construct models with such DOs. This would be the case, if several subsets of species do not always appear together at one location where their concentrations are measured. Besides the long-term behavior transient behavior can also be explained with respect to organizations, for example by defining a projection from a system state to an organization, as demonstrated for the Handel model (Figures 3.26 and 3.27). It is a task for future work to systematically analyze the transition dynamics between organizations [64, 39].

Our approach is not limited to IAV or SARS-Cov-2 models, but can be directly applied to other viruses in the same way since their dynamics are similarly modeled by ODEs and PDEs [101]. Furthermore, the approach is open to include other dynamically relevant components like treatment and vaccination strategies.

Bibliography

- [1] Pablo Abuin, Alejandro Anderson, Antonio Ferramosca, Esteban A Hernandez-Vargas **and** Alejandro H Gonzalez. “Characterization of SARS-CoV-2 Dynamics in the Host”. **in:** *arXiv e-prints* (2020), arXiv–2006.
- [2] Linda Joy Allen. “Applications of differential inequalities to persistence and extinction problems for reaction-diffusion systems”. phdthesis. Knoxville: University of Tennessee, 1981.
- [3] Alexis Erich S Almcera, Esteban A Hernandez-Vargas **and** others. “Multi-scale model within-host and between-host for viral infectious diseases”. **in:** *Journal of mathematical biology* 77.4 (2018), **pages** 1035–1057.
- [4] Roy M Anderson, B Anderson **and** Robert M May. *Infectious diseases of humans: dynamics and control*. Oxford university press, 1992.
- [5] Prasith Baccam, Catherine Beauchemin, Catherine A Macken, Frederick G Hayden **and** Alan S Perelson. “Kinetics of influenza A virus infection in humans”. **in:** *Journal of virology* 80.15 (2006), **pages** 7590–7599.
- [6] Shan Bai. “Simulations of COVID-19 spread by spatial agent-based model and ordinary differential equations”. **in:** *International Journal of Simulation and Process Modelling* 15.3 (2020), **pages** 268–277.
- [7] Norman TJ Bailey. *The mathematical theory of epidemics*. techreport. 1957.
- [8] Wolfgang Banzhaf. “Self-replicating sequences of binary numbers. Foundations I: General”. **in:** *Biological cybernetics* 69.4 (1993), **pages** 269–274.
- [9] C. A. Beauchemin **and** A. Handel. “A review of mathematical models of influenza A infections within a host or cell culture: lessons learned and challenges ahead”. **in:** *BMC Public Health* 11 Suppl 1 (february 2011), S7.
- [10] G. A. Bocharov **and** A. A. Romanyukha. “Mathematical model of antiviral immune response. III. Influenza A virus infection”. **in:** *J. Theor. Biol.* 167.4 (1994), **pages** 323–360.
- [11] A. Boianelli, V. K. Nguyen, T. Ebsen, K. Schulze, E. Wilk, N. Sharma, S. Stegemann-Koniszewski, D. Bruder, F. R. Toapanta, C. A. Guzman, M. Meyer-Hermann **and** E. A. Hernandez-Vargas. “Modeling Influenza Virus Infection: A Roadmap for Influenza Research”. **in:** *Viruses* 7.10 (october 2015), **pages** 5274–5304.
- [12] James D Brunner **and** Gheorghe Craciun. “Robust persistence and permanence of polynomial and power law dynamical systems”. **in:** *SIAM Journal on Applied Mathematics* 78.2 (2018), **pages** 801–825.
- [13] P. Cao, A. W. Yan, J. M. Heffernan, S. Petrie, R. G. Moss, L. A. Carolan, T. A. Guarnaccia, A. Kelso, I. G. Barr, J. McVernon, K. L. Laurie **and** J. M. McCaw. “Innate Immunity and the Inter-exposure Interval Determine the Dynamics of Secondary Influenza Virus Infection and Explain Observed Viral Hierarchies”. **in:** *PLoS Comput. Biol.* 11.8 (august 2015), e1004334.

- [14] Pengxing Cao **and** James McCaw. “The mechanisms for within-host influenza virus control affect model-based assessment and prediction of antiviral treatment”. **in:** *Viruses* 9.8 (2017), **page** 197.
- [15] Florian Centler **and** Peter Dittrich. “Chemical organizations in atmospheric photochemistries—A new method to analyze chemical reaction networks”. **in:** *Planetary and Space Science* 55.4 (2007), **pages** 413–428.
- [16] Stanca M Ciupe **and** Jane M Heffernan. “In-host modeling”. **in:** *Infectious Disease Modelling* 2.2 (2017), **pages** 188–202.
- [17] Carsten Conradi, Dietrich Flockerzi, Jörg Raisch **and** Jörg Stelling. “Subnetwork analysis reveals dynamic features of complex (bio) chemical networks”. **in:** *Proceedings of the National Academy of Sciences* 104.49 (2007), **pages** 19175–19180.
- [18] Gheorghe Craciun, Fedor Nazarov **and** Casian Pantea. “Persistence and permanence of mass-action and power-law dynamical systems”. **in:** *SIAM Journal on Applied Mathematics* 73.1 (2013), **pages** 305–329.
- [19] Peter Dittrich **and** Pietro Speroni di Fenizio. “Chemical Organization Theory”. **in:** *Bull. Math. Biol.* 69.4 (2007), **pages** 1199–1231.
- [20] Peter Dittrich **and** Lars Winter. “Chemical organizations in a toy model of the political system”. **in:** *Advances in Complex Systems* 11.04 (2008), **pages** 609–627.
- [21] H. M. Dobrovolny, M. B. Reddy, M. A. Kamal, C. R. Rayner **and** C. A. Beauchemin. “Assessing mathematical models of influenza infections using features of the immune response”. **in:** *PLoS ONE* 8.2 (2013), e57088.
- [22] Sean Quan Du **and** Weiming Yuan. “Mathematical modeling of interaction between innate and adaptive immune responses in COVID-19 and implications for viral pathogenesis”. **in:** *Journal of Medical Virology* (2020).
- [23] Manfred Eigen. “Selforganization of matter and the evolution of biological macromolecules”. **in:** *Naturwissenschaften* 58.10 (1971), **pages** 465–523.
- [24] Sibel Eker. “Validity and usefulness of COVID-19 models”. **in:** *Humanities and Social Sciences Communications* 7.1 (2020), **pages** 1–5.
- [25] Jan Ewald, Patricia Sieber, Ravindra Garde, Stefan N Lang, Stefan Schuster **and** Bashar Ibrahim. “Trends in mathematical modeling of host–pathogen interactions”. **in:** *Cellular and Molecular Life Sciences* (2020), **pages** 1–14.
- [26] François Fages, Steven Gay **and** Sylvain Soliman. “Inferring reaction systems from ordinary differential equations”. **in:** *Theoretical Computer Science* 599 (2015), **pages** 64–78.
- [27] Martin Feinberg. “Lectures on chemical reaction networks”. **in:** *Notes of lectures given at the Mathematics Research Center, University of Wisconsin* 49 (1979).
- [28] P. Speroni di Fenizio **and** P. Dittrich. “Chemical Organizations at Different Spatial Scales”. **in:** *Advances in Artificial Life* (2007), **pages** 1–11.
- [29] P Speroni di Fenizio, Peter Dittrich, Wolfgang Banzhaf **and** Jens Ziegler. “Towards a theory of organizations”. **in:** *Proc. German Workshop on Artificial Life (GWAL 2000), Bayreuth, April 5-7, 2000*. **by editor** Holger Lange. (in print), available online: <https://users.fmi.uni-jena.de/~dittrich/p/SDZB2001gwal.pdf>. 2001.
- [30] WE Fitzgibbon, JJ Morgan, GF Webb **and** Y Wu. “ANALYSIS OF A REACTION–DIFFUSION EPIDEMIC MODEL WITH ASYMPTOMATIC TRANSMISSION”. **in:** *Journal of Biological Systems* 28.3 (2020), **pages** 561–587.

- [31] Walter Fontana **and** Leo W Buss. “The arrival of the fittest: Toward a theory of biological organization”. **in:** *Bulletin of Mathematical Biology* 56.1 (1994), **pages** 1–64.
- [32] LE Fraenkel. *An introduction to maximum principles and symmetry in elliptic problems*. Cambridge University Press, 2000.
- [33] Karin Gatermann, Markus Eiswirth **and** Anke Sesse. “Toric ideals and graph theory to analyze Hopf bifurcations in mass action systems”. **in:** *Journal of Symbolic Computation* 40.6 (2005), **pages** 1361–1382.
- [34] B. Hancioglu, D. Swigon **and** G. Clermont. “A dynamical model of human immune response to influenza A virus infection”. **in:** *J. Theor. Biol.* 246.1 (may 2007), **pages** 70–86.
- [35] Andreas Handel, Laura E Liao **and** Catherine AA Beauchemin. “Progress and trends in mathematical modelling of influenza A virus infections”. **in:** *Current Opinion in Systems Biology* (2018).
- [36] Andreas Handel, Ira M Longini Jr **and** Rustom Antia. “Neuraminidase inhibitor resistance in influenza: assessing the danger of its generation and spread”. **in:** *PLoS Computational Biology* 3.12 (2007), e240.
- [37] Andreas Handel, Ira M Longini Jr **and** Rustom Antia. “Towards a quantitative understanding of the within-host dynamics of influenza A infections”. **in:** *Journal of the Royal Society Interface* 7.42 (2009), **pages** 35–47.
- [38] Mads Christian Hansen, Wiuf Carsten **and others**. “Existence of a unique quasi-stationary distribution in stochastic reaction networks”. **in:** *Electronic Journal of Probability* 25 (2020).
- [39] Richard Henze, Chunyan Mu, Mate Puljiz, Nishanthan Kamaleson, Jan Huwald, John Haslegrave, Pietro Speroni di Fenizio, David Parker, Christopher Good, Jonathan E Rowe **and others**. “Multi-scale stochastic organization-oriented coarse-graining exemplified on the human mitotic checkpoint”. **in:** *Scientific reports* 9.1 (2019), **page** 3902.
- [40] A Esteban Hernandez-Vargas **and** Michael Meyer-Hermann. “Innate immune system dynamics to influenza virus”. **in:** *IFAC Proceedings Volumes* 45.18 (2012), **pages** 260–265.
- [41] Esteban A Hernandez-Vargas. *Modeling and Control of Infectious Diseases in the Host: With MATLAB and R*. Academic Press, 2019.
- [42] Esteban A Hernandez-Vargas **and** Jorge X Velasco-Hernandez. “In-host Mathematical Modelling of COVID-19 in Humans”. **in:** *Annual Reviews in Control* (2020).
- [43] Georg Hetzer **and** Wenxian Shen. “Uniform persistence, coexistence, and extinction in almost periodic nonautonomous competition diffusion systems”. **in:** *SIAM journal on mathematical analysis* 34.1 (2002), **pages** 204–227.
- [44] Francis Heylighen, Shima Beigi **and** Tomas Veloz. “Chemical Organization Theory as a modeling framework for self-organization, autopoiesis and resilience”. **in:** *International Journal Of General Systems, submitted* (2015).
- [45] Josef Hofbauer, Karl Sigmund **and others**. *Evolutionary games and population dynamics*. Cambridge university press, 1998.
- [46] Wim Hordijk **and** Mike Steel. “Autocatalytic networks at the basis of life’s origin and organization”. **in:** *Life* 8.4 (2018), **page** 62.

- [47] Fritz Horn **and** Roy Jackson. “General mass action kinetics”. *in: Archive for rational mechanics and analysis* 47.2 (1972), **pages** 81–116.
- [48] Franziska Hufsky, Kevin Lamkiewicz, Alexandre Almeida, Abdel Aouacheria, Cecilia Arighi, Alex Bateman, Jan Baumbach, Niko Beerenwinkel, Christian Brandt, Marco Cacciabue **and others**. “Computational Strategies to Combat COVID-19: Useful Tools to Accelerate SARS-CoV-2 and Coronavirus Research”. *in:* (2020).
- [49] Bashar Ibrahim, Richard Henze, Gerd Gruenert, Matthew Egbert, Jan Huwald **and** Peter Dittrich. “Spatial rule-based modeling: a method and its application to the human mitotic kinetochore”. *in: Cells* 2.3 (2013), **pages** 506–544.
- [50] Bashar Ibrahim, Dino P McMahon, Franziska Hufsky, Martin Beer, Li Deng, Philippe Le Mercier, Massimo Palmarini, Volker Thiel **and** Manja Marz. “A new era of virus bioinformatics”. *in: Virus research* 251 (2018), **pages** 86–90.
- [51] Sanjay Jain **and** Sandeep Krishna. “Autocatalytic sets and the growth of complexity in an evolutionary model”. *in: Physical Review Letters* 81.25 (1998), **page** 5684.
- [52] Christoph Kaleta, Stephan Richter **and** Peter Dittrich. “Using chemical organization theory for model checking”. *in: Bioinformatics* 25.15 (2009), **pages** 1915–1922.
- [53] Stuart A Kauffman. “Cellular homeostasis, epigenesis and replication in randomly aggregated macromolecular systems”. *in: Journal of Cybernetics* 1.1 (1971), **pages** 71–96.
- [54] Florian Krammer, Gavin JD Smith, Ron AM Fouchier, Malik Peiris, Katherine Kedzierska, Peter C Doherty, Peter Palese, Megan L Shaw, John Treanor, Robert G Webster **and** Adolfo García-Sastre. “Influenza”. *in: Nature Reviews Disease Primers* 4.1 (2018). DOI: [10.1038/s41572-018-0002-y](https://doi.org/10.1038/s41572-018-0002-y).
- [55] P. Kreyssig, G. Escuela, B. Reynaert, T. Veloz, B. Ibrahim **and** P. Dittrich. “Cycles and the qualitative evolution of chemical systems”. *in: PLoS ONE* 7.10 (2012), e45772.
- [56] Peter Kreyssig, Christian Wozar, Stephan Peter, Tomas Veloz, Bashar Ibrahim **and** Peter Dittrich. “Effects of small particle numbers on long-term behaviour in discrete biochemical systems”. *in: Bioinformatics* 30.17 (2014), **pages** i475–i481.
- [57] M Veera Krishna **and** J Prakash. “Mathematical modelling on phase based transmissibility of Coronavirus”. *in: Infectious Disease Modelling* 5 (2020), **pages** 375–385.
- [58] H. Y. Lee, D. J. Topham, S. Y. Park, J. Hollenbaugh, J. Treanor, T. R. Mosmann, X. Jin, B. M. Ward, H. Miao, J. Holden-Wiltse, A. S. Perelson, M. Zand **and** H. Wu. “Simulation and prediction of the adaptive immune response to influenza A virus infection”. *in: J. Virol.* 83.14 (july 2009), **pages** 7151–7165.
- [59] Naoki Matsumaru, Florian Centler, Pietro Speroni di Fenizio **and** Peter Dittrich. “Chemical organization theory applied to virus dynamics”. *in: it-Information Technology* 48.3 (2006), **pages** 154–160.
- [60] Naoki Matsumaru, Pietro Speroni di Fenizio, Florian Centler **and** Peter Dittrich. “On the Evolution of Chemical Organizations”. *in: Proceedings of the 7th German Workshop of Artificial Life*. **by editor** Stefan Artmann und Peter Dittrich. IOS Press, 2006, **pages** 135–146.

- [61] H. Miao, J. A. Hollenbaugh, M. S. Zand, J. Holden-Wiltse, T. R. Mosmann, A. S. Perelson, H. Wu **and** D. J. Topham. “Quantifying the early immune response and adaptive immune response kinetics in mice infected with influenza A virus”. *in: J. Virol.* 84.13 (july 2010), **pages** 6687–6698.
- [62] Maya Mincheva **and** David Siegel. “Nonnegativity and positiveness of solutions to mass action reaction–diffusion systems”. *in: Journal of mathematical chemistry* 42.4 (2007), **pages** 1135–1145.
- [63] Maya Mincheva **and** David Siegel. “Stability of mass action reaction–diffusion systems”. *in: Nonlinear Analysis: Theory, Methods & Applications* 56 (march 2004), **pages** 1105–1131. doi: [10.1016/j.na.2003.10.025](https://doi.org/10.1016/j.na.2003.10.025).
- [64] Chunyan Mu, Peter Dittrich, David Parker **and** Jonathan E Rowe. “Organisation-Oriented Coarse Graining and Refinement of Stochastic Reaction Networks”. *in: IEEE/ACM Transactions on Computational Biology and Bioinformatics* (2018).
- [65] Chunyan Mu, Peter Dittrich, David Parker **and** Jonathan E Rowe. “Organisation-oriented coarse graining and refinement of stochastic reaction networks”. *in: IEEE/ACM transactions on computational biology and bioinformatics* 15.4 (2018), **pages** 1152–1166.
- [66] James D Murray. “Mathematical biology: I. An introduction. Interdisciplinary applied mathematics”. *in: Mathematical Biology, Springer* (2002).
- [67] Faten Nabli, Thierry Martinez, François Fages **and** Sylvain Soliman. “On enumerating minimal siphons in Petri nets using CLP and SAT solvers: theoretical and practical complexity”. *in: Constraints* 21.2 (2016), **pages** 251–276.
- [68] Igor Nesteruk. “Statistics-based predictions of coronavirus epidemic spreading in mainland China”. *in:* (2020).
- [69] Gunter Neumann **and** Stefan Schuster. “Continuous model for the rock–scissors–paper game between bacteriocin producing bacteria”. *in: Journal of Mathematical Biology* 54.6 (june 2007), **pages** 815–846. ISSN: 1432-1416. doi: [10.1007/s00285-006-0065-3](https://doi.org/10.1007/s00285-006-0065-3). URL: <https://doi.org/10.1007/s00285-006-0065-3>.
- [70] K. A. Pawelek, G. T. Huynh, M. Quinlivan, A. Cullinane, L. Rong **and** A. S. Perelson. “Modeling within-host dynamics of influenza virus infection including immune responses”. *in: PLoS Comput. Biol.* 8.6 (2012), e1002588.
- [71] Alan S Perelson. “Modelling viral and immune system dynamics”. *in: Nature Reviews Immunology* 2.1 (2002), **pages** 28–36.
- [72] S. Peter **and** P. Dittrich. “On the Relation between Organizations and Limit Sets in Chemical Reaction Systems”. *in: Advances in Complex Systems* 14.1 (2011), **pages** 77–96.
- [73] Stephan Peter, Peter Dittrich **and** Bashar Ibrahim. “Structure and Hierarchy of SARS-CoV-2 Infection Dynamics Models Revealed by Reaction Network Analysis”. *in: Viruses* 13.1 (2021), **page** 14.
- [74] Stephan Peter, Fanar Ghanim, Peter Dittrich **and** Bashar Ibrahim. “Organizations in reaction-diffusion systems: Effects of diffusion and boundary conditions”. *in: Ecological Complexity* 43 (2020), **page** 100855.
- [75] Stephan Peter, Martin Hölzer, Kevin Lamkiewicz, Pietro Speroni di Fenizio, Hassan Al Hwaeer, Manja Marz, Stefan Schuster, Peter Dittrich **and** Bashar Ibrahim. “Structure and Hierarchy of Influenza Virus Models Revealed by Reaction Network Analysis”. *in: Viruses* 11.5 (2019), **page** 449.

- [76] Stephan Peter, Bashar Ibrahim **and** Peter Dittrich. "Linking Network Structure and Dynamics to Describe the Set of Persistent Species in Reaction Diffusion Systems". **in:** *SIAM Journal on Applied Dynamical Systems* 20.4 (2021), **pages** 2037–2076.
- [77] Velislava N Petrova **and** Colin A Russell. "The evolution of seasonal influenza viruses". **in:** *Nature Reviews Microbiology* 16.1 (2018), **page** 47.
- [78] Alessandro Ravoni. "Long-term behaviours of Autocatalytic Sets". **in:** *arXiv preprint arXiv:2010.08523* (2020).
- [79] Otto E Rössler. "Ein systemtheoretisches Modell zur Biogenese/A System Theoretic Model of Biogenesis". **in:** *Zeitschrift für Naturforschung B* 26.8 (1971), **pages** 741–746.
- [80] R. A. Saenz, M. Quinlivan, D. Elton, S. Macrae, A. S. Blunden, J. A. Mumford, J. M. Daly, P. Digard, A. Cullinane, B. T. Grenfell, J. W. McCauley, J. L. Wood **and** J. R. Gog. "Dynamics of influenza virus infection and pathology". **in:** *J. Virol.* 84.8 (april 2010), **pages** 3974–3983.
- [81] S. Schuster, T. Pfeiffer, F. Moldenhauer, I. Koch **and** T. Dandekar. "Structural Analysis of Metabolic Networks: Elementary Flux Modes, Analogy to Petri Nets, and Application to Mycoplasma pneumoniae". **in:** *Proceedings of the German Conference on Bioinformatics 2000*. **by editor** E. Bornberg-Bauer **and** M. Vingron U. Rost J. Stoye. Berlin: Logos Verlag, 2000, **pages** 115–120.
- [82] Anke Sensse **and** Markus Eiswirth. "Feedback loops for chaos in activator-inhibitor systems". **in:** *The Journal of chemical physics* 122.4 (2005), **page** 044516.
- [83] Peng Shao **and** Yingji Shan. "Beware of asymptomatic transmission: Study on 2019-nCoV prevention and control measures based on extended SEIR model". **in:** *BioRxiv* (2020).
- [84] A. M. Smith **and** A. S. Perelson. "Influenza A virus infection kinetics: quantitative data and models". **in:** *Wiley Interdiscip Rev Syst Biol Med* 3.4 (2011), **pages** 429–445.
- [85] A. M. Smith **and** A. P. Smith. "A Critical, Nonlinear Threshold Dictates Bacterial Invasion and Initial Kinetics During Influenza". **in:** *Sci Rep* 6 (december 2016), **page** 38703.
- [86] Amanda P Smith, David J Moquin, Veronika Bernhauerova **and** Amber M Smith. "Influenza virus infection model with density dependence supports biphasic viral decay". **in:** *Frontiers in microbiology* 9 (2018), **page** 1554.
- [87] Sylvain Soliman **and** Monika Heiner. "A unique transformation from ordinary differential equations to reaction networks". **in:** *PloS one* 5.12 (2010), e14284.
- [88] Mike Steel, Joana C Xavier **and** Daniel H Huson. "The structure of autocatalytic networks, with application to early biochemistry". **in:** *Journal of the Royal Society Interface* 17.171 (2020), **page** 20200488.
- [89] Klaus Stöhr. "Influenza – WHO cares". **in:** *The Lancet infectious diseases* 2.9 (2002), **page** 517.
- [90] Zhaoqian Su **and** Yinghao Wu. "A multiscale and comparative model for receptor binding of 2019 novel coronavirus and the implication of its life cycle in host cells". **in:** *BioRxiv* (2020).

- [91] Alla L'vovna Tasevich, Gennady Alexeevitch Bocharov **and** Vitalii Aizikovich Vol'pert. "Reaction-diffusion equations in immunology". **in:** *Zhurnal Vychislitel'noi Matematiki i Matematicheskoi Fiziki* 58.12 (2018), **pages** 2048–2059.
- [92] Vladimir K Vanag **and** Irving R Epstein. "Cross-diffusion and pattern formation in reaction–diffusion systems". **in:** *Physical Chemistry Chemical Physics* 11.6 (2009), **pages** 897–912.
- [93] Francisco G Varela, Humberto R Maturana **and** Ricardo Uribe. "Autopoiesis: The organization of living systems, its characterization and a model". **in:** *Biosystems* 5.4 (1974), **pages** 187–196.
- [94] Esteban Abelardo Hernandez Vargas **and** Jorge X Velasco-Hernandez. "In-host modelling of covid-19 kinetics in humans". **in:** *medRxiv* (2020).
- [95] Tomas Veloz. "The Complexity–Stability Debate, Chemical Organization Theory, and the Identification of Non-classical Structures in Ecology". **in:** *Foundations of Science* 25.1 (2020), **pages** 259–273.
- [96] Jin Wang. "Mathematical models for COVID-19: Applications, limitations, and potentials". **in:** *Journal of public health and emergency* 4 (2020).
- [97] Joshua S Weitz **and** Jonathan Dushoff. "Modeling post-death transmission of Ebola: challenges for inference and opportunities for control". **in:** *Scientific reports* 5 (2015), **page** 8751.
- [98] Oliver Weller-Davies, Mike Steel **and** Jotun Hein. "Complexity results for autocatalytic network models". **in:** *Mathematical Biosciences* (2020), **page** 108365.
- [99] Roman Wölfel, Victor M Corman, Wolfgang Guggemos, Michael Seilmaier, Sabine Zange, Marcel A Müller, Daniela Niemeyer, Terry C Jones, Patrick Vollmar, Camilla Rothe **and others**. "Virological assessment of hospitalized patients with COVID-2019". **in:** *Nature* 581.7809 (2020), **pages** 465–469.
- [100] Joseph T Wu, Kathy Leung **and** Gabriel M Leung. "Nowcasting and forecasting the potential domestic and international spread of the 2019-nCoV outbreak originating in Wuhan, China: a modelling study". **in:** *The Lancet* 395.10225 (2020), **pages** 689–697.
- [101] Carolin Zitzmann **and** Lars Kaderali. "Mathematical Analysis of Viral Replication Dynamics and Antiviral Treatment Strategies: From Basic Models to Age-Based Multi-Scale Modeling". **in:** *Frontiers in microbiology* 9 (2018).

Appendix A

Reactions of Influenza-A virus infection dynamics models

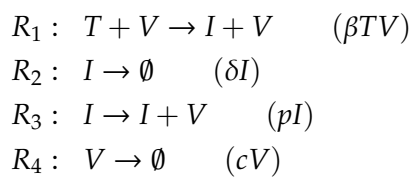


FIGURE A.1: Reactions of Baccam model [5].

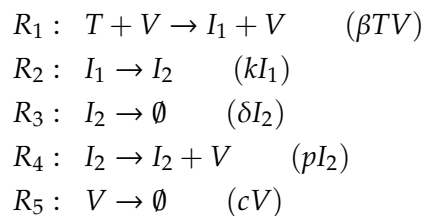


FIGURE A.3: Reactions of Baccam II model [5] with delayed virus production.

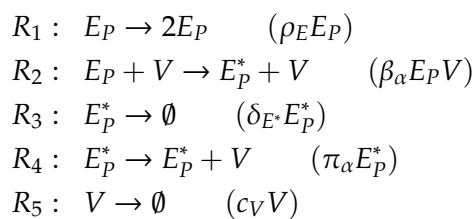


FIGURE A.2: Reactions of Miao model [61].

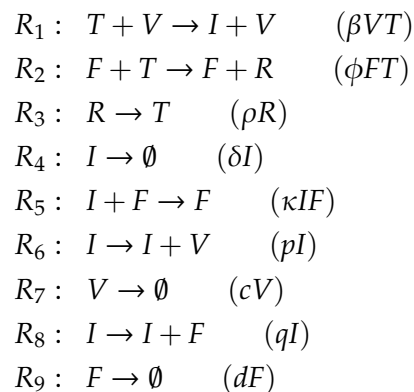


FIGURE A.4: Reactions of Pawelek model [70]

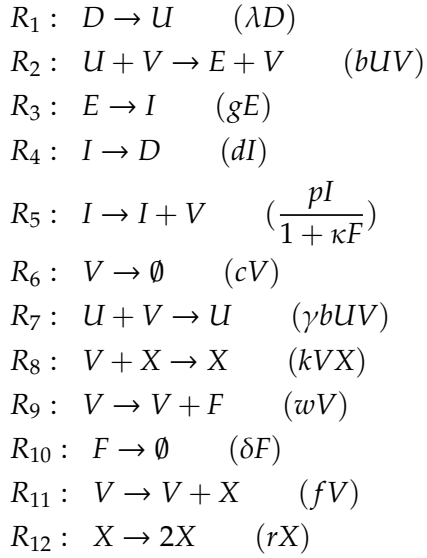


FIGURE A.5: Reactions of Handel model [37]

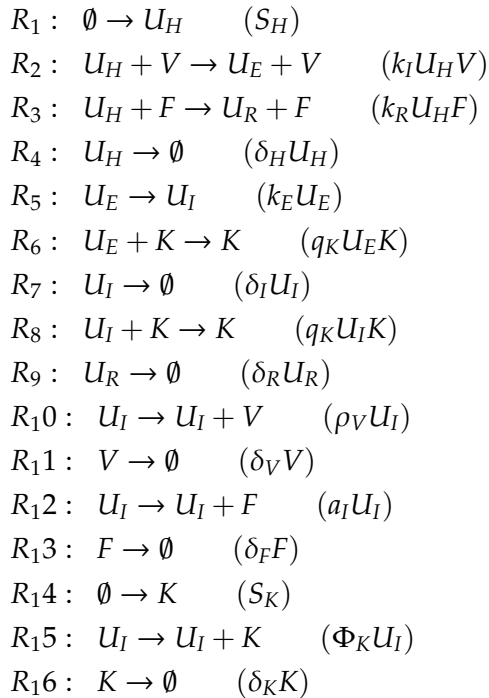


FIGURE A.6: Reactions of Hernandez model [40]

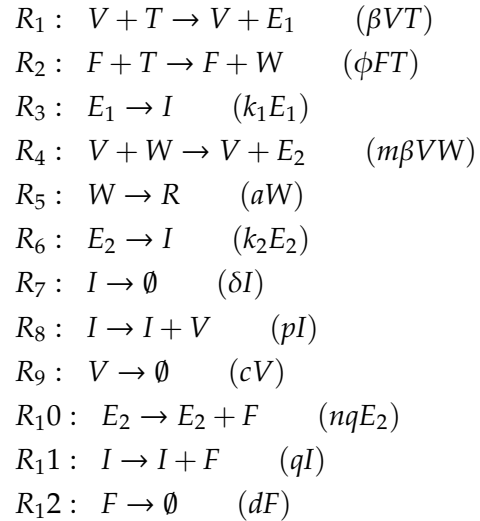


FIGURE A.7: Reactions of Saenz model [80]

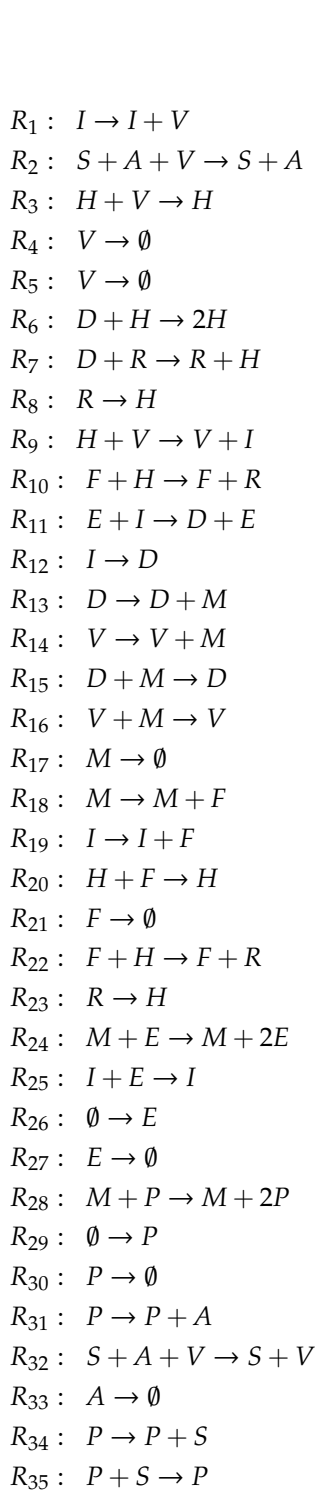


FIGURE A.8: Reactions
of Hancioglu model
[34]

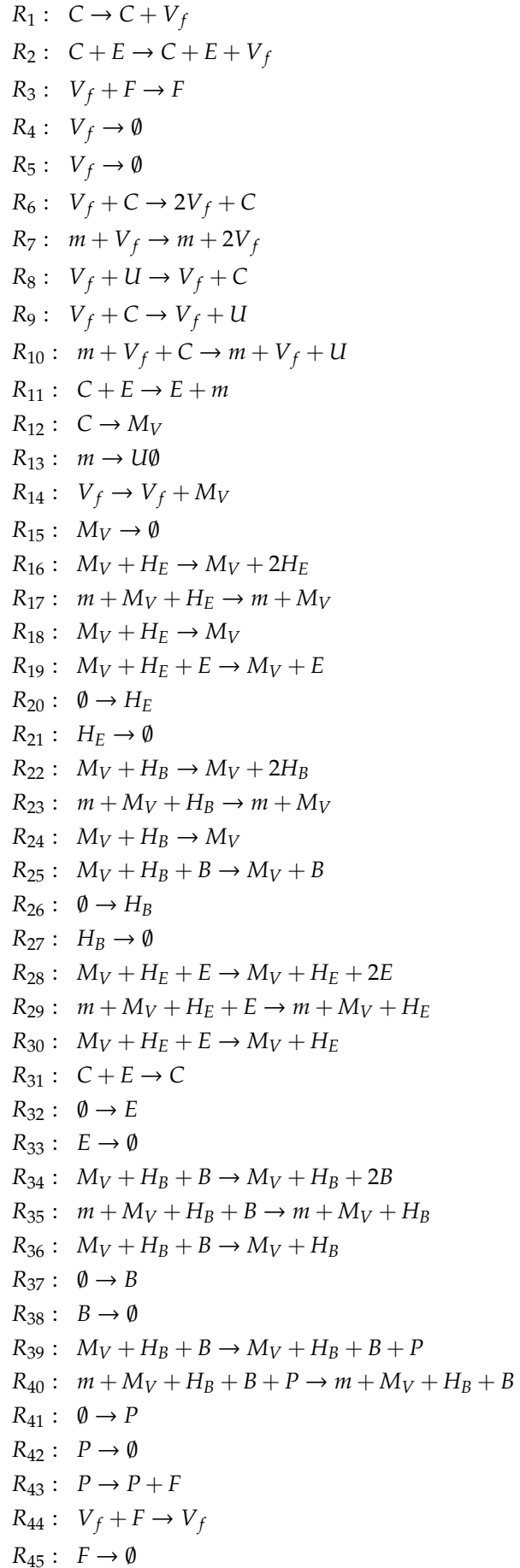


FIGURE A.9: Reactions
of Bocharov model
[10]

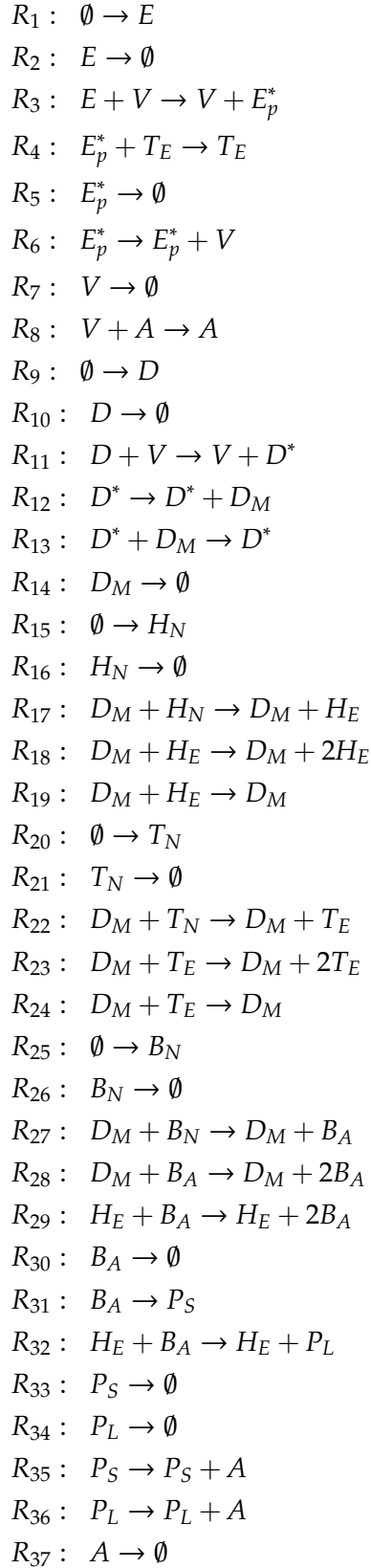
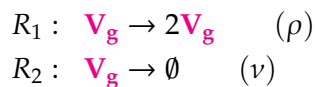


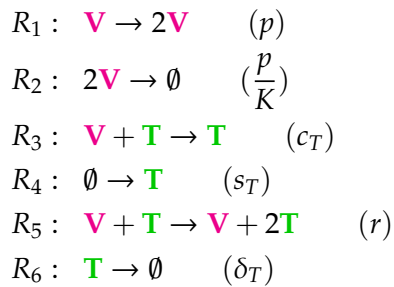
FIGURE A.10: Reactions of Lee model [58]

Appendix B

Reactions of SARS-Cov-2 virus infection dynamics models

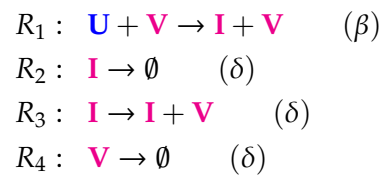


(A) Vargas-I Model

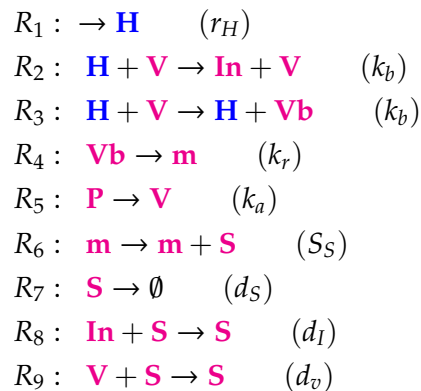


(B) Vargas-II Model

FIGURE B.1: Lists of reactions of the **Vargas Models**.

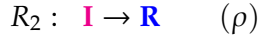
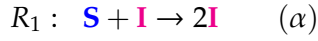


(A) Abuin Model

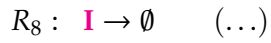
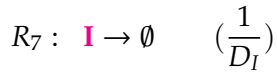
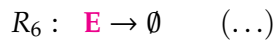
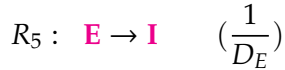
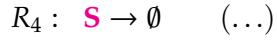
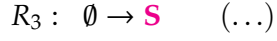
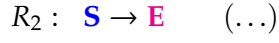
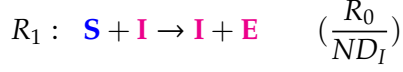


(B) Su Model

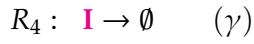
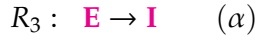
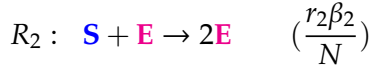
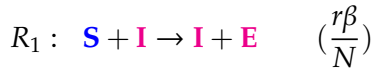
FIGURE B.2: Lists of reactions of the **Abuin Model** and the **Su Model**.



(A) Nesteruk Model

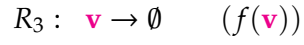
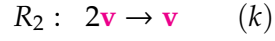
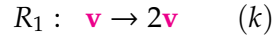


(B) Wu Model

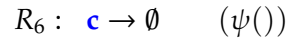
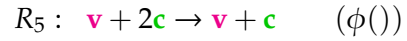
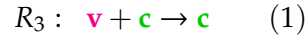
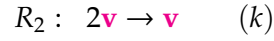
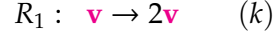


(c) Bai Model

FIGURE B.3: Lists of reactions of the **Nesteruk Model**, the **Wu Model**, and the **Bai Model**.

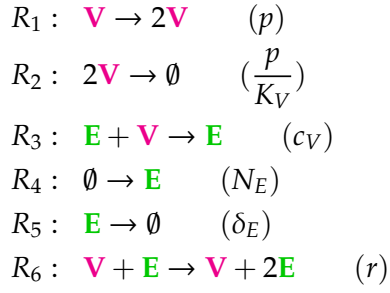


(A) Bocharov-I Model

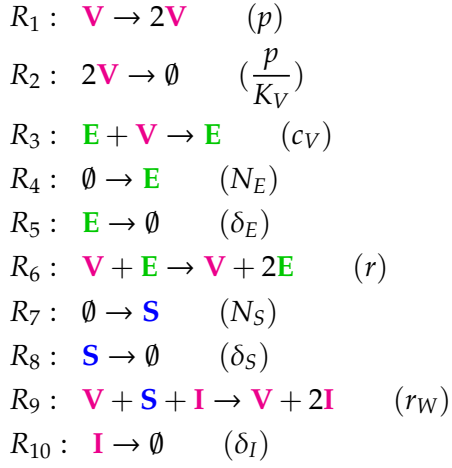


(B) Bocharov-II Model

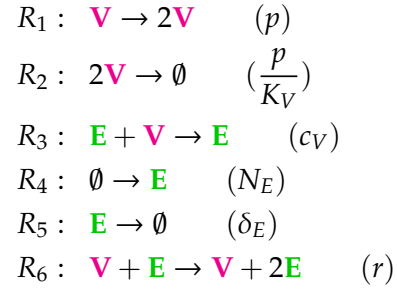
FIGURE B.4: Lists of reactions of the **Bocharov Models**.



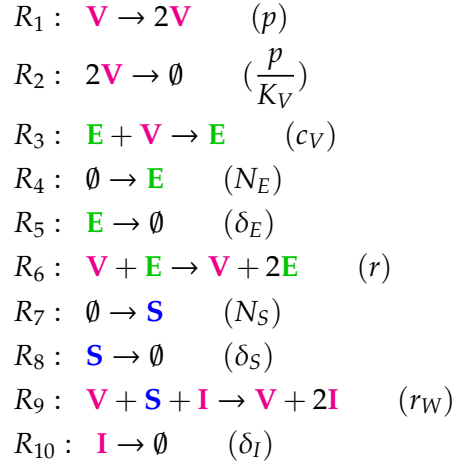
(A) Fitzgibbon-I Model



(B) Fitzgibbon-II Model

FIGURE B.5: Lists of reactions of the **Fitzgibbon Models**.

(A) In-host model



(B) Linked model

FIGURE B.6: Lists of reactions of the **Almocera Model**.

Selbstständigkeitserklärung

Hiermit erkläre ich, Stephan Peter, dass ich die beigefügte Dissertation mit dem Titel "*Chemische Organisationstheorie für Reaktionsdiffusionssysteme und ihre Anwendung auf Vireinfektionsmodelle*" selbstständig verfasst und keine anderen als die angegebenen Hilfsmittel genutzt habe. Alle wörtlich oder inhaltlich übernommenen Stellen habe ich als solche gekennzeichnet.

Ort, Datum: Jena, den 04.04.2022

Unterschrift:
